Reviews of

Physiology Biochemistry and Pharmacology 133

M. Ullrich
Effects of Streptolysin on Endothelial Cells and Platelets

W. Meyerhof
The Elucidation of Somatostatin Receptor Functions: A Current View

M. Lenz, F. Lentes, E. Kilimann and A. Noack
Cytokine-Mediated Hepatic Apoptosis

Springer

Reviews of Physiology, Biochemistry and Pharmacology 133

Reviews of

133 Physiology Biochemistry and Pharmacology

With 18 Figures and 5 Tables

Springer

ISSN 0303-4240
ISBN 3-540-63945-4 Springer-Verlag Berlin Heidelberg New York

Library of Congress-Catalog-Card Number 74-3674

Printed in Germany

Production: PRO EDIT GmbH, D-69126 Heidelberg
SPIN: 10551728 27/3136-5 4 3 2 1 0 – Printed on acid-free paper

Contents

Effects of Veratridine on Sodium Currents and Fluxes
By W. Ulbricht, Kiel, Germany
(With 7 Figures) 1

The Elucidation of Somatostatin Receptor Functions:
A Current View
By W. Meyerhof, Potsdam-Rehbrücke, Germany
(With 5 Figures and 3 Tables) 55

Cytokine-Mediated Hepatic Apoptosis
By M. Leist, F. Gantner, G. Künstle, and A. Wendel,
Konstanz, Germany
(With 6 Figures and 2 Tables) 109

Indexed in Current Contents

Effects of Veratridine on Sodium Currents and Fluxes

W. Ulbricht

Department of Physiology, University of Kiel, Olshausenstraße 40, D-24098 Kiel, Germany

Contents

1 Introduction 2
1.1 The Alkaloid 2
1.2 Early Experiments 2
2 Voltage Clamp Experiments 5
2.1 Slow Secondary Sodium Current 5
2.2 Activation of Modified Sodium Channels 6
2.3 Slow-Current Kinetics and Alkaloid Binding 8
2.4 The Pool of Free Veratridine Molecules 11
3 Single Channel Experiments 14
3.1 Natural Membranes 14
3.2 Artificial Membranes 16
4 Reduced Selectivity 17
5 Veratridine Binding and Its Modulation 19
5.1 Catterall's Neurotoxin Binding Sites 19
5.2 Experiments with Radiolabeled Toxins and Radioactive Isotopes 19
5.3 Electrophysiological Experiments with Activators 23
5.4 Remarks on Concentration-Effect Relationship 26
5.5 Block by Guanidinium Toxins 27
5.6 Block by Local Anesthetics 28
6 Temperature Effects 32
7 Modeling 35
7.1 Various Models 35
7.2 Computations 38
8 The Veratridine Binding Site 41
9 Summary and Conclusion 43
References 44

1 Introduction

1.1 The Alkaloid

Veratrum alkaloids are produced by lilaceous plants of the suborder Melanthaceae of which *Veratrum album*, the hellebore of Europe and northern Asia, *Veratrum viride*, the swamp hellebore or Indian poke of North America, and *Schoenocaulon officinale* of Central and South America are the best known. The latter yields the sabadilla seed which was used as an insecticide by Indians in pre-Columbian times (Crosby 1971). The alkaloid fraction of the seeds, often termed "veratrine," is a poorly defined mixture mostly of the ester alkaloids, veratridine, and cevadine and of the alkamine veracevine or its isomer cevine.

Sensible pharmacological research requires pure alkaloids. This was emphasized by Krayer (Krayer and Acheson 1946) who devoted decades of his working life to the study on veratrum alkaloids and who provided many investigators with pure compounds (Goldstein 1987). Nevertheless, veratrine continued to be used in numerous studies until pure alkaloids, especially veratridine, became commercially available in about 1970. It is interesting to note that since then the price of veratridine has risen more than 100-fold, for several reasons, such as booming demand (which will continue for at least another decade), scarcity of (wild) sabadilla seeds due to a lack of collectors, and improved purification. The latter is concerned particularly with the separation of veratridine from cevadine by high-performance liquid chromatography (Holan et al. 1984; Reed et al. 1986; Hare 1996).

1.2 Early Experiments

The earliest description of the action of veratrine on the neuromuscular system appeared about 130 years ago (Prévost 1866; von Bezold and Hirt 1867). For the next 90 years or so many experiments were carried out on the "veratrine response" of muscle, a twitch followed, after a relaxation, by a second slow rise and fall of tension. Its electrophysiological basis, a sizeable afterdepolarization following a spike potential, and giving rise to a series of spikes, was studied for decades (see summaries by Krayer and

Acheson 1946; Shanes 1958; Ulbricht 1969a). Experiments with the pure alkaloid veratridine on the membrane level made it clear that the afterpotential was caused by characteristic changes in the sodium permeability, in particular keeping channels open by preventing fast inactivation (Ulbricht and Flacke 1965; Ulbricht 1969a).

The idea that veratrine increases the stationary sodium permeability evolved gradually from the observed membrane depolarization and the concomitant Na^+-K^+ exchange (summarized by Fleckenstein 1955; Shanes 1958a,b) leading to the concept of "depolarizing agents" and "labilizers," antagonized by "stabilizers" such as local anesthetics and Ca^{2+}. This antagonism is dealt with in more detail in later sections. The connection to our present-day understanding was provided by Straub (1956), who showed that the veratridine-induced depolarization of desheathed bundles of myelinated frog nerve fibers requires Na^+ in the external medium. These findings were confirmed on continuously superfused single nerve fibers that permitted a much better temporal resolution (Ulbricht and Flacke 1965). However, a more accurate description could not be given until voltage clamp experiments on this preparation became available (Ulbricht 1965). Such electrophysiological studies, including those on single channels, continued to be carried out for another two decades, as described in Sects. 2 and 3.

The alkaloid acts from either side of the membrane (Meves 1966; Scruggs 1973); it modulates the Na^+ permeability of various excitable membranes, including that of nerve endings where it increases firing. In sensory endings this may initiate reflexes such as the famous Bezold-Jarisch reflex originating in the myocardium and leading to bradycardia via vagus branches (for a historical account see Krayer 1961). In presynaptic endings veratrum alkaloids cause massive release of transmitter, in most cases by the depolarization-induced increase in Ca^{2+} influx, as shown, for example, with potential-sensitive fluorescent dye in synaptosomes by Blaustein (1975; see also Blaustein and Goldring 1975; and the review of Minchin 1980); for this reason veratridine has been used as a pharmacological tool until today (see, e.g., Fontana and Blaustein 1993; Bouron and Reuter 1996).

Other secondary veratridine effects include increased Na^+-K^+ pump activity in rat myotubes due to increased Na^+ influx (Brodie and Sampson 1990) and the related increased cellular (or synaptosomal) respiration (see, e.g., Mata et al. 1980; Urenjak et al. 1991) or intracellular acidification of repetitively stimulated frog nerve fibers as protons increasingly flow

through Na^+ channels that are kept open (Khodorov et al. 1994). Increased Na^+ influx into cerebral cortex cells due to depolarization by veratridine and other means cause cell swelling (Lipton 1973; Churchwell et al. 1996). Such secondary effects, including membrane depolarization, are beyond the scope of this review, and therefore only some representative papers are described.

It may be mentioned here that veratridine is also reported to partially *block* Na^+ channels in jellyfish neurones which, however, are tetrodotoxin-insensitive and show other unusual pharmacological features (Spafford et al. 1996). In neuroblastoma cells veratridine-induced *block* of Ca^{2+} channels was observed at concentrations which stimulate Na^+ channels (Romey and Lazdunski 1982). Such suppression of Ca^{2+} current, however, at relatively large concentrations of veratridine, is also seen in frog muscle fibers (Nánási et al. 1994). Even the *block* of voltage-gated K^+ channels in T lymphocytes and neuroblastoma cells has been reported (Verheugen et al. 1994). The mechanism of such blocking action remains unclear.

Another application of veratridine emerged in the early 1970s with the first experiments with solubilized and purified Na^+ channels, identified by their tetrodotoxin binding (Henderson and Wang 1972; Benzer and Raftery 1973). Proof that functioning channels had indeed been isolated was eventually provided by incorporating them into phospholipid vesicles and measuring $^{22}Na^+$ fluxes. Such fluxes are considerably increased in the presence of veratridine or batrachotoxin, another lipid-soluble alkaloid from Colombian frogs. Although this review focuses on veratridine, results obtained with batrachotoxin (which nowadays outnumber those with veratridine) are sometimes considered. In this context the reader may consult more recent reviews on this neurotoxin (Khodorov 1985; Brown 1988; Moczydlowski and Schild 1994); other excellent reviews on neurotoxins in general have also been published (e.g., Strichartz et al. 1987; Hille 1992). The more easily available (although less effective) veratridine was widely used as a channel opener (see summaries by Villegas et al. 1988; Catterall 1992).

A different approach is to incorporate channels in lipid bilayers that allow current measurements through them under voltage control. However, recording conditions are not very favorable for following the short openings of unmodified Na^+ channels, and they are therefore usually treated with veratridine or batrachotoxin to lengthen their opening. It is also reported that these activating neurotoxins are a prerequisite for the insertion per se, although it has been shown that mild trypsin treatment

(which, as with veratridine, prevents fast inactivation) is sufficient if not superior (Shenkel et al. 1989). The chemical studies have yielded a wealth of information on interactions of veratridine with other neurotoxins. They led to the definition of at least five toxin binding sites on the Na^+ channel that are in part allosterically linked (Catterall 1992). These results are described in more detail and compared to the electrical measurements in Sect. 5.

2 Voltage Clamp Experiments

2.1 Slow Secondary Sodium Current

The frog node of Ranvier was the first preparation on which the pure alkaloid was tested under voltage clamp conditions (Ulbricht 1965, 1969a). After equilibration with 15 μM veratridine (pH 8.1, room temperature) a moderately depolarizing impulse of a few milliseconds elicits an almost normal current pattern *during* the pulse: the fast inward Na^+ current, I_{Na}, followed by the outward K^+ current, I_K. However on repolarization the fast inward current tail (time constant of about 0.1 ms) does not return fully to the prepulse level but subsides in a second phase very slowly (time constant τ_s of about 1 s; Fig. 1a). In a series of pulses these slow tails add up and after cessation of the train are followed by a large and equally slowly decaying current (Fig. 1b,c). Comparable results have been obtained on frog muscle fibers (Sutro 1986). If depolarizing pulses of several seconds duration are applied, the inward current following the fast transient I_{Na} continues to grow very slowly to a constant value with a time constant on the order of 1 s. This current continues flowing as long as the membrane is depolarized, i.e., it does not inactivate. Repolarization again induces a slow tail current (see Sect. 5.6, Fig. 6a, trace 1). This secondary slow current, whose amplitude is at best only about one-tenth that of the peak I_{Na} (Ulbricht 1969a), flows through modified Na^+ channels, as discussed below. It too is carried mostly by Na^+ ions and depends on the external Na^+ concentration in quantitative agreement with theoretical predictions. In Na-free solutions only outward currents are measured, and this effect takes place within a fraction of a second if, during a pulse, the solution is rapidly changed (Fig. 6b; Ulbricht and Stoye-Herzog 1984).

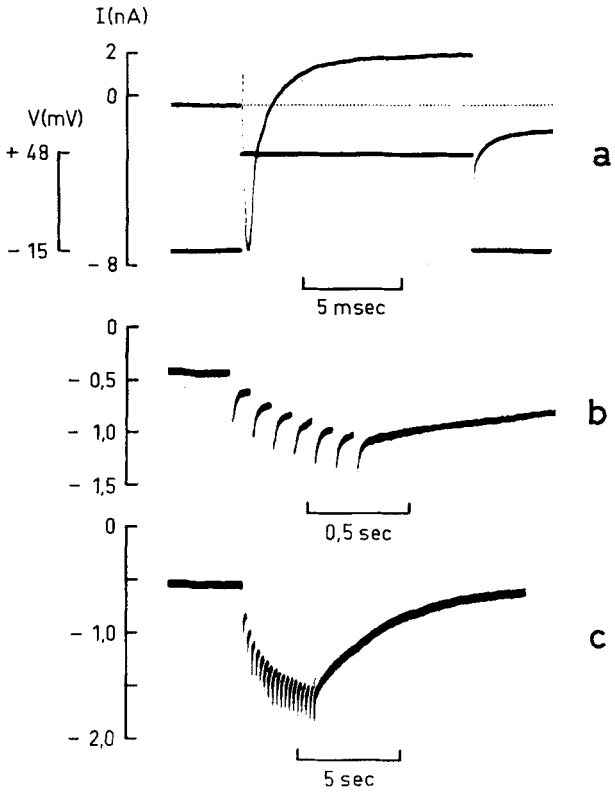

Fig. 1a–c. Additive after-effects of short depolarizing pulses in 15 μ*M* veratridine (pH 8.1; 21°C). **a** Time course of current during a 12-ms pulse (second trace) from V_H=–15 mV (holding potential) to V=48 mV, both potentials relative to the resting value (V=0 mV). Note that the pulse is followed by a fast and a much slower current tail whose start is shown. **b** After-effects of a 10-Hz train of seven 12-ms impulses from V_H=–6 mV to a value close to the reversal potential. **c** After-effects of a 4-Hz train of 18 pulses (12-ms, V_H=–20 mV, V=128 mV). The after-effects increase as V_H becomes more negative (compare **b** and **c**). (With permission from Ulbricht 1969a)

2.2
Activation of Modified Sodium Channels

The very slow kinetics of Na^+ current and the absence of inactivation are the most conspicuous effects of veratridine. However, modified channels may shut and reopen also on the millisecond scale, but under extreme

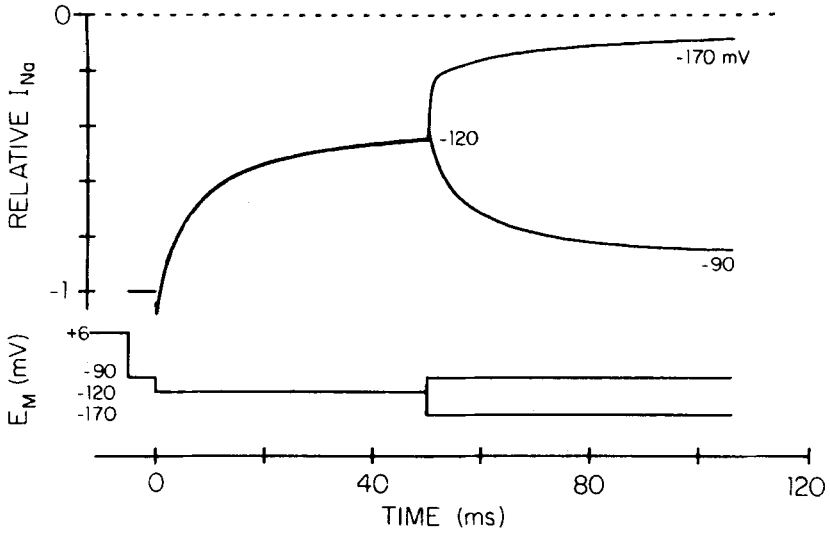

Fig. 2. Fast closing and reopening of Na^+ channels of frog muscle modified by veratridine following a series of conditioning pulses. The further pulse sequence was: +6 mV for 10 ms, -90 mV for 5 ms, -120 mV for 50 ms, and then either -170 or -90 mV. Note that stepping from -120 to -170 mV (or -90 mV) led to a double-exponential closing (or reopening) of channels. All traces are normalized to the initial I_{Na} at -90 mV. (With permission of Rockefeller University Press from Leibowitz et al. 1986)

hyperpolarization (Sutro 1986; Leibowitz et al. 1986; Rando 1989), and this feature therefore escaped attention in the early voltage clamp experiments (frog nerve: Ulbricht 1969a; squid axon: Scruggs 1979). The fast current changes were first studied in detail on frog muscle fibers. Figure 2 shows that the inward current immediately after a series of depolarizing impulses was almost abolished within about 1 ms on hyperpolarizing the membrane, for example, from -90 to -170 mV. Return to -90 mV caused the current to increase again more slowly in about 15 ms (at 9°C; Sutro 1986; not shown). At closer inspection these "fast" changes turned out to be biexponential, which must be taken into account on creating kinetic models (see below). The steady-state behavior of modified channels can be viewed as a ca. -90-mV shift of the activation gating, as compared to the peak current-potential curve of unmodified channels (Leibowitz et al. 1986). In frog nodes of Ranvier very similar phenomena were observed,

but the fast current changes illustrated by Fig. 2 were monoexponential (Rando 1989).

2.3 Slow-Current Kinetics and Alkaloid Binding

The modifications described in the previous section are thought to occur while veratridine is bound to the channel. The early experiments also attributed the *slow* current changes to the (much slowed) kinetics of channels to which veratridine is permanently bound. This interpretation served well under conditions in which the fast transient Na^+ current was negligible but could not satisfactorily explain why, after a short flow of early current, the slow component started at a higher level ("priming action"; Ulbricht 1969a). Later the following concept developed, mostly by analogy to results with other lipid soluble neurotoxins such as batrachotoxin (see Khodorov 1985, who also discusses extensively veratridine results) that bind to the same site (Catterall 1975b). Veratridine binds only to open channels and prevents their fast inactivation. The slowly developing current observed during long depolarizing pulses then reflects the rate of modification of channels previously inactivated that enter the conducting state. Since the latter event is fairly rare, the short supply of "precursor" determines the slow kinetics (Sutro 1986; Hille et al. 1987).

Such interpretation is best discussed by means of kinetic schemes as shown in detail in Sect. 7. Here it may suffice to introduce three states of unmodified sodium channels, resting (R), open (O), and inactivated (I) which are passed through (R–O–I) on depolarization, and their modified counterparts R*, O*, and I*, of which O* is permanently conducting and originating from O; for most cases O can be neglected because of its very short lifetime. The fast changes described by Fig. 2 are thought to be due to transitions between O* and R* whereas a very slow decrease in or inactivation of the maintained current, observed in frog muscle (Sutro 1986) but not in frog nerve (Ulbricht 1969a, Rando 1989) is attributed to an O*–I* transition. Rando (1989), in contrast postulates, for reasons discussed below, that the time course of the slow permeability is determined by a transition from an inactivated modified state I* to O*.

In agreement with the binding hypothesis it is observed that agents which suppress inactivation of Na^+ channels also enhance the veratridine action, obviously by increasing the probability of state O which in turn feeds O*. This is true for pronase (Scruggs and Narahashi 1982),

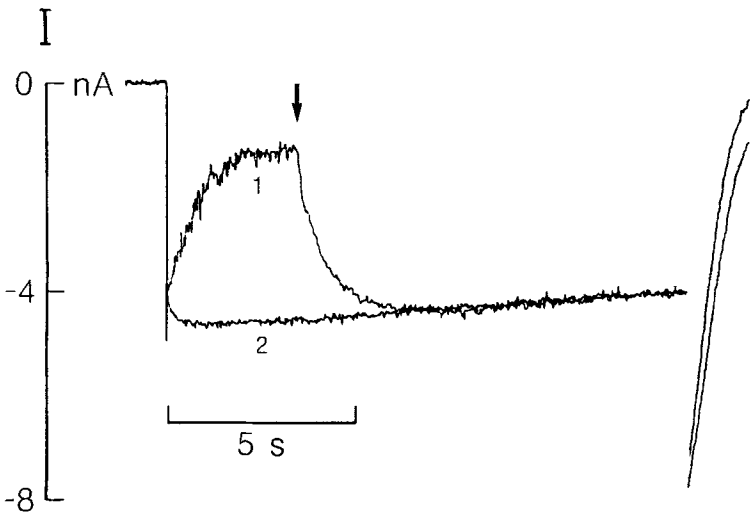

Fig. 3. Enhanced rate of veratridine action on the nodal membrane after pretreatment with chloramine-T. *Trace 1* shows, after the treatment, the slow and incomplete decay of Na^+ current following the peak (cutoff because of the slow time base) during the first 3 s of a 15-s depolarizing impulse. *Arrow*, 60 μM veratridine was applied leading to a fast increase in inward current with a time constant of 0.75 s. *Trace 2*, ca. 20 s later. In either case a large current tail was observed after the pulse. 18.2°C. (With permission from Ulbricht 1990)

chloramine-T, (Ulbricht and Stoye-Herzog 1984), *N*-bromoacetamide, *Leiurus quinquestriatus* toxin (LqTX; Sutro 1986), and *Anemonia sulcata* toxin II (ATX II; Ulbricht 1990). Pretreatment of a node of Ranvier with chloramine-T considerably accelerates the onset of veratridine action, as illustrated by Fig. 3. Trace 2 of this figure also shows that the persistent current starts at a much larger level and slightly declines during the 14-s pulse whereas without pretreatment the slow current sets in gradually with no signs of inactivation (see, e.g., Fig. 6 in Sect. 5.6). In cardiac cells the inactivation inhibitor BDF 9145 also increases the veratridine effect (Wang et al. 1990; Zong et al. 1992).

Other consequences of the binding hypothesis are as follows. During trains of depolarizing pulses the peak Na^+ current (corresponding to O) should decrease at the rate with which the tail current (O^*) increases. This has been found in frog muscle (Sutro 1986), neuroblastoma cells (Barnes and Hille 1988), and frog nerve in which, however, the reverse process,

recovering of peak Na^+ current, took clearly longer than the tail current to vanish (Rando 1989). The rate of modification by veratridine (VT, assumed to be due to a one-to-one alkaloid-channel reaction, $O+VT \rightarrow O^*$) should be linearly related to the free veratridine concentration, [VT]. In frog muscle this was confirmed by measuring initial rates of modification by applying a conditioning pulse to a rested fiber *equilibrated* in various veratridine concentrations (Leibowitz et al. 1986). Comparable results have been obtained in cardiac cells coactivated with BDF 9145 (Zong et al. 1992). In frog nerve the steady-state current increased with [VT] but not its rate of development (Rando 1989). Likewise, in the more classical approach of suddenly applying alkaloid to the depolarized frog nerve, the time constant (several seconds) of the slowly developing inward current depended only weakly on [VT] (Ulbricht 1972a). These results are presented in more detail below (Sect. 2.4).

If the slow current tail following a train of impulses is due to unbinding of veratridine it should be solely determined by the dissociation of veratridine leading to O^*-O and thus monoexponential and independent of alkaloid concentration. Monoexponential tails have indeed been observed in frog nodes of Ranvier (Ulbricht 1972a), frog muscle fibers (Leibowitz et al. 1986), neuronal sodium channels expressed in oocytes (Sigel 1987) and BDF 9145-treated cardiac cells (Zong et al. 1992). In these preparations (except in frog muscle) and in neuroblastoma cells (Yoshii and Narahashi 1984; Barnes and Hille 1988) the tail time constant decreased at more negative potentials. For the frog nerve this potential dependence is illustrated by the two-pulse experiment of Fig. 4 which shows a threefold faster time constant for repolarizations to the holding potential, V_H, than for V_H+38 mV. This has also been reported for snail neurones (Leicht et al. 1971a,b). Obviously it must be postulated that the dissociation is, directly or indirectly, potential dependent (see also Zong et al. 1992). Biphasic relaxation, mentioned above for the O^*–I^* transition in muscle, is also observed in neuroblastoma cells, where tails following long (but not short) trains of impulses show a biexponential decay (Barnes and Hille 1988), thus requiring an extended kinetic model. Such details and other problems with the binding hypothesis are discussed below and in Sect. 7. Incidentally, in snail neurones the veratridine-induced current is insensitive to tetrodotoxin but absent in Na-free solutions (Leicht et al. 1971a,b), in agreement with observations on unmodified Na^+ channels in this preparation (Kostyuk et al. 1977). Veratridine effects on other tetrodotoxin-insensitive channels are discussed in Sect. 5.2.

Fig. 4. Slow currents, I_s, in arbitrary units (*a.u.*), during a two-pulse experiment on a frog node of Ranvier. A first 6.3-s pulse to V=57 mV during which I_s increased with $\tau_{s,on}$=1.7 s was followed by a second pulse of 11.5 s duration (trace 2: 9.6 s) to various potentials: -10, 7, 14, and 28 mV for traces 1, 2, 3, and 4 with tail time constants, $\tau_{s,off}$, of 1.0, 2.0, 2.5, and 3.1 s, respectively; the tail amplitude decreased with the driving force on Na^+. The fast peak I_{Na} does not show at the slow time base. 60 μ*M* veratridine, 20.4°C; holding potential V_H=-10 mV, all potentials relative to the resting potential; I_s: 1 a.u.≈2.5 nA, set at I_s=0 for V_H. (Unpublished experiment of W. Ulbricht and M. Stoye-Herzog)

2.4 The Pool of Free Veratridine Molecules

Since the binding hypothesis assumes the channel modification to be due to de novo drug binding from a pool of free alkaloid molecules (Leibowitz et al. 1986), the location of such a pool is of particular interest. Pertinent points are: (a) the reactions to fast application and washout of veratridine, (b) reversibility, and (c) pH effects and related evidence.

The superfused node of Ranvier is particularly suited to fast perfusate changes. As mentioned above, when veratridine (4.5 or 45 μ*M* at pH 8.1) is suddenly applied to the moderately depolarized nodal membrane, an inward current develops exponentially, with a time constant, τ_{on} of 3.8 and 3.2 s, respectively. Early (after 6 s) washout of these concentrations causes the current to disappear exponentially, but unexpectedly with a time constant, τ_{off}, that depends on the previously applied [VT], 5.6 and 7.5 s, respectively. Longer applications are best monitored by measuring tail currents at the end of 2-s depolarizing pulses elicited every 5 s (see also

Sect. 5.3, Fig. 5). These yield two time constants during onset, τ_{on}, comparable to those measured during continuous depolarization, although the membrane is at rest 60% of the time between pulses. The second time constant, τ'_{on} is about ten times τ_{on}. For the offset time constants, τ_{off} and τ'_{off}, a similar relationship is found with τ'_{off} being independent of concentration. Interestingly, τ'_{on} is more clearly related to [VT] in the expected manner (Ulbricht 1972b). These results suggest that on application the alkaloid diffuses, in its uncharged lipid-soluble form, both into the myelin and through the membrane into the axoplasm from where it continues to feed the membrane during washout.

It remains, however, unclear why only the longer time constants behave as those of a reaction. Diffusion through the membrane and intracellular accumulation is also thought to account for the onset of veratridine action on cardiomyocytes, with a time constant of about 1 min (20°C; Zong et al. 1992). In crayfish giant axons most veratridine effects persist, but the maintained current at the holding potential between pulses during a train vanishes on washout (Warashina 1985). Only partial recovery is reported for externally applied alkaloid to squid giant axons (Ohta et al. 1973), but when this preparation is perfused internally, full reversibility is achieved, possibly because washing on either side of the membrane was feasible (Meves 1966). In this connection it is interesting to note that externally applied veratridine (100 μM at 5°C) slowly but markedly depolarizes non-perfused squid axons whereas depolarization is much less if at the same time the axons are internally perfused and thus washed with toxin-free solution (Seyama et al. 1988).

Reversibility is good only after short veratridine applications to the node of Ranvier, whereas recovery is only partial after prolonged treatment even though a first fast decline of the effect is always observed on washing. After a very short (1 s) application to depolarized nodes the slow inward current continues to rise for 1–2 s before it decreases again. Such delay on washing is clearly longer than that with which the effect sets in on addition of alkaloid (0.16 s) but is, at least qualitatively, imitated by diffusion through a plane sheet on applying a short ($<0.5\ Dt/l^2$) concentration "pulse" where l is the thickness of the sheet and D the diffusion constant, quantities which one can only roughly estimate (Ulbricht 1972a). At any rate the slow current is not expected to follow closely the drug concentration in the immediate vicinity of the receptor if the concentration changes at a rate comparable to or even faster than normal channels happen to open. This may well be the case. Indeed after treatment with chloramine-T

the onset of veratridine action on first application was about four times faster (see Fig. 3), with no conceivable change in diffusional access.

A different and earlier interpretation of these and related phenomena assumed a fast reaction of drug with channels of unspecified conformation, but a slow potential-dependent opening kinetics once drug was bound. Delayed offset could then result in a decreasing number of modified channels which, however, continued to open as the membrane stayed depolarized (Ulbricht 1972a). This early interpretation implied that resting channels of frog nerve can also be modified. This was deduced from equal effects of impulses that started only 15 s after veratridine application either during a long depolarizing impulse or to the resting membrane, where it often immediately caused a small inward current (see Ulbricht 1972b, Fig. 5). By the same token, τ_{on} during a long pulse or a series of shorter pulses was the same, as mentioned. Although these results may point to *some* channel modification at rest, they have been interpreted differently as veratridine binding afresh on opening channels by depolarizations (Sutro 1986). In frog muscle such resting current is absent (Leibowitz et al. 1986). Another experiment of possible relevance to the binding hypothesis shows that fast application of a strong veratridine solution *during* the current tail (elicited in a weak solution) does not at all change its time course, as if additional modification cannot be achieved when modified channels close (early interpretation; Ulbricht 1972a) or, less plausible, when they unbind alkaloid (binding hypothesis).

Additional evidence of the alkaloid pool and its accessibility has been obtained by studying pH effects. Veratridine is a weak base with pK_a=9.54 (in 155 m*M* NaCl at 25°C; McKinney et al. 1986), and increasing the pH by one unit therefore increases the fraction of uncharged molecules by a factor of ten. In cardiac myocytes equilibrated in 30 μ*M* veratridine at pH 7.3 and pulsed every 5 s, a rapid change to pH 8.3 leads to a considerable but relatively slow increase in tail currents comparable to a tenfold increase in $[VT]_o$ at pH 7.3. From such results and those on changes also in internal pH it was concluded that veratridine acts, in its protonated form, from inside the membrane to which it gains access by diffusing through the membrane in its uncharged form (Honerjäger et al. 1992). These sophisticated experiments have been interpreted to suggest that alkaloid dissociates exclusively into the intracellular space, excluding the extracellular space or the lipid environment of the Na^+ channel, favored by most other authors, to function as the alkaloid pool.

The importance of the intracellular space is supported by experiments with solutions of increased viscosity, η, to reduce the diffusion coefficient, D, of veratridine because of the Stokes-Einstein inverse relation of D and η. When applied to the intracellular, but not the extracellular, side of cardiomyocytes this leads to an increased tail time constant in approximate relation to the viscosity. Moreover, this result suggests that the decaying tail current is directly linked to a diffusion-controlled reaction; this is an independent argument for the binding hypothesis (Honerjäger et al. 1992). Unfortunately, comparable experiments have not been carried out on other preparations. Incidentally, in frog nerve cooling not only considerably slows the current tails, as expected for an unbinding reaction, but also reduces the current in a biphasic fashion, which is less easily explained (Ulbricht 1969b).

3 Single Channel Experiments

3.1 Natural Membranes

Even in solutions of maximally tolerated veratridine concentrations the current through modified channels is always only a fraction of that which unmodified channels can pass (Ulbricht 1969a). In frog muscle during a train of depolarizing pulses the decrease in peak Na^+ current and the increases in late current (just before the end of the impulse) and tail current can best be fitted taking the conductance, γ^*, of modified channels to be about one-third of γ of unmodified channels (Leibowitz et al. 1986). Comparable results have been obtained in single-channel measurements, however, on N18 (γ^*/γ=4 pS/16 pS=0.25; Barnes and Hille 1988) and N1E-115 neuroblastoma cells ($\gamma^*/\gamma \approx 0.5$; Yoshii and Narahashi 1984), ventricular myocytes of fetal rats ($\gamma^*/\gamma \approx 0.25$; Wang et al. 1990), adult rats γ^*=5 pS (Schreibmayer et al. 1989) vs γ=15 pS (Cachelin et al. 1983), and in the presence of the inactivation inhibitor S-DPI 201-106 ($\gamma^*/\gamma \approx 0.33$; Schreibmayer et al. 1989) and of guinea pigs with low and higher conductance ($\gamma^*/\gamma \approx 0.19$ and 0.48; Sunami et al. 1993). Veratridine also reduced γ of chick neuronal Na^+ channels expressed in *Xenopus* oocytes to ca. 25% (γ^*=5–6 pS, γ=21–25 pS, Sigel 1987). Embryonic cockroach neurones in culture that normally lack Na^+ channels reveal, in the presence of veratrid-

ine, such channels with at least two low conductance levels (Amar et al. 1991). Activation of other "silent" channels have been reported for inexcitable C_9 brain tumor cells (Romey et al. 1979), fibroblasts (Frelin et al. 1982), Schwann cells of squid axons (J. Villegas et al. 1976), glioma cells (Reiser and Hamprecht 1983), and other preparations. In most of these preparations certain polypeptide toxins (e.g., from sea anemones or scorpions) act synergistically, as in spiking cells, but in contrast are often less sensitive to tetrodotoxin (equilibrium constant of inhibition $K_i \approx 1$ μM in C_9 cells; Romey et al. 1979).

As expected from the macroscopic current, modified channels stay open for longer periods of time, although the preparations differ considerably in this respect. At least some of these differences may be due to the heavy filtering required because of the small amplitude of current through modified channels. Usually the long openings were interrupted by short closures, and hence termed "bursts" or "flicker." In connection with the idea that a channel must open before it can be modified by veratridine, particular interest is placed in records in which a normal-sized opening is followed by a long opening of reduced amplitude. This was indeed observed in N18 cells although not without ambiguity since patches with only one Na^+ channel could not be obtained (Barnes and Hille 1988). In this preparation unmodified channels had a mean open time of 0.25 ms whereas that of modified channels was 1.6 s. In most records of Na^+ channels (≥ 2 per patch) expressed in oocytes (Sigel 1987) normal openings preceded long openings of reduced conductance. The latter mostly persisted for several hundred milliseconds *after* a depolarizing pulse and are thus the substrate of tail currents. Interestingly, spontaneous modified openings could be observed at holding potentials more positive than -90 mV that were never preceded by normal openings.

Single-channel records of guinea pig cardiomyocytes in the presence of 50 μM veratridine (internally applied) show short events of normal conductance. As noted above, these records also demonstrate two types of events after modification that would require another bound state, O**, of intermediate conductance with a mean open time of 19 ms (E=–120 mV), rising to 86 ms at E=–10 mV. The analogous values for state O* were 4.5 and 16 ms, respectively (22°–25°C; Sunami et al. 1993). From the sequence of events the authors conclude that O** should connect with O but also with two more states, I** and R**. Interestingly, state O* proves to be more resistant to tetrodotoxin than O**, in contrast to observations in other preparations (see Sect. 5.5).

In cultured cardiac myocytes of fetal rats the low-conductance state during long-lasting depolarizations has a mean open time (bursts) of ca. 450 ms (20°C, 250 μM veratridine). In the presence of the coactivator BDF 9145, which induces long bursts of normal amplitude, the mean open time of the low-conductance bursts is independent of [VT] (0.3–5 μM), but increasing [VT] augments the number of such bursts at the expense of the normal-conductance ones (Wang et al. 1990). Analysis of the bursting behavior suggests that veratridine and BDF 9145 act allosterically and are synergistic, and that veratridine dominates the conductance during co-modification. Analysis also arrives at a forward rate constant for alkaloid binding in the presence of coactivator k_f=4.3×10^6 M^{-1} s^{-1} and the dissociation (backward) constant k_b=2.2 s^{-1} yielding K_d=k_b/k_f=0.51 μM (20°C, E=–30 mV).

3.2 Artificial Membranes

As mentioned above, experiments on Na^+ channels incorporated in planar lipid bilayers require measures to keep the channels open since, with the heavy filtering necessary (because of the unfavorable signal-to-noise ratio), normal short openings would not be detected. In most experiments veratridine or batrachotoxin is used as "agonist" with veratridine being considered a "partial agonist" and batrachotoxin a "full agonist." The reason is that the latter alkaloid keeps the channels open almost continuously on depolarization whereas in veratridine, even at maximal concentrations, the channels close part of the time. Also, γ_{max}, measured at saturating Na^+ concentrations, is about twice as high in the presence of batrachotoxin than of veratridine, independent of the channel origin as in rat skeletal muscle: 21 vs 10 pS (Garber and Miller 1987), rat brain: 30 vs 9 pS (Krueger et al. 1983; Corbett and Krueger 1989), and in another study 24 vs 10 pS (Cukierman 1991), eel electroplax: 25 vs 13 pS (Recio-Pinto et al. 1987) and lobster nerve: 16 vs 10 pS (Castillo et al. 1992). Veratridine-modified channels in *natural* membranes show lower conductances (see previous section), most probably because they have been determined at lower (natural) cation concentrations. In some preparations conductance sublevels are found in the presence of veratridine, for example, in eel electroplax (Duch et al. 1989); this may, however, result from unresolved rapid channel closings. Also, some rat brain channels modified by vera-

tridine or batrachotoxin have another lower conductance state (ca. 50%) which differs in its response to scorpion toxin (Corbett and Krueger 1990).

Mean open times of veratridine-modified electroplax channels increase on depolarization but vary considerably among preparations of the same kind, even if expressed as fractional open times, f_o. Thus in the rare case of one-channel patches the potential at which f_o=0.5 varied by 30 mV. In other cases the results are complicated since depolarization also increases the number of conducting channels (Duch et al. 1989). Membranes with single lobster nerve channels show closures on the order of milliseconds (fast process), seconds (slow process), and minutes, leading to fast and slow types of f_o that increased with depolarization and have different midpoint potentials of −122 and −95 mV, respectively. Due to closures lasting for several minutes the *overall* $f_o(E)$ is rather shallow, with a midpoint potential of −24 mV. The modified channels display a noisy (flickery) substate which is most prominent at positive potentials, and at $E > +30$ mV slow inactivation is observed (Castillo et al. 1992). Flickering states are also seen in inserted rat brain channels (Corbett and Krueger 1990). Other bilayer results concerning selectivity, coactivation by other toxins, and block are discussed below.

4
Reduced Selectivity

Modification by veratridine obviously involves profound structural changes which manifest themselves not only in large open times and reduced conductance but also in a reduction of selectivity, i.e., the capability to discriminate among permeating cations. The best way in which to study selectivity is to determine the potential, E_{rev}, at which the current through a modified channel reverses sign, if the cation concentration on either side of the membrane is known or predetermined as in bilayer experiments. To ensure that inserted channels with incorrect orientation are eliminated a high concentration of tetrodotoxin is added to one side of the membrane. In veratridine-modified channels of rat muscle relative permeabilities for Na^+:Li^+:K^+=1.0:0.91:0.34 are found whereas in batrachotoxin-modified channels these values, 1.0:0.91:0.11, are closer to those in unmodified channels (Garber and Miller 1987), i.e., 1.0:0.96:0.048 (frog muscle; Campbell 1976). Similar measurements on veratridine-modified rat brain sodium channels yield P_K/P_{Na}=0.42 (Cukierman 1991)

but 0.16 on eel electroplax channels (Duch et al. 1989). The different changes in selectivity caused by veratridine and batrachotoxin have been studied in detail and interpreted by a two-barrier pore model with higher energy barriers for veratridine than for batrachotoxin, symmetrical for the permeation of Na^+ and Li^+, but asymmetrical for K^+ (Garber 1988).

In preparations whose intracellular space is not accessible, permeability ratios can be determined from differences, ΔE_{rev}, of reversal potential on changing the external cation concentration. Thus in frog muscle fibers treated with veratridine $P_{NH4}/P_{Na}=0.67$ as compared to 0.11 in unmodified channels (Leibowitz et al. 1987). In frog nerve fibers treated with the alkaloid mixture veratrine $P_{Na}:P_{NH4}:P_K=1.0:0.61:0.29$ was determined (Naumov et al. 1979), compared with control values for this preparation of 1.0:0.16:0.086 (Hille 1972). At any rate in modified channels discrimination deteriorates. In modified rat muscle channels $\gamma_{Li}=0.34$ γ_{Na} (inserted in bilayer; Garber and Miller 1987) whereas in unmodified muscle channels $I_{li}\approx 0.8$ I_{Na} (frog; Campbell 1976). In normal channels of frog nerve $I_{Li}\approx 0.7$ I_{Na} (Hille 1972); modification may lead to a comparably drastic reduction of Li^+ conductance and thus be responsible for the reversible absence of veratridine-induced afterpotentials in Li^+-Ringer solution (see Ulbricht 1969a, Fig. 16). Similarly, in squid axons treated with veratridine the amplitude of slow tail current in Li^+ artificial seawater was only one-half of that in Na^+- artificial seawater (Scruggs 1979).

In neuroblastoma cells (N1E-115) selectivity of modified channels has been derived from influx measurements of radioisotopes $^{42}K^+$ and $^{86}Rb^+$ and of [^{14}C]guanidinium and [^{14}C]methylamine in relation to that of $^{22}Na^+$, which yielded for 10 μM veratridine 0.39, 0.12, 0.35, 0.06, respectively, as compared to Hille's (1971, 1972) permeability ratios for unmodified channels in frog nerve of 0.086, 0.012, 0.13, 0.07. Coactivation with 1 μM ATX II or 10 nM LqTX does not fundamentally change the relations (Frelin et al. 1981). Selectivity has also been determined from half-lives of cation equilibration of vesicles containing reconstituted Na^+ channels in the presence of veratridine whereby fluxes of isotopes $^{42}K^+$, $^{86}Rb^+$, and $^{137}Cs^+$ were compared with those of $^{22}Na^+$. The ratios were 0.83, 0.50, and 0.38, respectively, indicating reduced selectivity (Tanaka et al. 1983). Such flux results, however, cannot be compared directly with permeability ratios obtained from E_{rev} measurements.

5
Veratridine Binding and Its Modulation

5.1
Catterall's Neurotoxin Binding Sites

Extensive studies of chemical neurotoxin binding to Na^+ channels have led to the definition of five binding sites (see review by Catterall 1992), which have been supplemented by other authors. Site 1 binds the water-soluble guanidine derivatives tetrodotoxin and saxitoxin and one type of marine snail polypeptide toxins, μ-conotoxins. These toxins block Na^+ channels. Site 2 binds, in addition to veratridine, the other lipid-soluble alkaloids batrachotoxin (from arrow-poison frogs) and aconitine (from monk's hood) and the lipid-soluble, nonalkaloid grayanotoxins (from *Ericaceae* plants). These toxins keep Na^+ channels open to varying degrees. Site 3 binds polypeptide toxins from scorpions (α-toxins) and sea anemones; they slow inactivation and enhance the persistent activation of site-2 toxins interpreted as an allosteric interaction of the two sites. Site 4 binds a different kind of scorpion toxins (β-toxins) which shift the voltage dependence of activation. Site 5 binds lipid-soluble polyether brevetoxins and ciguatoxins (from red tide and deep sea dinoflagellates, respectively) which also shift the voltage dependence of activation, cause repetitive firing of nerves and inhibit inactivation; they enhance the action of site-2 and site-4 neurotoxins but do not influence the action of site-1 or site-3 toxins. Recently a sixth site has been added which, in vertebrate and invertebrate Na^+ channels, binds another conotoxin (from *Conus textile*), δTxVIA. However only in mollusks does binding cause an effect, slowing of inactivation, whereas in channels of other phyla (including insects) binding remains "silent" but veratridine has a negative allosteric effect on both "silent" and "effective" binding (Fainzilber et al. 1994; Shichor et al. 1996).

5.2
Experiments with Radiolabeled Toxins and Radioactive Isotopes

The experiments underlying the site definition involved either the binding of radiolabeled toxins or the displacement of such toxins. As for site-2 toxins the binding of [^{3}H]veratridine is unsatisfactory due to its comparatively low affinity and the high nonspecific binding to membrane lipids

(Balerna et al. 1975). This is true to varying extents for batrachotoxin, but after coactivation with site-3 scorpion toxin the equipotent labeled derivative [^{3}H]batrachotoxinin A 20-α-benzoate has proved to be a valuable tool to test site 2, for example, of rat brain synaptosomes depolarized by 135 m*M* K^+. Unlabeled site-2 neurotoxins displaced labeled batrachotoxin with a K_d=0.05, 7, and 1.2 μ*M* for batrachotoxin, veratridine, and aconitine, respectively (Catterall et al. 1981).

In many papers neurotoxin effects on cells, synaptosomes or lipid vesicles containing purified channels were studied by means of $^{22}Na^+$ uptake. Recently the intravesicular increase in Na^+ concentration has also been monitored with fluorescent indicators (Daniell 1992; Deri and Adma-Vizi 1993). The techniques employed in the $^{22}Na^+$ experiments, especially those of purification and insertion, are rather variable, as are the *quantitative* data whereas *qualitatively* most of the results agree, in particular the sequence of effectiveness as revealed by the displacement experiments. One must consider that the influx experiments are complicated since small cells or vesicles are soon swamped with label. To obtain true permeability values from influx measurements one should incubate cells in neurotoxin in the absence of an ionic gradient (high K^+, Na^+-free solution, at E=0 mV), determine the initial uptake at low $[Na^+]_o$ and keep the membrane potential, E, constant (Catterall 1977). At negative internal potential and $[^{22}Na^+]_i$ greater $[Na^+]_o$ the approach to equilibrium is effectively slowed, which improves the measurement of initial influx rates. To reach the same effect in reconstituted vesicles requires a different technique (for details see Tamkun et al. 1984). Note that authors differ in describing their results, with equilibrium dissociation constants, K_d, implying a known stoichiometry, or with the operational concentration, $K_{0.5}$, causing a half-maximum effect. If the meaning is clear, the authors' expressions are used. This also applies to the action of inhibitory drugs (K_i or IC_{50}).

In N18 neuroblastoma cells the activation of uptake yields K_d=80 μ*M* for veratridine and 0.4 μ*M* for batrachotoxin. The two neurotoxins also differ in the maximum uptake velocity with veratridine inducing only 34% of that by batrachotoxin, in agreement with the notion of partial and full agonists. The main reason may be differences in single-channel conductance and open times (see Sect. 3). $^{22}Na^+$ uptake induced by 1 μ*M* batrachotoxin is reduced by high concentrations (100 μ*M*) of veratridine, eventually to the level observed in veratridine alone, as one would expect of two ligands competing for site 2 (Catterall 1975a). Similar uptake results have been obtained with rat brain synaptosomes, yielding $K_{0.5}$ of 0.5, 13,

and 14 μ*M* for batrachotoxin, veratridine, and aconitine, respectively; the maximum uptake in the presence of veratridine or aconitine is 57%, or 19% of that in batrachotoxin (Tamkun and Catterall 1981). In mouse brain synaptosomes the respective $K_{0.5}$ values are 0.5, 34.5 and 19.6 μ*M* (Ghiasuddin and Soderlund 1984). Uptake into lipid vesicles containing electroplax Na^+ channels is activated by veratridine with $K_{0.5}$=18 μ*M* (Rosenberg et al. 1984); uptake through highly purified sodium channels (α-unit only) of this preparation has a K_d of 14 μ*M* (Duch and Levinson 1987).

Oddly, in synaptosomes of rainbow trout brain aconitine is clearly more potent than veratridine ($K_{0.5}$ of 7.7 vs 66 μ*M*) and maximum uptake, likewise, is 76% vs 29% of that in batrachotoxin (Stuart et al. 1987). Another deviating result has been reported for purified channels from rat brain, reconstituted into phosphatidylcholine vesicles where batrachotoxin activates a smaller fraction of channels than veratridine, and K_d for the latter is larger (30 μ*M*) than in native channels (Tamkun et al. 1984); a similarly high value ($K_{0.5}$=35 μ*M*) is observed with purified channels from rat sarcolemma (Weigele and Barchi 1982). In N18 cells neurotoxin-induced activation is inhibited by divalent cations, with Mn^{2+} being most effective and Sr^{2+} least effective. The inhibition constants for Ca^{2+} are 0.84 m*M* and 1.2 m*M* (veratridine- and batrachotoxin-dependent uptake; Catterall 1975a). In a rat brain preparation stimulated by veratridine 55 μ*M* Ca^{2+} has been shown to be sufficient for reducing uptake by one-half (Matthews et al. 1981). $^{22}Na^+$ uptake through several types of tetrodotoxin-sensitive channels activated by veratridine is also inhibited by Zn^{2+} and Cd^{2+} with a half-inhibitory concentration (IC_{50}) of ca. 2 and 5 m*M*, respectively, whereas the IC_{50} of tetrodotoxin-resistant channels, for example, from heart cells, is much lower: 50 μ*M* and 0.2 m*M* (Frelin et al. 1986).

$^{22}Na^+$ uptake into synaptosomes has also been used to study the potentiation of veratridine by site-3 toxins of a scorpion (LqTX) and the sea anemone *Anthopleura xanthogrammica* (AxTX). Thus on coactivation with 0.1 μ*M* LqTX or 1 μ*M* AxTX the veratridine concentration for half-activation drops approximately from 20 to 1 μ*M*; LqTX in the absence of veratridine increases uptake by ca. 60% and AxTX by only ca. 20% (Krueger and Blaustein 1980). Very similar results were obtained on this preparation by Tamkun and Catterall (1981) who found that 0.2 μ*M* LqTX decreases $K_{0.5}$ of batrachotoxin, veratridine, and aconitine to 0.1, 0.07, and 0.13, respectively, of the value without scorpion toxin; only the two latter toxins also increase the maximum uptake. Likewise, $^{22}Na^+$ uptake into vesicles from lobster leg nerves, modified by veratridine, is accelerated by

toxin II of a different sea anemone *Anemonia sulcata* (ATX II), of which 50 n*M* decreases $K_{0.5}$ from 20 to ca. 2 μ*M* veratridine whereas the maximum uptake is only slightly increased (Correa et al. 1987). Also, in cultured rat heart cells 300 n*M* ATX II enhances veratridine-induced $^{22}Na^+$ uptake, whose maximum value P_∞, normalized to that in batrachotoxin, increases from 0.23 to 0.76, whereas $K_{0.5}$ decreases from 17 to 6.5 μ*M* veratridine.

However the situation is complicated by the fact that ATX II binding is voltage dependent (see, e.g., Catterall 1980), and that its binding site seems to have two subclasses (Catterall and Coppersmith 1981). Veratridine-stimulated uptake into N1E-115 neuroblastoma cells yields $K_{0.5}$=330 μ*M*, which on addition of another anemone toxin, ATX V, is halved (Honerjäger et al. 1982). Uptake into N18 neuroblastoma cells has been studied in the presence of up to 200 μ*M* veratridine and up to 100 n*M* LqTX, which increases P_∞ from 0.08 to 0.56 with little change in $K_{0.5}$. This is typical of "poor activators" (partial agonists: veratridine and aconitine) in contrast to "good activators" (full agonists) such as batrachotoxin and grayanotoxin whose P_∞ remains maximal whereas $K_{0.5}$ is reduced to less than one-tenth (Catterall 1977). Similar results have been obtained with N1E-115 neuroblastoma cells in which veratridine and ATX II enhance uptake synergistically (Jacques et al. 1978). In fitting kinetic schemes to their data these authors postulated an additional silent-channel population which is, nevertheless, tetrodotoxin-sensitive. In three papers mentioned above (Catterall 1977; Krueger and Blaustein 1980; Tamkun and Catterall 1981) comparable kinetic models (assuming a homogeneous channel population) of allosteric interaction of site-2 and site-3 neurotoxins have been fitted to the numerous data. The models are discussed in Sect. 7. Incidentally, the effects of site-2 toxins and their enhancement by site-3 toxins are also observed in tetrodotoxin-insensitive ($K_i \geq 1$ μ*M*) channels such as the Na^+ channels of cultured cells of rat muscle (Lawrence and Catterall 1981), rat heart (Catterall and Coppersmith 1981), and of hamster lung fibroblasts (Frelin et al. 1982). In summary there is ample evidence from $^{22}Na^+$ uptake studies that site-3 toxins enhance the action of site-2 toxins.

Brevetoxins which bind to site 5, enhance the veratridine-activated $^{22}Na^+$ influx in neuroblastoma cells (Catterall and Risk 1981); they increase P_∞ rather than reduce $K_{0.5}$ (Catterall and Gainer 1985). However in veratridine-treated adrenal medullary cells the brevetoxin PbTx-3 increases both P_∞ and affinity, again determined by $^{22}Na^+$ influx measurements (Wada et al. 1994). Brevetoxins also enhance batrachotoxin binding, and this effect is very much potentiated by certain pyrethroids, for example,

RU 39568, which alone increases binding about 400-fold; addition of a high concentration of veratridine (300 μ*M*) reduces batrachotoxin binding to 1%, demonstrating the specific allosteric effect of this pyrethroid (Trainer et al. 1993; see also Sect. 8). Another site-5 neurotoxin, ciguatoxin, enhances $^{22}Na^{+}$ uptake in neuroblastoma cells and myoblasts in synergy with veratridine at even lower concentration (Bidard et al. 1984). A common feature of these site-5 toxins is that, by themselves, they do not increase fluxes.

5.3
Electrophysiological Experiments with Activators

Except for tetrodotoxin and saxitoxin (discussed below), neurotoxins binding to Catterall's original sites have been infrequently tested in electrophysiological experiments on veratridine-modified membranes. As mentioned above (Sect. 2.1), LqTX (50 n*M* on frog muscle; Sutro 1986) and ATX II (5 μ*M*, frog nerve; Ulbricht 1990) enhance the action of veratridine. The latter case is illustrated in Fig. 5 on a node of Ranvier subjected to a train of impulses which caused a current pattern as described for onset studies in Sect. 2.4. The enhancing effect of ATX II was fully reversible, and set in and recovered with a time course comparable to the ATX II effect in the absence of veratridine in this preparation (appearance of a persistent current component; Schmidtmayer et al. 1982). Current clamp experiments on frog nerve bundles show that the addition of LqTX shifts the relationship between membrane depolarization and veratridine concentration shifted to lower alkaloid concentrations by about one order of magnitude (Rando et al. 1986).

One other constituent of veratrine, cevadine, differs from veratridine by the acid moiety, angelic acid instead of veratric acid, which makes it less lipophilic. It causes sustained depolarizations, although less effectively than veratridine, in axons of squid, crayfish (Ohta et al. 1973), and lobster (Honerjäger 1973). It too seems to bind to site 2. It shows similar effects although the tail currents observed in its presence decline more than four times faster in rat ventricular myocytes pretreated with the coactivator BDF 9145, with 4 μ*M* cevadine inducing half-maximum tails (Honerjäger et al. 1992). In veratridine-cevadine mixtures at low concentrations (1 and 2 μ*M*) diphasic tails are seen with time constants corresponding to those in the single-alkaloid experiments. At saturating concentrations veratridine-cevadine mixtures yield results that strongly suggest competitive in-

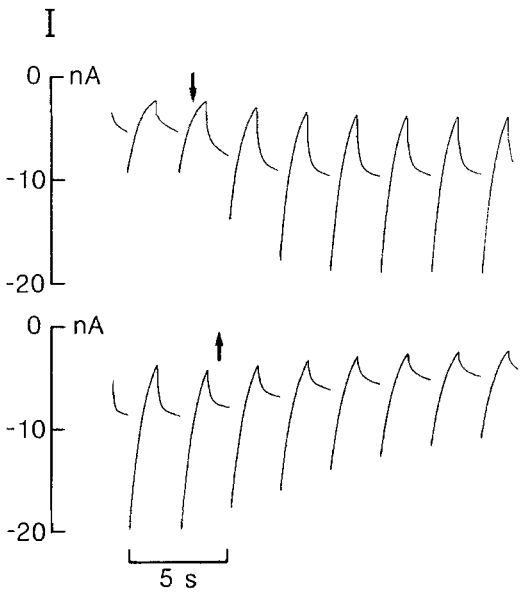

Fig. 5. ATX II reversibly increases the effect of veratridine (60 μ*M*) on a node of Ranvier as studied with a train of 1.1-s impulses elicited every 2.5 s. During each pulse (to V=40 mV) the inward current slowly increased, followed by a slowly decaying tail current on repolarization to the holding potential, V_H=–20 mV; both potentials relative to the resting potential. *Arrow, upper trace*, 5 μ*M* ATX II was added which considerably increased both inward currents during and after the impulse. The enhancing effect was fully reversible, as shown by the lower trace where after returning to veratridine alone (*arrow pointing up*) the tail current amplitude soon assumed its original value. Fitting exponentials to these amplitudes yielded onset and offset time constants of 2.1 and 8.7 s, respectively. 20.2°C. (With permission from Ulbricht 1990)

teraction. Strangely, in neuroblastoma cells uptake of $^{22}Na^+$ is not stimulated by cevadine, and in flux studies employing alkaloid mixtures therefore cevadine acts as a competitive inhibitor (Honerjäger et al. 1982). In frog muscle 100 μ*M* cevadine is about twice as efficacious at inducing tail currents as equimolar concentrations of veratridine. Analysis of the cevadine experiments suggests that channel complexes with this alkaloid have life times of 1.5 s in the open state and 6 s in the closed state (Leibowitz et al. 1987). This compares with 2.9 and 25 s, respectively, for veratridine (Leibowitz et al. 1986).

A better understanding of the activator-veratridine interaction would require single-channel experiments which, however, are scarce. In cultured cardiomyocytes a mixture of veratridine and ATX II induces, on steady depolarization, frequent openings to a low conductance substate (γ=4.6 pS). This can be seen in veratridine alone only after voltage jumps and for a short time whereas in ATX II alone a different substate (γ=11.5 pS) is observed. In the mixture the state of low conductance is often preceded by openings of the largest conductance (γ=14.2 pS; all values in $[Na^+]_o$=140 m*M*; Schreibmayer et al. 1989). Comparable (although not identical) results have been obtained with Na^+ channels of lobster leg nerve incorporated in lipid bilayers (Castillo et al. 1996). In this preparation ATX II induces two conductance states of 10 and 65 pS ($[Na^+]_o$=$[Na^+]_i$=500 m*M*) whereas in a mixture with veratridine or in the latter neurotoxin alone only the low-conductance state is observed. In this preparation open and closed times were studied in more detail, revealing rather complex patterns; the studies were, however, limited by the temporal resolution of bilayer experiments.

The results show that positive cooperativity between veratridine and ATX II, which is observed only at negative membrane potentials, results from channel gating but not from conductance changes. Interestingly, the midpoint potential of the overall fractional open time in the mixture is shifted markedly to more negative membrane potentials than in either veratridine or ATX II alone. In cultured cardiomyocytes the artificial coactivator S-DPI 201-106 (possibly binding to a site different from that for ATX II; Scholtysik et al. 1986) induces several conductance substates with that of 14 pS predominating (Schreibmayer et al. 1989). In a mixture with veratridine this conductance level becomes increasingly resolvable in addition to that typical of the neurotoxin effect (5 pS). In fetal cultured cardiomyocytes the coactivator BDF 9145 leads to long bursts of normal-level conductance which, on addition of the neurotoxin, alternate many times with the low-conductance bursts that represent the veratridine-bound state dominating in the mixture (Wang et al. 1990). This section thus demonstrates how complicated the electrical counterpart of the seemingly simpler flux results on comodified channels may be.

5.4
Remarks on Concentration-Effect Relationship

The veratridine concentrations employed in the various studies differ widely. Some such differences can be explained by the different temperatures at which the experiments are performed since the effects are much reduced in the cold (see Sect. 6). The alkaloid action also depends on pH, with, as mentioned above, more alkaline values increasing the effect. Another modulator may be the Ca^{2+} concentration, whose increase shifts the relationship between the permeability of modified channels and membrane potential to more positive potentials and leads to a reduced effect over a wider potential range (see Ulbricht 1969a, Fig. 31). This paper also discusses earlier hypotheses of a more direct veratridine-calcium interaction. More recently a direct competition between Ca^{2+} and veratridine has been postulated from $^{22}Na^+$ uptake studies, as mentioned above (Catterall 1975a). For frog muscle the apparent K_d of such veratridine-enhanced uptake is reported to decrease considerably when the membrane is depolarized by doubling $[K^+]_o$ from 2.5 to 5 m*M* (McKinney and Ratzlaff 1987).

$^{22}Na^+$ uptake measurements usually provide dose-response curves to test stoichiometry and to determine $K_{0.5}$ or even K_d values. However, seldom do these curves really saturate at high veratridine concentrations (in contrast to batrachotoxin curves), a prerequisite for the exact determination of K_d. Moreover, depending on the technique, they may not represent equilibrium results. The reported K_d values are between ca. 10 and 30 μ*M*. On the lower end are inhibitory constants, K_i, for the displacement of labeled batrachotoxin by veratridine: 7 μ*M* (rat brain synaptosomes, Catterall et al. 1981) and 8 μ*M* (guinea pig cortex preparation, Creveling et al. 1983). Clearly larger values stem from flux measurements on N18 neuroblastoma cells (K_d=80 μ*M*; Catterall 1975a) and various other cell lines with apparent K_d values higher than 100 μ*M*, attributed to higher Ca^{2+} concentrations than employed in other experiments (Stallcup 1977).

Dose-response curves from Na^+ *currents* are hard to determine since saturation seems to require damagingly high concentrations. However, if one assumes a one-to-one stoichiometry one can attempt to fit the equilibrium results at lower concentrations. Thus in frog nerve fibers the relative stationary permeability in 1.5, 4.5, 15, and 45 μ*M* veratridine is 1, 2.5, 4.0, and 4.9, which can be reasonably fitted with $K_d \approx 5$ μ*M* (at pH 8.1; Ulbricht 1972b). At pH 7.2 the average K_d derived from tail currents is 7.9 μ*M*

(M. Stoye-Herzog and W. Ulbricht, unpublished results). Much lower values are deduced from kinetics as $K_d=k_b/k_f$ with k_f the forward, k_b the backward rate constant of the veratridine-receptor reaction. For frog muscle $K_d=0.3\ s^{-1}/2\times10^6\ M^{-1}\ s^{-1}=0.15\ \mu M$ has been reported, an unusually low value for 7°C (Leibowitz et al. 1986). Another low value was determined for ventricular myocytes, however, coactivated with BDF 9145, as $K_d=0.51\ \mu M$ (see Sect. 3.1; Wang et al. 1990). This value compares with half-saturating veratridine concentrations of 3.5 and 60 μM as derived from tail currents, at the end of 50-ms pulses, in this preparation in the presence and absence of coactivator (Zong et al. 1992). A possible explanation for these discrepancies in K_d is presented in Sect. 7.2.

5.5 Block by Guanidinium Toxins

The site-1 toxins tetrodotoxin (TTX) and saxitoxin (STX) are highly potent blockers of most native voltage-gated sodium channels, effective at nanomolar concentrations. This is true also after modification by veratridine, as shown in $^{22}Na^+$ uptake experiments in vesicles of rat sarcolemma (K_i=5 nM STX, Barchi and Tanaka 1984) and rat brain (K_i=14 nM TTX, Tamkun et al. 1984), rat brain synaptosomes ($K_{0.5}$=5–10 nM STX, Krueger and Blaustein 1980; K_i=6 nM STX, Tamkun and Catterall 1981). Na^+ flux measurements on veratrinized frog muscle yield K_i=8 nM TTX, comparable to the figure observed in unmodified preparations (McKinney and Ratzlaff 1987). In frog nerve rates and extent of block by TTX, determined either from tail currents during periodic (ca. 0.2 Hz) depolarizing pulses (Ulbricht 1974) or during a single 14-s pulse (Ulbricht and Stoye-Herzog 1984; see also Sect. 5.6, Fig. 6b), were found to be very similar to those of unmodified channels in the same preparation: $k_f=3.4\times10^6\ M^{-1}\ s^{-1}$ and $k_b=1.14\times10^{-2}\ s^{-1}$ vs $2.9\times10^6\ M^{-1}\ s^{-1}$ and $1.4\times10^{-2}\ s^{-1}$ in alkaloid-free solutions at the same temperature (20°C; Schwarz et al. 1973).

Decreases in TTX sensitivity, however, are also reported. Thus the $^{22}Na^+$ uptake in a lobster nerve preparations requires higher blocking concentration ($K_{0.5}\approx27$ nM TTX) than in intact lobster nerves ($K_{0.5}$=3.1 nM of [^{3}H]TTX binding, R. Villegas et al. 1976). In N1E-115 neuroblastoma cells $K_{0.5}$ of block increases almost linearly from 5 nM to ca. 18 nM TTX on raising the veratridine concentration from 0 to 130 μM; coactivation with ATX II increases $K_{0.5}$ even further (Jacques et al. 1978).

Na^+ channels incorporated into lipid bilayers with the aid of veratridine show clear voltage-dependent block by TTX with K_d increasing with depolarization. This has been reported for electroplax channels (Duch et al. 1989) as well as those from lobster walking leg nerves. In both preparations batrachotoxin-modified channels are also blocked in a potential-dependent fashion (Levinson et al. 1986; Castillo et al. 1992). Comparable results have been obtained with other preparations (for an extensive discussion see Moczydlowski and Schild 1994). Block of unmodified neuronal Na^+ channels is not or is only little affected by membrane potential. Thus in frog nodes of Ranvier shifts of holding potential between –50 and –90 mV does not influence block by TTX (Ulbricht and Wagner 1975) nor is block by STX affected by a change in test pulse frequency from 1 to 10 Hz (Wagner and Ulbricht 1976). However, hyperpolarizing the membrane by 40–50 mV between pulses (0.8 Hz) intensifies block by both TTX and STX during the trains of pulses (Lönnendonker 1989). Other authors report no such use dependence of STX block in Ranvier nodes unless the membrane is pretreated with batrachotoxin, possibly because STX binding to (maintained) open channels is voltage dependent (Rando and Strichartz 1986), as has been suggested for TTX binding to modified brain Na^+ channels (Wang and Wang 1994). A more detailed hypothesis of state-dependent toxin affinity of *unmodified* channels is presented by Lönnendonker (1989); an extended interpretation involving external cation concentrations is found in Salgado et al. (1986) and Lönnendonker (1991).

Closures of veratridine-modified channels last much longer than events of blocking by TTX or STX. Therefore direct measurements of blocking kinetics in single channels require either a shorter average block time or a lengthening of channel openings. The former is achieved by using the low-affinity STX derivative C1 (21-sulfo-11-α-hydroxysaxitoxin) of 100-ms block time on muscle Na^+ channels inserted in bilayers (Garber and Miller 1987). The latter is achieved by using ordinary TTX on cultured cardiac cells treated with the veratrum alkaloid, germitrine (Dugas et al. 1989).

5.6 Block by Local Anesthetics

Sodium channels modified by veratridine are blocked by local anesthetics, but the mechanism seems to differ from that by TTX. The agents dealt with here are "local anesthetics" in the broadest sense, including antiarrhyth-

mics, anticonvulsants, etc. Straub (1956) reported that the veratridine-induced (7.5 μM) depolarization of frog nerve bundles can be fully counteracted by cocaine (ca. 2.9 mM). This is compatible with the observation in this preparation that lidocaine shifts the dose-response curve, membrane depolarization as a function of veratridine concentration, to higher alkaloid values with $K_i \approx 100$ μM anesthetic (Rando et al. 1986). This K_i value lies, for unmodified nodal channels, between that for the resting and that for the depolarized (inactivated) membrane, 150 and 30 μM lidocaine, respectively. Voltage clamp experiments on single frog fibers show that the antiarrhythmic *N*-propyl ajmaline preferentially blocked channels kept open by veratridine (Khodorov and Zaborovskaya 1983). Likewise in Purkinje fibers the antiarrhythmic agent R56865 blocked the veratridine-induced noninactivating Na^+ current more effectively than the peak current (Verdonck et al. 1991).

In single nodes of Ranvier the effect of benzocaine on the veratridine-induced persistent current has been studied in more detail. The steady-state current through channels modified by 60 μM veratridine, measured at the end of 14-s depolarizing impulses, are reduced to 69%, 30%, and 10% in the presence of 0.025, 0.25, and 1 mM benzocaine, respectively (Ulbricht and Stoye-Herzog 1984). This reduction is clearly larger than that of peak I_{Na} in unmodified channels, which is only to 91%, 73%, and 47% in these respective concentrations. These values were obtained with short test pulses following 30-ms hyperpolarizing prepulses to abolish inactivation (Meeder and Ulbricht 1987). When, however, the prepulses are omitted (leading to about 20% inactivation), the apparent K_i decreases to less than one-quarter (Schmidtmayer and Ulbricht 1980), supporting the hypothesis that inactivated channels bind local anesthetics with higher affinity.

More interestingly, after veratridine treatment the onset of benzocaine block during 14-s impulses is very slow, as illustrated in Fig. 6a with τ_{on} of several seconds although access to the membrane, for example, for Na^+-free solution, is unimpeded (Fig. 6b). In contrast, in unmodified fibers (Rimmel et al. 1978) and during long pulses applied to channels kept open by chloramine-T treatment the onset rate is much faster (half time < 100 ms; Ulbricht and Stoye-Herzog 1984) and appears to be limited by the speed of solution change. Strangely, the offset time constant, τ_{off}, is shorter than τ_{on}, and the latter depends little on benzocaine concentration. When benzocaine is added to the veratridine solution during a 0.4-Hz train of 1.1-s depolarizing pulses, the amplitude of the ensuing tails soon reaches a new reduced stationary value, with a time constant that is clearly

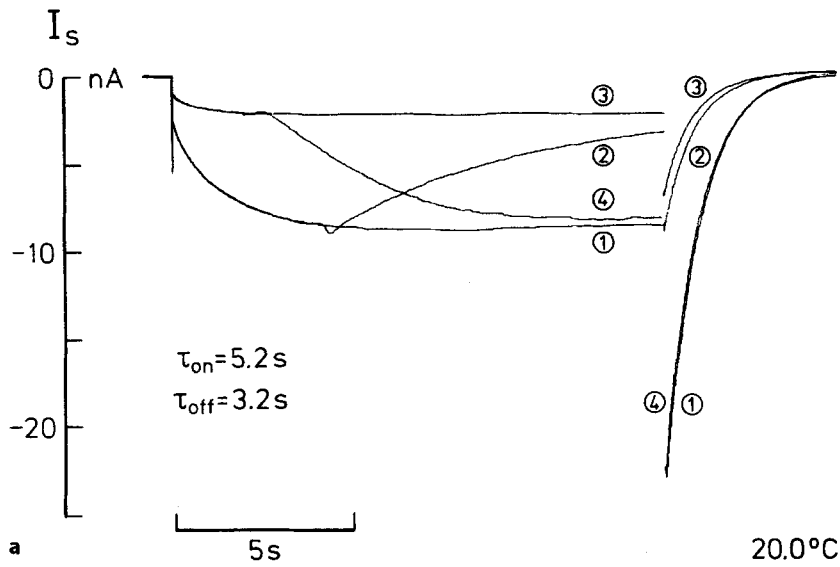
Is
0
nA
-10
-20
τon=5.2s
τoff=3.2s
5s
20.0°C
a

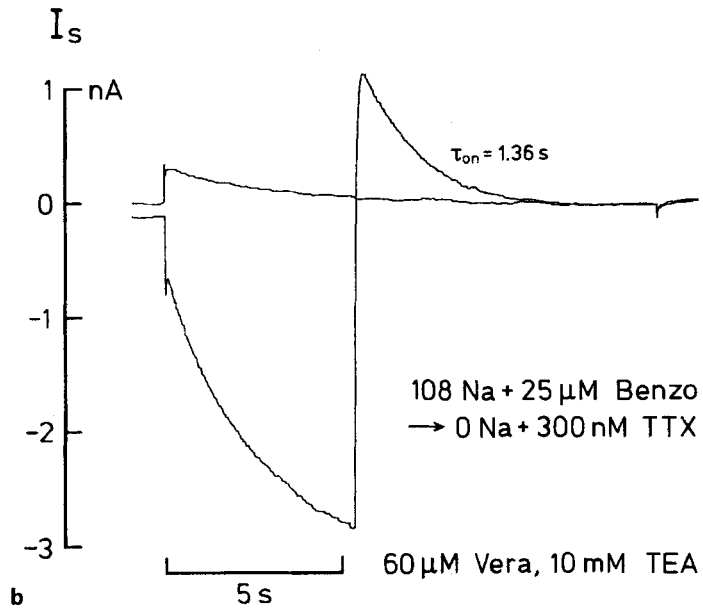
Is
1
nA
0
-1
-2
-3
τon = 1.36 s
108 Na + 25 µM Benzo
→ 0 Na + 300 nM TTX
60 µM Vera, 10 mM TEA
5 s
b

shorter than that obtained at the same potential and concentration during long pulses. It seems that repeated returns to the resting potential enhances the block. Applying benzocaine 1–2 s before the start of the long pulse greatly reduces the persistent current right from the beginning. Also, onset is further slowed on cooling by only a few degrees; this is not seen in unmodified channels but is typical of the veratridine-induced current (see below). These facts suggest that a channel modified by veratridine cannot be blocked by local anesthetics (and vice versa), and that the observed current decrease is determined by the rate at which channels become unmodified. It should be mentioned in passing that block of modified channels by *n*-pentanol is also slow (τ_{on}=3.7 s; 10 m*M*) whereas peak I_{Na} of unmodified channels is blocked much more rapidly (Ulbricht and Stoye-Herzog 1984).

The veratridine-induced $^{22}Na^+$ uptake into frog muscle is inhibited by the antiepileptic drug 5,5'-diphenylhydantoin (McKinney 1985). Uptake into neuroblastoma cells is reduced by yohimbine, a use-dependent Na^+ channel blocker (Huang et al. 1978) or by lidocaine (and other antiarrhythmics) in a manner suggesting that these blocking agents are allosteric inhibitors acting at a site separate from that for veratridine (Catterall 1981). The latter study introduced the inhibition by antiarrhythmics into an allosteric model of neurotoxin action (Catterall 1977) to explain why these inhibitors exert mixed effects on the partial agonist veratridine (both IC_{50}, the apparent dissociation constant, and P_∞, the maximum response, are affected) whereas in the presence of the full agonist batracho-

Fig. 6a,b. Effect of the blocking agent benzocaine (**a**) and of tetrodotoxin in Na^+-free solution (**b**) in the presence of 60 μ*M* veratridine during 14-s depolarizing pulses. **a** *Trace 1*, after a short transient I_{Na} (not fully recorded at the slow time base), the slowly increasing (time constant 1.19 s) noninactivating inward current is followed by a large, slowly decaying tail current (time constant 0.94 s). During a second run (*trace 2*) 0.25 m*M* benzocaine is added 4.3 s after the start of the pulse leading to slow current decrease (τ_{on}=5.2 s) followed by a much reduced tail current of unchanged time course. After equilibration in the veratridine-benzocaine solution (*trace 3*) benzocaine washout was started after 2.5 s (*trace 4*) on which the inward current during the pulse recovered (τ_{off}=3.2 s) as did the tail current. 20°C. **b** In the presence of veratridine+25 μ*M* benzocaine the Na^+ concentration is suddenly changed 5 s after the start of the impulse from 108 to 0 m*M*+300 n*M* tetrodotoxin (*trace 1*), which resulted in an immediate current reversal (Na^+ effect) followed by a slow decline (τ_{on}=1.36 s, tetrodotoxin effect). *Trace 2*, recorded in the tetrodotoxin solution. A different fiber at 19.3 °C. (With permission from Ulbricht and Stoye-Herzog 1984)

toxin only IC_{50} is affected. A similar extended model was presented by Rando et al. (1986) to explain the different actions on membrane potential of the two neurotoxins and their interactions with local anesthetics.

6 Temperature Effects

More than 110 years ago Brunton and Cash (1883) reported that cooling reduces the action of veratrine on frog muscle. Comparable observations, first on mechanical responses, later with potential measurements, were made in the following decades (see quotations in Ulbricht 1969b). In frog nerve fibers the influence of temperature on veratridine effects has been studied in detail both in the current and voltage clamp (Ulbricht 1969b). The main results are that cooling (a) increases the time constant of the onset of this current on depolarization and of the slow tail current on repolarization (tail: Q_{10} of 3.9 between 8° and 23°C) and (b) remarkably reduces the alkaloid-induced steady I_{Na} during long depolarizing pulses, most conveniently obtained from the amplitude of the following tail (Q_{10} of 3.3 between 8° and 22°C). The large effect on steady-state currents after equilibration at a given temperature differ clearly from effects on fast temperature changes (achieved by rapid changes of the superfusate) as illustrated by Fig. 7. This figure shows how sudden temperature changes affect the subsiding tail current. Short (ca. 1 s) changes from 20° to 10°C and back (upper half, two "cold pulses") lead to an immediate current reduction followed by a slowed decay during the "cold pulse"; rewarming causes a sudden current increase and a resumed faster decay. The lower half of Fig. 7 shows that three "warm pulses" to 20°C superimposed on a steady superfusion at 10°C yield the reciprocal effects. Interestingly, if the temperature steps are taken at face value, one arrives at $Q_{10} \approx 2$ for the step changes in current; this value may be a lower limit but is clearly smaller than that expected from the behavior of tail current amplitudes after equilibration (ca. −5 nA vs ca. −1 nA in this figure). Incidentally, Khodorov and Zabarovskaya (1983) were able to work on frog nerve with 300 μM veratridine, however, at 14°C; at room temperature this concentration would soon destroy the nodal membrane.

The current clamp experiments of this series show that when the membrane is depolarized by 15 μM veratridine at room temperature (pH 8.1; about 50 mV), cooling leads to a slow but reversible repolarization (or

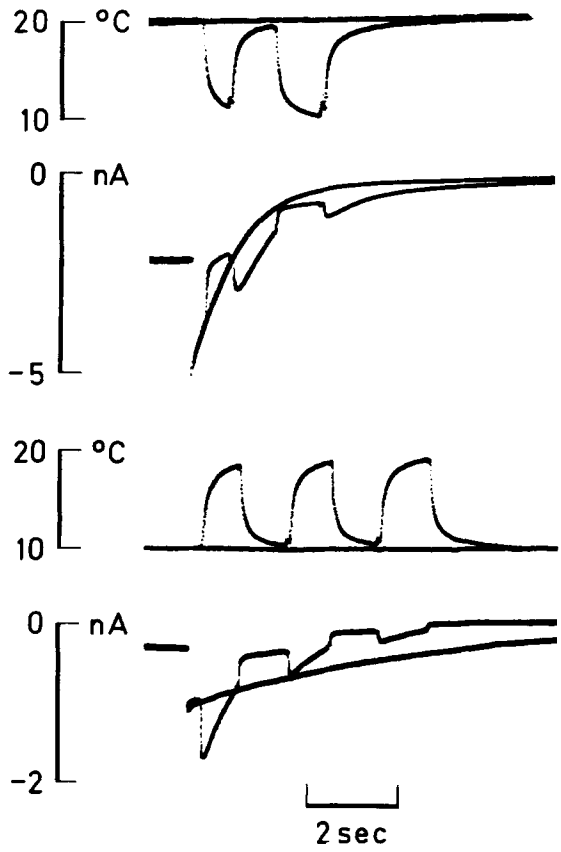

Fig. 7. Effects of fast temperature changes during tail currents upon repolarization to V=0 (resting potential) following 6 s at V=30 mV. Superimposed records at constant temperature (*above*, 20°C; *below*, 10°C) and during short (ca. 1-s) temperature changes (*above*, two "cold pulses" to 10°C; *below*, three "warm pulses" to 20°C). The temperature in the vicinity of the node of Ranvier (10 mm upstream at continuous superfusion) was recorded with a small thermocouple of limited temporal response; the true temperature step achieved by a fast change of perfusates and estimated to be completed within 0.1 s, induced step changes in current and immediate changes in the time constants of tails. At constant temperatures the time constants of tail currents were 0.9 s (20°C) and 3.8 s (10°C). (With permission from Ulbricht 1969b)

even hyperpolarization), the extent of which depends on temperature (range between 8° and 24°C tested), but the responses of individual preparations differ considerably. Obviously the veratridine-induced depolarization, which is a secondary phenomenon (Ulbricht 1969a), is less suitable for studying the temperature effect. The effect of temperature has also been observed in crab giant axons, in which hardly any effect is found on membrane potential below 8°C (Romey at al. 1980). The interpretation of this postulated that the Na^+ channel exists in two thermodynamically stable states above 20°C and below 8°C, and that only the former is sensitive to veratridine. In frog nerve there is little evidence of two such states since the tail time constant increases on cooling, without a break (Ulbricht 1969b). In squid giant axons the veratridine-induced (10–300 μM) depolarization is clearly reduced on cooling from 21° to 5°C. The apparent permeability derived from ^{22}Na efflux measurements in 30, 100, and 300 μM is maximal in 100 μM at 21°C; at 5°C it is 30% in this concentration but less than that in 30 or 300 μM (Siem-Fung and Sevcik 1983). This strange behavior remains unexplained.

If the slow increase and decrease in I_{Na} during and after a long depolarizing pulse ($Q_{10}>3$; Ulbricht 1969b) reflects the binding and unbinding of veratridine (Sutro 1986), the drastic reduction in steady-state current on cooling is then due to an increase in the equilibrium dissociation constant, K_d. In the simplest case, $K_d=k_b/k_f$, the ratio of backward to forward rate constants, an increase in K_d would require the rates of onset and offset to be affected much differently by temperature, which was not observed. Rather, it appears that equilibration in the cold drastically reduces the veratridine concentration in the immediate vicinity of the binding site or reduces the number of channels that can be opened (see also Romey et al. 1980), a differentiation that clearly would require single-channel experiments. At any rate such processes could involve rearrangements in the membrane lipids which would explain why equilibration takes minutes whereas I_{Na} kinetics responds within a fraction of seconds (see Fig. 7). The next section shows that K_d can be an apparent constant depending on the rate of inactivation; as an explanation, however, this would help very little as it requires another, much slower effect of temperature on inactivation.

Influx of $^{22}Na^+$ through purified Na^+ channels reconstituted in phophatidylcholine vesicles has been found to depend markedly on temperature when the channels are stimulated by veratridine (500 μM, 10°–36°C). Arrhenius plots of initial rates of $^{22}Na^+$ uptake are linear and yield an activation energy of 23.6 kcal/mol (98.8 kJ/mol). Uptake of $^{86}Rb^+$ (which is

slower and hence more easily monitored) has been studied both through veratridine-activated and batrachotoxin-activated (5 μM) channels with very different activation energies of 31.0 and 7.6 kcal/mol (129.8 and 31.8 kJ/mol), corresponding to Q_{10} values greater than 3.0 and approx. 1.8, respectively (Tanaka at al. 1983). These authors, considering the much lower rates of uptake in the presence of veratridine than of batrachotoxin, hypothesize that with the former alkaloid the rate-limiting step is the channel opening rather than permeation. Indeed the conductance of single batrachotoxin-modified Na^+ channels of squid axons changes with a Q_{10} of only 1.53 (at E=–60 mV; Correa et al. 1991), a lower value than the $Q_{10}\approx 2$ derived from step changes in the veratridine-modified nodal membrane, as mentioned above (Ulbricht 1969b). Although the squid study was carried out at 5°C, batrachotoxin was applied at 15°C to enhance modification which, interestingly, remained after recooling.

7 Modeling

7.1 Various Models

The diverse effects observed in veratridine-modified Na^+ channels gave rise to several kinetic models connecting channel states with and without bound alkaloid. The simplest or most general kinetic scheme, based on the allosteric model of Monod et al. (1965) and applied to flux measurements was presented by Catterall (1977) to deal with the interaction of site-3 neurotoxins (e.g., α-scorpion toxins) with site-2 toxins such as veratridine or batrachotoxin. In essence the model distinguishes only between an active and an inactive state whose distribution is governed by the allosteric constant. To these states site-2 toxin binds with different affinities whereas the effect of site-3 toxin is taken into account by a change of the allosteric constant (see also Tamkun and Catterall 1981). Krueger and Blaustein (1980) added a closed state R (resting) and identified the active state with an open state O and another closed, inactivated (in the sense of electrophysiology) state I. The activator, A, (e.g., veratridine) binds both to O and to I, again, with different affinities, to yield O* and I* (Scheme 1).

Note that $K_4/K_3=K_r$ determines the preference of A for the open state. Krueger and Blaustein (1980) have fit their flux results on synaptosomes

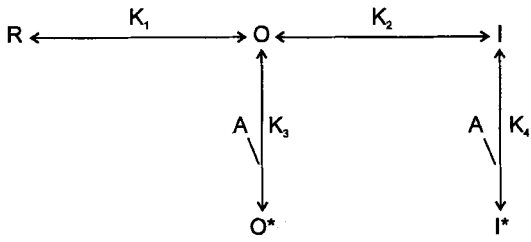

(1)

with the full agonist batrachotoxin with $K_r \geq 10^4$ vs 600 for the partial agonist veratridine. Site-3 toxins increase K_2 thus keeping channels open in state O at the expense of I. In this model the membrane depolarization decreases K_1 and K_2 as channels move from R to O and I; it allows a satisfactory fit of the results described in Sect. 5.2. In synaptosomes (but not in neuroblastoma cells; Catterall 1977) there was a clear effect of site-3 scorpion toxin in the absence of A.

Scheme 1 was developed to fit equilibrium results obtained with fluxes. Description of the electrophysiological results (many of which are kinetic and of a higher temporal resolution) requires rate constants of the transitions between states, for example, obtained by single-channel analysis. Such analysis has been carried out on cultured ventricular myocytes and led to the kinetic Scheme 2 where O' stands for channels kept open by the coactivator BDF 9145, a state with much increased affinity for veratridine so that the doubly bound state O'* predominates over O* with possible transitions between these states as BDF dissociates and reassociates. O' can be distinguished during bursts by its current amplitude as compared with the small (one-quarter) amplitude of veratridine-associated states (Wang et al. 1990; Scheme 2).

Because of the low veratridine concentration necessary in the presence of coactivator the O–O* transition can be neglected whereas the O'*–O* equilibrium on depolarization (E=–30 mV) is determined by $K_d = 2.2\ s^{-1}/4.3 \times 10^6\ M^{-1}\ s^{-1} = 0.5\ \mu M$. Bursts are terminated by steps O*–O or O'–O. Further considerations and computations are based on the more detailed Scheme 3.

Some of the constants of Scheme 1 can be immediately identified such as $K_1 = k_{or}/k_{ro}$, $K_2 = k_{io}/k_{oi}$ (where k_{io} may contain the site-3 toxin concentration), $K_3 = k_{-Vo}/k_{+Vo}$, $K_4 = k_{-Vi}/k_{+Vi}$ (where k_{+Vo} and k_{+Vi} contain the concentration of the agonist veratridine). Additionally introduced are the R–R*, O*–R* and I*–R* transitions; k_{+Vr} again contains the veratridine concentration.

Sutro's (1986) original kinetic scheme (Scheme 4) as applied to frog muscle is simpler as it does not directly assign rate constants to the state transitions. The observed fast decrease in current through modified channels and reincrease on return to the normal resting potential are interpreted as transition between O* and R* whereby the biexponential time course would actually require two modified open states, but could also be due to other mechanisms. The biexponential tails following long trains of depolarizing pulses in neuroblastoma cells (Barnes and Hille 1988) are also not easily accounted for by such a scheme. In frog muscle the secondary decrease in tail currents during high-frequency trains of impulses is interpreted as a slow inactivation process due to population of the I* pool. Leibowitz et al. (1986) analyzed use-dependent veratrinization during a train of 10-ms impulses by comparing the time courses of peak current decrease and increases in "late" current after 10 ms and the following tail current. For the sake of a good description allowance had to be made for

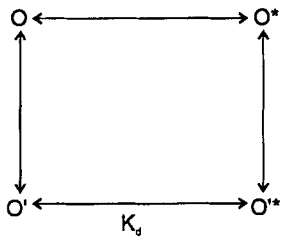

(2)

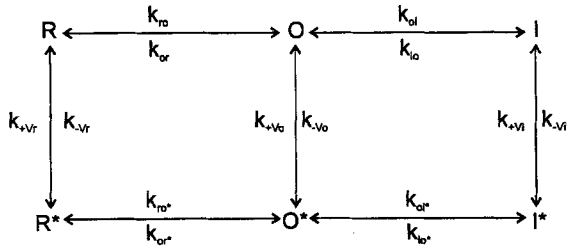

(3)

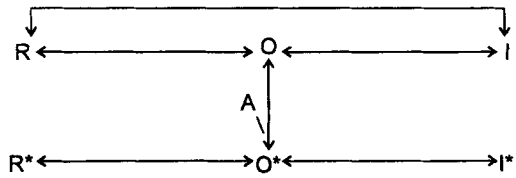

(4)

an O*–I*–N transition, where N stands for normal, unmodified channels in all possible states (i.e., R, O, and I), a feature not included in Scheme 3.

In complementary experiments on frog nerve fibers Rando (1989) studied the recovery of peak current and the decrease in the "late" current *after* a series of impulses. This process was clearly faster (complete within 20 s) than the former, which developed in two phases. This led to the interpretation that the peak current recovering later than 20 s must flow through channels after unbinding of veratridine from modified nonconducting channels, i.e., in the I* state, since modified "resting" channels would be conducting at the holding potential (see Sect. 2.2). Rando (1989) emphasizes the special nature of I* in this context (being favored by more negative potentials); he proposes that the slow current tails on repolarization are caused by a very slow O*–I* transition and not by the dissociation of veratridine from the channel. The slowly developing modified current during depolarizations is thought to reflect the opposite I*-O* process.

Still another kinetic scheme has been proposed by Gola et al. (1982) to describe phenomena (mostly observed in the current clamp) in veratridine-treated snail neurones: O* additionally connects I, and O*–I–R is the exclusive route on repolarization. R* is absent, but O*–I* is potential independent and accounts for the very slow inactivation observed during maintained depolarizations. Veratridine concentration does not directly enter, leaving the model rather vague for further computations. In particular one would like to test hypotheses of electrical phenomena such as slow current changes during and following long depolarizing pulses, kinetics of block by local anesthetics, etc. The following section presents pertinent computational attempts to fit the frog nerve results.

7.2 Computations

A crucial test of models is whether they describe quantitatively, in addition to the fast changes during trains of short impulses, the above slow current changes (τ_s=1–2 s) in terms of veratridine binding/unbinding to open channels. The simplest approach would be with a model of unmodified channel states R–O–I in which only O connects to the modified open state O*, i.e., Scheme 1 without the I–I* transition. Experiments on frog muscle (Sutro 1986; Leibowitz et al. 1986; Hille et al. 1987) led to the idea, mentioned above, that the slow current kinetics is due to the scarce I–O transitions during maintained depolarizations, controlled by k_{io} in the nomen-

clature of Scheme 3. The forward rate constant k_{+Vo}, although directly proportional to the veratridine concentration [VT], should not be rate limiting since it is too fast. Even at 9°C its value has been estimated to be $2\times10^6\ M^{-1}\ s^{-1}$, which at a concentration of 100 μM leads to a rate of 200 s^{-1}, i.e., a time constant of 5 ms (Leibowitz et al. 1986) vs τ_s of ca. 1 s in Ranvier nodes even at room temperature (Ulbricht 1969a,b).

Computing the results from frog nerve began by estimating the equilibrium fraction, O*, of modified channels from K_1, K_2, and K_3 of Scheme 1 without the I–I* transition as given by Krueger and Blaustein (1980). However, early in a depolarizing pulse the fraction, R, of channels in the resting state becomes negligible, and thus O* is given simply by $K_2/(K_2+K_3+K_2K_3)$. Note that $K_2=k_{io}/k_{oi}$ and $K_3=k_{-Vo}/k_{+Vo}$, a dimensionless constant in contrast to that defined by Krueger and Blaustein (1980). The results with frog nerve suggest that the maximum permeability of modified channels is only about 10% of the maximum P_{Na} (Ulbricht 1969a). Considering that $\gamma^*=\gamma/4$ (Barnes and Hille 1988), we expect the maximum O* to be 0.4, and for the following considerations we may therefore settle for 0.3. At E=–40 mV we assume $k_{io}=6\ s^{-1}$ and $k_{oi}=820\ s^{-1}$ (following α_h and β_h at 20°C, Frankenhaeuser and Huxley 1964) so that $K_2=0.0073$. With these quantities $K_3=0.0172$ yields O*=0.3.

Finally, for reasons given below, k_{-Vo} is chosen to be 1 s^{-1} so that $k_{+Vo}=59\ s^{-1}$, leading at [VT]=60 μM to a forward rate constant for the binding reaction of $59\ s^{-1}/6\times10^{-5}\ M=9.8\times10^5\ M^{-1}\ s^{-1}$. With these values one calculates (with a Runge-Kutta routine) the time courses of O* which in most cases can be readily approximated by single exponentials with onset and offset time constants, $\tau_{s,on}=0.75$ s and $\tau_{s,off}=1.0$ s. The latter time constant obviously is close to $1/k_{-Vo}$, and it was actually chosen to fit the observed tail time constants. However, the computed $\tau_{s,on}$ was always shorter than $\tau_{s,off}$, as expected for a binding reaction; this is rate limiting but contrary to the experiments which always yielded $\tau_{s,on}>\tau_{s,off}$ if the off-time constant is measured at the holding potential. For the computed time course this is true for a wide variety of assumed rate constants. However, one feature of the experimental results, the step with which the slowly increasing current starts (see, e.g., Fig. 6), is well reproduced by the computation. In the example above the relative step was 20%, similar to that in a real experiment. One should note that an equilibrium dissociation constant of veratridine binding determined from the equilibrium fraction O*, for example, those mentioned in Sect. 5.4, leads to K'_d, which is much larger than the true K_d of the O–O* reaction, since $K'_d\approx K_d/K_2$.

For a given veratridine concentration the equilibrium fraction, O*, of modified channels in frog nodes of Ranvier increases monotonically with increasing depolarization (Ulbricht 1969a; Rando 1989). On the other hand, in the absence of veratridine the fraction, O, of precursor peaks near E=−40 mV and decreases on further depolarization, at least if calculated with the equations of Frankenhaeuser and Huxley (1964; see also Table 1 of Hille 1967). This discrepancy may be apparent since the classical description, resting mainly on extrapolation, ignores a small fraction of channels that fail to inactivate even at large depolarizations (Dubois and Bergman 1975; see also Neumcke 1990). A more serious inconsistency may be that, on partial repolarization, i.e., to potentials between the holding potential and the test pulse potential, $\tau_{s,off}$ increases in real experiments, as shown by Fig. 4. This cannot easily be explained by the binding hypothesis in its simplest form since the reciprocal of k_{-Vo} (supposedly independent of potential) sets the upper limit of $\tau_{s,off}$. Computations with constant k_{-Vo}, but with changes in other rate constants to imitate incomplete repolarization (increased k_{ro} and k_{oi}, decreased k_{or} and k_{io}), gave $\tau_{s,off} < 1/k_{-Vo}$. These discrepancies may be related to those reported by Leibowitz et al. (1986) who, as mentioned above, had to introduce a direct route from I* to the unmodified state(s) to describe recovery on repolarization. Unfortunately only a lumped scheme was presented, which is unsuited for computing $\tau_{s,off}$. It may be added here that the R–O transition used in the computations was also lumped from R_1–R_2–R_3–O (see, e.g., Neumcke 1990), but sample calculations with the more unwieldy extended form did not yield basically different results.

Rando's (1989) alternative interpretation of the slow current changes as due to I*–O* transitions allows a fit of $\tau_{s,on}$ and $\tau_{s,off}$ by choosing the appropriate values of k_{io*} and k_{oi*}. Transitions from unmodified states do not enter Rando's equations, but when his values for the (fast) R*–O* conversion are extrapolated to depolarizations, the computations yield a current step as described above. Also, if another state, I', is connected to I* to represent channels blocked by benzocaine, onset and offset of this block behave *qualitatively* as in the experiments described in Sect. 5.6, i.e., with $\tau_{on} > \tau_{off}$ and τ_{on} depending little on [VT]. However the computed time constants are too short.

As for the block by benzocaine, Ulbricht and Stoye-Herzog (1984) obtained a clearly better fit of its rates, both during long pulses and trains of shorter pulses. They used a simple formalism in which closed, unblocked channels could either turn to a permanently open form (depending on

potential) or a blocked form (depending on benzocaine concentration). They employed kinetic data from previous work on benzocaine (Schmidtmayer and Ulbricht 1980) and assumed permanently modified channels with the typical slow kinetics (Ulbricht 1969a). Introduction of such formalism into the kinetic Scheme 3, however, gives unsatisfactory results. For example, if I stands for the unblocked closed state, I* (with no connection to O*) and O* would then play the respective roles of blocked and permanently open states. The values of k_{io}, k_{oi}, k_{+Vo}, and k_{-Vo} mentioned above then yield O*=0.3 at equilibrium. From this one calculates, on applying 0.25 m*M* benzocaine (k_{on}=100 s^{-1} and k_{off}=29 s^{-1} for the benzocaine-channel reaction; see Ulbricht and Stoye-Herzog 1984), a stationary block to 29%, τ_{on}=1 s, and on washout τ_{off}=0.75 s; again $\tau_{on}>\tau_{off}$, but this is far off in terms of absolute time constants (5.2 and 3.2 s, respectively). Changing k_{on} and/or k_{off} over a wide range does not improve the fit as they are not rate limiting.

In summary, the computations based on veratridine binding exclusively to open channels whose availability determines the slow kinetics are only partially successful. Perhaps a better fit would require the inclusion of all possible transitions in Scheme 3 plus those not included like direct pathways, O*-R etc. leaving too many degrees of freedom for a meaningful fit even under the constraint of microscopic reversibility.

8
The Veratridine Binding Site

The decade following the pioneering work of Numa and coworkers (Noda et al. 1984) has provided us with an enormous amount of structural details of the Na^+ channel, especially its α-subunit (for recent reviews see Hille 1992; Catterall 1992; Noda 1993; Sato and Matsumoto 1995; Aidley and Stanfield 1996). Clearly one would like to know where on this macromolecule veratridine binds, and how to explain its many effects. Hille and coworkers (1987) proposed that, on channel opening, the binding site becomes exposed to the hydrophobic interior of the lipid membrane phase; they placed the site at the junction between two of the four domains of the α-subunit. Bound veratridine could function as a wedge between domains that stabilizes the open state and impedes channel closing by deactivation (on repolarization) or by inactivation (during maintained depolarization). This wedge is thought to distort the α-subunit, thereby

widening the selectivity filter and reducing its power of discrimination. A *modified* channel may close but the trapped veratridine molecule constitutes a strain that favors reopening even at potentials considerably more negative than the normal resting value (see Fig. 2); veratridine may leave the closed trap, however very slowly, despite the pressure put on the alkaloid molecule. Other neurotoxins such as batrachotoxin with a higher affinity for site 2 dissociate from it so slowly that the channel may open and close very many times while the toxin is bound. Batrachotoxin also seems to exert less strain as a wedge and hence shifts activation along the potential axis only half as much as does veratridine.

The model of veratridine action presented above leaves, of course, the chemical nature of the binding site unexplained. Earlier attempts to characterize site 2 were based on common structural features of the toxins binding to it, veratridine, batrachotoxin, and aconitine. Extending an idea of Masutani et al. (1981), Codding (1983) and Kosower (1983) proposed a triangular arrangement of oxygens at a distance of ca. 5–6 Å from a tertiary nitrogen considered a hydrogen-bond acceptor; this function is supposedly taken over by a different group in grayanotoxin, another site-2 ligand lacking the nitrogen. An extensive report on these papers is found in Khodorov's (1985) review of batrachotoxin. Because of its higher affinity for site 2, batrachotoxin is, as mentioned, nowadays the preferred ligand in binding studies.

Only very recently a successful attempt was made to characterize site 2 within the known channel structure. Mapping of this site had not been feasible because of the low affinity of ligand binding, even of batrachotoxin. Only after additionally employing pyrethroids and brevetoxin PbTx-1 (a site-5 toxin) was the affinity for the photoreactive and radiolabeled derivative [^{3}H]BTX-OAB (batrachotoxinin-A orthoazidobenzoate) enhanced by a factor of 1000 (Trainer et al. 1996). The experiments were carried out on purified Na^+ channel α-subunits incorporated in lipid vesicles. The photolabeled regions were identified by antibody mapping of proteolytic fragments to belong to the transmembrane region S6 of domain I. The batrachotoxin receptor site is formed in part by this region between the amino acids Asn-388 and Glu-429. This region may be relatively inaccessible at rest, but access is thought to change dramatically on repetitive depolarization and in the presence of the activators mentioned. The underlying conformational changes must reach far, for example, to sites 1 (TTX) and 3 (α-scorpion toxins), and are thought to cause the decrease in channel conductance and selectivity and the great shift of

potential dependence of the conductance. In labeling experiments 300 μM veratridine has proven able to prevent labeling, as expected if the two toxins have identical or overlapping binding sites. The structural details will eventually be characterized by site-directed mutagenesis. Natural channel mutants already exist since muscles of the batrachotoxin-producing tropical frogs are insensitive to their own toxin but sensitive (although to a lesser extent than other frog muscles) to veratridine (Daly et al. 1980).

9
Summary and Conclusion

Veratridine causes Na^+ channels to stay open during a sustained membrane depolarization by abolishing inactivation. The consequential Na^+ influx, either by itself or by causing a maintained depolarization, leads to many secondary effects such as increasing pump activity, Ca^{2+} influx, and in turn exocytosis. If the membrane is voltage clamped in the presence of the alkaloid, a lasting depolarizing impulse induces, following the "normal" transient current, another much more slowly developing Na^+ current that reaches a constant level after a few seconds. Repolarization then is followed by an inward tail current that slowly subsides. Development of these slow currents is enhanced by additional treatment with agents that inhibit inactivation. Most of these phenomena can be satisfactorily explained by assuming that Na^+ channels must open before veratridine binds to them, and that the slow current changes reflect the kinetics of binding and unbinding. It is unclear, however, where the alkaloid stays when it is not bound. Although the effect sets in promptly, once this pool is filled, access to it from outside must be impeded since in most preparations veratridine can only partially be washed out. Cooling acts as if the available concentration is reduced, but this reversible "reduction" takes much longer to develop than the cold-induced changes in kinetics. Several authors assume that the binding site, site 2, is accessed from the lipid phase of the membrane. Considerations of this kind are often based on experiments with batrachotoxin, the widely used site-2 ligand which has a much higher affinity and acts as a full agonist in contrast to the partial agonist veratridine. Batrachotoxin thus lends itself to binding studies using radiolabeled derivatives. Such experiments may eventually lead to the characterization of neurotoxin site 2; the first promising steps have been taken. Modern techniques of molecular biology will almost certainly be success-

ful, and one hopes for point-mutated channels with distinctly different reactions also to veratridine. A considerable amount of research is still required to clarify the structural basis for the numerous allosteric interactions with other sites, the mechanism of the very large potential shift of activation, the reduced single-channel conductance and selectivity, and the chemical nature of the different affinities of the site-2 toxins.

Note Added in Proof. A report on point mutations with effects on neurotoxin site 2 (see Sect. 8) has just appeared: Wang S-Y, Wang GK (1988) Point mutations in segment I-S6 render voltage-gated Na^+ channels resistent to batrachotoxin. Proc Natl Acad USA 95:2653–2658. In μ1 muscle Na^+ channels expressed in mammalian cells, mutation Asn434Lys leads to complete, Asn434Ala to partial insensitivity to 5m*M* batrachotoxin. (Asn434 corresponds to Asn419 of Trainer et al. 1996). The mutant channel displays almost normal current kinetics and in the presence of veratridine little, if any, slow tail current. However, veratridine inhibits peak Na^+ currents in the mutant which may point to a complex structure of site 2.

References

Aidley DJ, Stanfield PR (eds) (1996) Ion channels: molecules in action. Cambridge University Press, Cambridge

Amar M, Pichon Y, Inoue I (1991) Micromolar concentrations of veratridine activate sodium channels in embryonic cockroach neurones in culture. Pflügers Arch 417:500–508

Balerna M, Fosset M, Chicheportiche R, Romey G, Lazdunski M (1975) Constitution and properties of axonal membranes of crustacean nerves. Biochemistry 14:5500–5511

Barnes S, Hille B (1988) Veratridine modifies open sodium channels. J Gen Physiol 91:421–443

Benzer TI, Raftery MA (1973) Solubilization and partial characterization of the tetrodotoxin binding component from nerve axons. Biochem Biophys Res Comm 51:939–944

Bidard J-N, Vijverberg HPM, Frelin C, Chungue E, Legrand, A-M, Bagnis R, Lazdunski M (1984) Ciguatoxin is a novel type of Na^+ channel toxin. J Biol Chem 259:8353–8357

Blaustein MP (1975) Effects of potassium, veratridine and scorpion venom on calcium accumulation and transmitter release by nerve terminals in vitro. J Physiol (Lond) 247:617–655

Blaustein MP, Goldring JM (1975) Membrane potentials in pinched-off presynaptic nerve terminals monitored with a fluorescence probe: evidence that synaptosomes have potassium diffusion potentials. J Physiol (Lond) 247:589–615

Bouron A, Reuter H (1996) A role of intracellular Na^+ in the regulation of synaptic transmission and turnover of the vesicular pool of cultured hippocampal cells. Neuron 17:969–978

Brodie C, Sampson SR (1990) Veratridine-induced oscillations in membrane potential of cultured rat skeletal muscle: Role of the Na-K pump. Cell Mol Neurobiol 10:217–226

Brown GB (1988) Batrachotoxin: a window on the allosteric nature of the voltage-sensitive sodium channel. Int Rev Neurobiol 29:77–116

Brunton L, Cash T (1883) Influence of heat and cold upon muscles poisoned by veratria. J Physiol (Lond) 4:1–17

Cachelin AB, De Peyer JE, Kokubun S, Reuter H (1983) Sodium channels in cultured cardiac cells. J Physiol (Lond) 340:389–401

Campbell DT (1976) Ionic selectivity of the sodium channel of frog skeletal muscle. J Gen Physiol 67:295–307

Castillo C, Villegas R, Recio-Pinto E (1992) Alkaloid-modified sodium channels from lobster walking leg nerves in planar lipid bilayers. J Gen Physiol 99:897–930

Castillo C, Piernavieja C, Recio-Pinto E (1996) Interactions between anemone toxin II and veratridine on single neuronal sodium channels. Brain Res 733:243–252

Catterall WA (1975a) Activation of the action potential Na^+ ionophore of cultured neuroblastoma cells by veratridine and batrachotoxin. J Biol Chem 250:4053–4059

Catterall WA (1975b) Cooperative activation of action potential Na^+ ionophore by neurotoxins. Proc Natl Acad Sci USA 72:1782–1786

Catterall WA (1977) Activation of the action potential Na^+ ionophore by neurotoxins. An allosteric model. J Biol Chem 252:8669–8676

Catterall WA (1980) Neurotoxins that act on voltage-sensitive sodium channels in excitable membranes. Annu Rev Pharmacol Toxicol 20:15–43

Catterall WA (1981) Inhibition of voltage-sensitive sodium channels in neuroblastoma cells by antiarrhythmic drugs. Mol Pharmacol 20:356–362

Catterall WA (1992) Cellular and molecular biology of voltage-gated sodium channels. Physiol Rev 72 [Suppl]:S15–S48

Catterall WA, Coppersmith J (1981) Pharmacological properties of sodium channels in cultured rat heart cells. Mol Pharmacol 20:533–542

Catterall WA, Gainer M (1985) Interaction of brevetoxin A with a new receptor site on the sodium channel. Toxicon 23:497–504

Catterall WA, Risk M (1981) Toxin T_{46} from *Ptychodiscus brevis* (formerly *Gymnodinium breve*) enhances activation of voltage-sensitive sodium channels by veratridine. Mol Pharmacol 19:345–348

Catterall WA, Morrow CS, Daly JW, Brown GB (1981) Binding of batrachotoxinin A 20-α-benzoate to a receptor site associated with sodium channels in synaptic nerve ending particles. J Biol Chem 256:8922–8927

Churchwell KB, Wright SH, Emma F, Rosenberg PA, Strange K (1996) NMDA receptor activation inhibits neuronal volume regulation after swelling induced by veratridine-stimulated Na^+ influx in rat cortical cultures. J Neurosci 16:7447–7457

Codding PW (1983) Structural studies of channel neurotoxins. II. Crystal structure and absolute configuration of veratridine perchlorate. J Am Chem Soc 105:3172–3176

Colquhoun D, Henderson R, Ritchie JM (1972) The binding of labelled tetrodotoxin to nonmyelinated nerve fibres. J Physiol (Lond) 227:95–126

Corbett AM, Krueger BK (1989) Polypeptide neurotoxins modify gating and apparent single-channel conductance of veratridine-activated sodium channels in planar bilayers. J Membrane Biol 110:199–207

Corbett AM, Krueger BK (1990) Isolation of two saxitoxin-sensitive sodium channel subtypes from rat brain with distinct biochemical and functional properties. J Membrane Biol 117:163–176

Correa AM, Latorre R, Bezanilla F (1991) Ion permeation in normal and batrachotoxin-modified Na^+ channels in the squid giant axon. J Gen Physiol 97:605–625

Correa AM, Villegas GM, Villegas R (1987) Anemone toxin II receptor site of the lobster nerve sodium channel: Studies in membrane vesicles and in proteoliposomes. Biochim Biophys Acta 897:406–422

Creveling CR, McNeal ET, Daly JW, Brown GB (1983) Batrachotoxin-induced depolarization and [^{3}H]-batrachotoxinin-A 20α-benzoate in a vesicular preparation from guinea pig cerebral cortex. Inhibition by local anesthetics. Mol Pharmacol 23:350–358

Crosby DG (1971) Minor insecticides of plant origin. In: Jacobson MJ, Crosby DG (eds) Naturally occurring insecticides. Dekker, New York, pp 177–239

Cukierman S (1991) Inactivation modifiers of Na^+ currents and the gating of rat brain Na^+ channels in planar lipid membranes. Pflügers Arch 419:514–521

Daly JW, Myers CW, Warnick JE, Albuquerque EX (1980) Levels of batrachotoxin and lack of sensitivity to its action in poison-dart frogs (*Phyllobates*). Science 208:1383–1385

Daniell LC (1992) Determination of the intravesicular ionized sodium concentration in a cell-free brain membrane vesicle preparation using the fluorescent indicator, SBFI. Anal Biochem 202:239–244

Deri Z, Adam-Vizi V (1993) Detection of intracellular free Na^+ concentration of synaptosomes by a fluorescent indicator, Na^+-binding benzofuran isophthalate: the effect of veratridine, ouabain, and α-latrotoxin. J Neurochem 61:818–825

Dubois JM, Bergman C (1975) Late sodium current in the node of Ranvier. Pflügers Arch 357:145–148

Duch DS, Levinson SR (1987) Neurotoxin-modulated uptake of sodium by highly purified preparations of the electroplax tetrodotoxin-binding glycopeptide reconstituted into lipid vesicles. J Membrane Biol 98:43–55

Duch DS, Recio-Pinto E, Frenkel C, Levinson SR, Urban BW (1989) Veratridine modification of the purified sodium channel α-polypeptide from eel electroplax. J Gen Physiol 94:813–831

Dugas M, Honerjäger P, Masslich U (1989) Tetrodotoxin block of single germitrine-activated sodium channels in cultured rat cardiac cells. J Physiol (Lond) 411:611–626

Fainzilber M, Kofman O, Zlotkin E, Gordon D (1994) A new neurotoxin binding site of sodium channels is identified by a conotoxin that affects sodium channel inactivation in molluscs and acts as an antagonist in rat brain. J Biol Chem 269:2574–2580

Fleckenstein A (1955) Der Kalium-Natrium-Austausch als Energieprinzip in Muskel und Nerv. Springer, Berlin Göttingen Heidelberg

Fontana G, Blaustein MP (1993) Calcium buffering and free Ca^{2+} in rat brain synaptosomes. J Neurochem 60:843–850

Frankenhaeuser B, Huxley AF (1964) The action potential in the myelinated nerve fibre of *Xenopus laevis* as computed on the basis of voltage clamp data. J Physiol (Lond) 171:302–315

Frelin C, Vigne P, Lazdunski M (1981) The specificity of the sodium channel for monovalent cations. Eur J Biochem 119:437–442

Frelin C, Lombet A, Vigne P, Romey G, Lazdunski M (1982) Properties of Na^+ channels in fibroblasts. Biochem Biophys Res Comm 107:202–208

Frelin C, Cognard C, Vigne P, Lazdunski M (1986) Tetrodotoxin-sensitive and tetrodotoxin-resistant Na^+ channels differ in their sensitivity to Cd^{2+} and Zn^{2+}. Eur J Pharmacol 122:245–250

Garber SS (1988) Symmetry and asymmetry of permeation through toxin-modified Na^+ channels. Biophys J 54:767–776

Garber SS, Miller C (1987) Single Na^+ channels activated by veratridine and batrachotoxin. J Gen Physiol 89:459–480

Ghiasuddin SM, Soderlund DM (1984) Mouse brain synaptosomal sodium channels: Activation by aconitine, batrachotoxin, and veratridine, and inhibition by tetrodotoxin. Comp Biochem Physiol 77 C:267–271

Gola M, Chagneux H, Argémi J (1982) An asymmetrical kinetic model for veratridine interactions with sodium channels in molluscan neurons. Bull Math Biol 44:231.258

Goldstein A (1987) Otto Krayer 1899–1982. Biographical memoirs, vol 57, pp 150–225. National Academic Press, Washington

Hare JD (1996) Purification and quantitative analysis of veratridine and cevadine by HPLC. J Agric Food Chem 44:149–152

Henderson R, Wang J (1972) Solubilization of a specific tetrodotoxin binding component from garfish olfactory nerve membrane. Biochemistry 11:4565–4569

Hille B (1967) A pharmacological analysis of the ionic channels in nerve. Thesis, Rockefeller University. University Microfilms International, Ann Arbor, no 689584

Hille B (1971) The permeability of the sodium channel to organic cations in myelinated nerve. J Gen Physiol 58:599–619

Hille B (1972) The permeability of the sodium channel to metal cations in myelinated nerve. J Gen Physiol 59:637–658

Hille B (1992) Ionic channels of excitable membranes, 2nd edn. Sinauer, Sunderland

Hille B, Leibowitz MD, Sutro JB, Schwarz JR, Holan G (1987) State-dependent modification of sodium channels by lipid-soluble agonists. In: Hille B, Fambrough DM (eds) Proteins of excitable membranes. Wiley, New York, pp 109–124

Holan G, Johnson WMP, Rihs K (1984) Separation of veratrine using high-performance liquid chromatography or droplet countercurrent chromatography. J Chromatogr 288:479–483

Honerjäger P (1973) Electrophysiological effects of various ceveratrum alkaloids on single nerve axons. Naunyn-Schmiedebergs Arch Pharmacol 280:391–416

Honerjäger P, Frelin C, Lazdunski M (1982) Actions, interactions, and apparent affinities of various ceveratrum alkaloids at sodium channels of cultured neuroblastoma and cardiac cells. Naunyn-Schmiedebergs Arch Pharmacol 321:123–129

Honerjäger P, Dugas M, Zong X-G (1992) Mutually exclusive action of cationic veratridine and cevadine at an intracellular site of cardiac sodium channel. J Gen Physiol 99:699–720

Huang LM, Ehrenstein G, Catterall WA (1978) Interaction between batrachotoxin and yohimbine. Biophys J 23:219–231

Jacques Y, Fosset M, Lazdunski M (1978) Molecular properties of the action potential Na^+ ionophore in neuroblastoma cells. Interaction with neurotoxins. J Biol Chem 253:7383–7392

Khodorov BI (1985) Batrachotoxin as a tool to study voltage-sensitive sodium channels of excitable membranes. Prog Biophys Mol Biol 45:57–148

Khodorov BI, Valkina O, Turovetsky V (1994) Mechanisms of stimulus-evoked intracellular acidification in frog nerve fibres. FEBS Lett 341:125–127

Khodorov BI, Zaborovskaya LD (1983) Blockade of sodium and potassium channels in the node of Ranvier by ajmaline and N-propyl ajmaline. Gen Physiol Biophys 2:233–268

Kosower EM (1983) A hypothesis for the mechanism of sodium channel opening by batrachotoxin and related toxins. FEBS Lett 163:161–164

Kostyuk PG, Krishtal OA, Shakhovalov YuA (1977) Separation of sodium and calcium currents in the somatic membranes of mollusc neurones. J Physiol (Lond) 270:545–568

Krayer O (1961) The history of the Bezold-Jarisch effect. Naunyn-Schmiedebergs Arch Pharmacol 240:361–368

Krayer O, Acheson GH (1946) The pharmacology of the veratrum alkaloids. Physiol Rev 26:383–446

Krueger BK, Blaustein MP (1980) Sodium channels in presynaptic nerve terminals. Regulation by neurotoxins. J Gen Physiol 76:287–313

Krueger BK, Worley JF, French RJ (1983) Single sodium channels from rat brain incorporated into planar lipid bilayer membranes. Nature 303:172–175

Lawrence JC, Catterall WA (1981) Tetrodotoxin-insensitive sodium channels. Ion flux studies of neurotoxin action in a clonal rat muscle cell line. J Biol Chem 256:6213–6222

Leibowitz MD, Sutro JB, Hille B (1986) Voltage-dependent gating of veratridine-modified Na channels. J Gen Physiol 87:25–46

Leibowitz MD, Schwarz JR, Holan G, Hille B (1987) Electrophysiological comparison of insecticide and alkaloid agonists of Na channels. J Gen Physiol 90:75–93

Leicht R, Meves H, Wellhöner H-H (1971a) The effect of veratridine on Helix pomatia neurones. Pflügers Arch 323:50–62

Leicht R, Meves H, Wellhöner H-H (1971b) Slow changes of membrane permeability in giant neurones of Helix pomatia. Pflügers Arch 323:63–79

Levinson SR, Duch DS, Urban BW, Recio-Pinto E (1986) The sodium channel from *Electrophorus electricus*. Ann NY Acad Sci 479:162–178

Lipton E (1973) Effects of membrane depolarization on light scattering by cerebral cortex slices. J Physiol 231:365–383

Lönnendonker U (1989) Use-dependent block of sodium channels in frog myelinated nerve by tetrodotoxin and saxitoxin at negative holding potentials. Biochim Biophys Acta 985:153–160

Lönnendonker U (1991) Use-dependent block with tetrodotoxin and saxitoxin at frog Ranvier nodes. II. Extrinsic influence of cations. Eur Biophys J 20:143–149

Masutani T, Seyama I, Narahashi T, Iwasa I (1981) Structure-activity relationship for grayanotoxin derivatives in frog skeletal muscle. J Pharmacol Exp Ther 217:812–819

Mata M, Fink DL, Gainer H, Smith CB, Davidsen L, Savaki H, Schwartz WJ, Sokoloff L (1980) Activity-dependent energy metabolism in rat posterior pituitary primarily reflects sodium pump activity. J Neurochem 34:213–215

Matthews JC, Warnick JE, Albuquerque EX, Eldefrawi ME (1981) Characterization of the electrogenic sodium channel from rat brain membranes using neurotoxin-dependent ^{22}Na uptake. Membr Biochem 4:71–104

McKinney LC (1985) Diphenylhydantoin reduces veratridine-induced sodium permeability on frog skeletal muscle. Neurosci Lett 55:173–178

McKinney LC, Ratzlaff RW (1987) Sodium permeability of frog skeletal muscle in absence and presence of veratridine. Am J Physiol 252:C190–C196

McKinney LC, Chakraverty S, De Weer P (1986) Purification, solubility, and pK_a of veratridine. Analyt Biochem 153:32–38

Meeder T, Ulbricht W (1987) Action of benzocaine on sodium channels of frog nodes of Ranvier treated with chloramine-T. Pflügers Arch 409:265–273

Meves H (1966) The effect of veratridine on internally perfused giant axons. Pflügers Arch 290:211–217

Minchin MCW (1980) Veratrum alkaloids as transmitter-releasing agents. J Neurosci Meth 2:111–121

Moczydlowski E, Schild L (1994) Unitary properties of the batrachotoxin-trapped state of voltage-sensitive sodium channels. In: Peracchia C (ed) Handbook of membrane channels. Molecular and cellular physiology. Academic, San Diego, pp 137–160

Monod J, Wyman J, Changeux J-P (1965) On the nature of allosteric transitions: A plausible model. J Mol Biol 12:88–118

Nánási PP, Varró A, Lathrop DA, Bryant SH (1994) Effects of veratridine on Na and Ca currents in frog skeletal muscle. Gen Pharmacol 25:1661–1666

Naumov AP, Negulyayev YuA, Nosyreva ED (1979) Change of selectivity of sodium channels in membrane of nerve fiber treated with veratrine (in Russian). Tsitologiya 21:692–696

Neumcke B (1990) Diversity of sodium channels in adult and cultured cells, in oocytes and in lipid bilayers. Rev Physiol Biochem Pharmacol 115:1–49

Noda M (1993) Structure and function of sodium channels. Ann NY Acad Sci 707:20–37

Noda M, Shimizu S, Tanabe T, Takai T, Kayano T, Ikeda T, Takahashi H, Nakayama H, Kanaoka Y, Minamino N, Kangawa K, Matsuo H, Raftery MA, Hirose T, Inayama LS, Hayashida H, Miyata T, Numa S (1984) Primary structure of *Electrophorus electricus* sodium channel deduced from cDNA sequence. Nature 312:121–127

Ohta M, Narahashi T, Keeler RF (1973) Effects of veratrum alkaloids on membrane potential and conductance of squid and crayfish giant axons. J Pharmacol Exp Ther 184:143–154

Prévost JL (1866) Recherches expérimentales relative à l'action de la vératrine. C R Soc Biol (Paris) 18:133 (cited by Krayer O, Acheson GH 1946)

Rando TA (1989) Rapid and slow gating of veratridine-modified sodium channels in frog myelinated nerve. J Gen Physiol 93:43–65

Rando TA, Strichartz GR (1986) Saxitoxin blocks batrachotoxin-modified sodium channels in the node of Ranvier in a voltage-dependent manner. Biophys J 49:785–794

Rando TA, Wang GK, Strichartz GR (1986) The interaction between the activator agents batrachotoxin and veratridine and the gating process of neuronal sodium channels. Mol Pharmacol 29:467–477

Recio-Pinto E, Duch DS, Levinson SR, Urban BW (1987) Purified and unpurified sodium channels from eel electroplax in planar lipid bilayers. J Gen Physiol 90:375–395

Reed JA, Gerrie J, Reed KL (1986) Purification of veratridine from veratrine using high-performance liquid chromatography. J Chromatogr 356:450–454

Reiser G, Hamprecht B (1983) Sodium-channels in non-excitable glioma cells, shown by the influence of veratridine, scorpion toxin, and tetrodotoxin on membrane potential and on ion transport. Pflügers Arch 297:260–264

Rimmel C, Walle A, Keßler H, Ulbricht W (1978) Rates of block by procaine and benzocaine and the procaine-benzocaine interaction at the node of Ranvier. Pflügers Arch 376:105–118

Romey G, Lazdunski M (1982) Lipid-soluble toxins thought to be specific for Na^+ channels block Ca^{2+} channels in neuronal cells. Nature 287:79–80

Romey G, Jacques Y, Schweitz H, Fosset M, Lazdunski M (1979) The sodium channels in non-impulsive cells. Interaction with specific neurotoxins. Biochim Biophys Acta 556:344–353

Romey G, Chicheportiche R, Lazdunski M (1980) Transition temperature of the electrical activity of ion channels in the nerve membrane. Biochim Biophys Acta 602:610–620

Rosenberg RL, Tomiko SA, Agnew WS (1984) Reconstitution of neurotoxin-modulated ion transport by the voltage-regulated sodium channel isolated from the electroplax of Electrophorus electricus. Proc Natl Acad Sci USA 81:1239–1243

Salgado VL, Yeh JZ, Narahashi T (1986) Use- and voltage-dependent block of the sodium channel by saxitoxin. Ann NY Acad Sci 479:84–95

Sato C, Matsumoto G (1995) Sodium channel function based on an octagonal structure model. J Membr Biol 147:45–70

Schmidtmayer J, Stoye-Herzog M, Ulbricht W (1982) Rate of action of *Anemonia sulcata* toxin II on sodium channels in myelinated nerve fibres. Pflügers Arch 394:313–319

Schmidtmayer J, Ulbricht W (1980) Interaction of lidocaine and benzocaine in blocking sodium channels. Pflügers Arch 387:47–54

Scholtysik G, Quast U, Schaad A (1986) Evidence for different receptor sites for the novel cardiotonic S-DPI, ATX II and veratridine on the cardiac sodium channel. Eur J Pharmacol 125:111–118

Schreibmayer W, Tritthart HA, Schindler H (1989) The cardiac sodium channel shows a regular substate pattern indicating synchronized activity of several ion pathways instead of one. Biochim Biophys Acta 986:172–186

Schwarz JR, Ulbricht W, Wagner H-H (1973) The rate of action of tetrodotoxin on myelinated nerve fibres of *Xenopus laevis* and *Rana esculenta*. J Physiol (Lond) 233:167–194

Scruggs VM (1973) The veratridine induced sodium conductance in the squid giant axon. Thesis, University of Miami. University Microfilms International, Ann Arbor, no 7921763

Seyama I, Yamada K, Kato R, Masutani T, Hamada M (1988) Grayanotoxin opens Na channels from inside the squid axonal membrane. Biophys J 53:271–274

Shanes AM (1958a) Electrochemical aspects of physiological and pharmacological action in excitable cells. I. The resting cell and its alteration by extrinsic factors. Pharmacol Rev 10:59–164

Shanes AM (1958b) Electrochemical aspects of physiological and pharmacological action in excitable cells. II. The action potential and excitation. Pharmacol Rev 10:165–273

Shenkel S, Cooper EC, James W, Agnew WS, Sigworth F (1989) Purified, modified eel sodium channels are active in planar bilayers in the absence of activating neurotoxins. Proc Natl Acad Sci USA 86:9592–9596

Shichor I, Fainzilber M, Pelhate M, Malecot CO Zlotkin E, Gordon D (1996) Interactions of δ-conotoxins with alkaloid neurotoxins reveal differences between the silent and effective binding sites on voltage-sensitive sodium channels. J Neurochem 67:2451–2460

Siem-Fung DJ, Sevcik C (1983) The effect of temperature on veratridine action in squid giant axons. Biochim Biophys Acta 728:305–310

Sigel E (1987) Effects of veratridine on single neuronal sodium channels expressed in Xenopus oocytes. Pflügers Arch 410:112–120

Spafford DJ, Grigoriev NG, Spencer AN (1996) Pharmacological properties of voltage-gated Na^+ currents in motor neurones from a hydrozoan jellyfish *Polyorchis penicillatus*. J Exp Biol 199:941–948

Stallcup WB (1977) Comparative pharmacology of voltage-dependent sodium channels. Brain Res 135:37–53

Straub R (1956) Die Wirkung von Veratridin und Ionen auf das Ruhepotential markhaltiger Nervenfasern des Frosches. Helv Physiol Acta 14:1–28

Strichartz G, Rando T, Wang GK (1987) An integrated view of the molecular toxinology of sodium channel gating in excitable cells. Annu Rev Neurosci 10:237–267

Stuart AM, Bloomquist JR, Soderlund DM (1987) Pharmacological characterization of the voltage-dependent sodium channels of rainbow trout brain synaptosomes. Brain Res 437:77–82

Sunami A, Sasano T, Matsunaga A, Fan Z, Sawanobori T, Hiraoka M (1993) Properties of veratridine-modified single Na^+ channels in guinea pig ventricular myocytes. Am J Physiol 264:H454–H463

Sutro JB (1986) Kinetics of veratridine action on Na channels of skeletal muscle. J Gen Physiol 87:1–24

Tamkun MM, Catterall WA (1981) Ion flux studies of voltage-sensitive sodium channels in synaptic nerve-ending particles. Mol Pharmacol 19:78–86

Tamkun MM, Talvenheimo JA, Catterall WA (1984) The sodium channel from rat brain. Reconstitution of neurotoxin-activated ion flux and scorpion toxin binding from purified components. J Biol Chem 259:1676–1688

Tanaka JC, Eccleston JF, Barchi RL (1983) Cation selectivity characteristics of the reconstituted voltage-dependent sodium channel purified from rat skeletal muscle. J Biol Chem 258:7519–7526

Trainer VL, Moreau E, Guedin D, Baden DG, Catterall WA (1993) Neurotoxin binding and allosteric modulation at receptor site 2 and 5 on purified and reconstituted rat brain sodium channels. J Biol Chem 268:17114–17119

Trainer VL, Brown GB, Catterall WA (1996) Site of covalent labeling by a photoreactive batrachotoxin derivative near transmembrane segment IS6 of the sodium channel α subunit. J Biol Chem 271:11261–11267

Ulbricht W (1965) Voltage clamp studies of veratrinized frog nodes. J Cell Comp Physiol 66:91–98

Ulbricht W (1969a) The effect of veratridine on excitable membranes of nerve and muscle. Ergeb Physiol 61:17–71

Ulbricht W (1969b) Effect of temperature on the slowly changing sodium permeability of veratrinized nodes of Ranvier. Pflügers Arch 311:73–95

Ulbricht W (1972a) Rate of veratridine action on the nodal membrane. I. Fast phase determined during sustained depolarization in the voltage clamp. Pflügers Arch 336:187–199

Ulbricht W (1972b) Rate of veratridine action on the nodal membrane. II. Fast and slow phase determined with periodic impulses in the voltage clamp. Pflügers Arch 336:201–212

Ulbricht W (1974) Drugs to explore the ionic channels in the axon membrane. In: Jaenicke L (ed) Biochemistry of sensory function. Springer, Berlin Heidelberg New York, pp 351–366

Ulbricht W (1990) The inactivation of sodium channels in the node of Ranvier and its chemical modification. In: Narahashi T (ed) Ion channels, vol 2. Plenum, New York, pp 123–168

Ulbricht W, Flacke W (1965) After-potentials and large depolarizations of single nodes of Ranvier treated with veratridine. J Gen Physiol 48:1035–1046

Ulbricht W, Stoye-Herzog M (1984) Distinctly different rates of benzocaine action on sodium channels of Ranvier nodes kept open by chloramine-T and veratridine. Pflügers Arch 402:439–445

Ulbricht W, Wagner H-H (1975) The influence of pH on equilibrium effects of tetrodotoxin on myelinated nerve fibres of *Rana esculenta*. J Physiol (Lond) 252:159–184

Urenjak J, Tegtmeier F, Beile A, Khan S, Peters T (1991) Synaptosomal respiration: a potent indicator of veratridine-induced Na influx. Pharmacology 43:26–35

Verdonck F, Bielen FV, Ver Donck L (1991) Preferential block of the veratridine-induced, non-inactivating Na^+ current by R56865 in single cardiac Purkinje cells. Eur J Pharmacol 203:371–378

Verheugen JAH, Oortgiesen M, Vijverberg HPM (1994) Veratridine blocks voltage-gated potassium current in human T lymphocytes and in mouse neuroblastoma cells. J Membr Biol 137:205–214

Villegas J, Sevcik C, Barnola FV, Villegas R (1976) Grayanotoxin, veratrine, and tetrodotoxin sensitive pathways in the Schwann cell membrane of squid nerve fibers. J Gen Physiol 67:369–380

Villegas R, Barnola FV, Sevcik C, Villegas GM (1976) Action of the sterol-binding form of filipin on the lobster axon membrane. Biochim Biophys Acta 426:81–87

Villegas R, Villegas GM, Rodriguez-Grille JM, Sorais-Landaez F (1988) The sodium channel of excitable and non-excitable cells. Q Rev Biophys 21:99–128

von Bezold A, Hirt L (1867) Über die physiologischen Wirkungen des essigsauren Veratrins. Untersuch Physiol Lab Würzburg 1:73–156

Wada A, Uezono Y, Arita M, Yuhi T, Kobayashi H, Yanagihara N, Izumi F (1992) Cooperative modulation of voltage-dependent sodium channels by brevetoxin and classical neurotoxins in cultured bovine adrenal medullary cells. J Pharmacol Exp Ther 263:1347–1351

Wagner H-H, Ulbricht W (1976) Saxitoxin and procaine act independently on separate sites of the sodium channel. Pflügers Arch 364:64–70

Wang G, Dugas M, Armah BI, Honerjäger P (1990) Sodium channel comodification with full activator reveals veratridine reaction dynamics. Mol Pharmacol 37:144–148

Wang GK, Wang S-Y (1994) Modification of cloned brain Na^+ channels by batrachotoxin. Pflügers Arch 427:309–316

Warashina A (1985) Frequency-dependent effects of aconitine and veratridine on membrane currents in the crayfish giant axon. Jap J Physiol 35:463–482

Weigele JB, Barchi RL (1982) Functional reconstitution of purified sodium channel protein from rat sarcolemma. Proc Natl Acad Sci USA 79:3651–3655

Yoshii M, Narahashi T (1984) Patch clamp analysis of veratridine-induced sodium channels (abstract). Biophys J 45:184a

Zong X-G, Dugas M, Honerjäger P (1992) Relation between veratridine reaction dynamics and macroscopic Na current in single cardiac cells. J Gen Physiol 99:683–697

Editor-in-charge: Professor M. P. Blaustein

The Elucidation of Somatostatin Receptor Functions: A Current View

W. Meyerhof

Department of Molecular Genetics, German Institute of Human Nutrition
and University of Potsdam, Arthur-Scheunert-Allee 114–116,
D-14558 Potsdam-Rehbrücke, Germany

Contents

1 Introduction 56
2 Molecular Cloning of Somatostatin Receptors 58
3 Molecular Biology 59
3.1 Primary Structures 59
3.2 Chromosomal Location, Gene Structure, and Regulation . . . 65
4 Pharmacology 67
4.1 Ligand Binding Studies 67
4.2 Mutational Analyses 70
5 Signal Transduction Mechanisms 73
5.1 G Protein- and Effector-Coupling in Native Membranes . . . 73
5.2 Signal Transduction Mediated by Somatostatin Receptors in Transfected Cell Lines 74
5.3 Desensitization and Internalization of Somatostatin Receptors 80
6 Tissue Distribution 84
6.1 Somatostatin Receptors in the CNS 84
6.2 Hypothalamic/Pituitary Axis 86
6.3 Peripheral Tissues 87
6.4 Ontogenesis 88
7 Physiology 91
8 Future Perspectives 92
References 93

1 Introduction

Somatostatin (SST) or somatotropin release-inhibiting factor (SRIF) was first discovered in hypothalamic extracts as an activity that inhibited growth hormone secretion from cultured anterior pituitaries (Krulich et al. 1968). Subsequently it was found that SST is widely distributed throughout the central nervous system (CNS) and peripheral tissues. It has attracted attention because of its diverse physiological actions. In addition to its function in the regulation of growth hormone release from the anterior pituitary (Brazeau et al. 1972), it is involved in the regulation of exocrine and endocrine secretion from various organs, such as pancreas, gut, and thyroid gland (Brown et al. 1977; Mandarino et al. 1981; Reichlin 1983; Epelbaum 1986; Feniuk et al. 1993; Epelbaum et al. 1994; Fujii et al. 1994). Furthermore, it has been suggested that SST serves as a neurotransmitter or neuromodulator in the CNS which influences locomotor activity and cognitive functions (Epelbaum 1986; Raynor and Reisine 1992; Epelbaum et al. 1994). SST has been identified as a cyclic 14 amino acid peptide (Brazeau et al. 1972). Besides SST-14, a second bioactive form with a N-terminal extension of 14 amino acids, SST-28, has been characterized (Pradayrol et al. 1980). In mammals both peptides are derived by tissue-specific proteolytic maturation from a single 116 amino acid preprohormone which in turn is the product of a single gene (reviewed in Patel and Galanopoulou 1995). Since both bioactive forms of SST cannot be iodinated, synthetic peptide analogs, such as Tyr^{11}-SST or Tyr^{1}-SST, have been used for ligand binding studies. SST analogs with increased half-life have become important for therapeutic treatment of neuroendocrine tumors (Lamberts et al. 1995). Recently, the complexity of the SST signaling system has been surprisingly and unexpectedly extended by the cDNA cloning of a 112 amino acid preprohormone, giving rise to two novel neuropeptides, cortistatin-14 and cortistatin-29 (de Lecea et al. 1996; Fukusumi et al. 1997). Cortistatin exhibits strong structural similarity to SST (Fig. 1), although it is the product of a different gene. By in situ hybridization cortistatin mRNA was detected in the cortex and hippocampus, where SST is also present, but not in the hypothalamus and some peripheral tissues where SST is abundant. Administration of cortistatin depresses neuronal electrical activity but, unlike SST, induces low-frequency waves in the cerebral cortex and antagonizes the effects of acetylcholine on hippocam-

```
rat somatostatin:        SANSNPAMAPRERKAG[CKNFFWKTFTSC]
                                 :   :   ::::::::: ::
rat cortistatin:         QERPPLQQPPHRDKKP[CKNFFWKTFSSC]
                         ::  : ::   ::  : : ::::::::::
human cortistatin:       QEGAPPQQSARRDRMP[CRNFFWKTFSSC]
```

Fig. 1. Alignment of the amino acid sequences of rat somatostatin-28 with those deduced from rat and human cortistatin cDNA predicted to form 29 amino acid peptides. Note that the conserved parts are located in the ring constituent (indicated by *square brackets*) and the extension of the ring structure by one amino acid in cortistatin. Also within the ring cortistatin displays the Trp-Lys motif that is essential for receptor binding (see Sect. 4)

pal and cortical measures of excitability, suggesting a mechanism for cortical synchronization related to sleep (de Lecea et al. 1996).

The various actions of SST are mediated through specific membrane receptors. The evidence for the existence of multiple somatostatin receptors was derived from several pharmacological and functional studies (reviewed by Rens-Domiano and Reisine 1992; Raynor and Reisine 1992). These experiments also suggested that receptors for SST belong to the superfamily of G protein-coupled receptors with seven transmembrane domains (Jakobs et al. 1983; Koch and Schonbrunn 1984; Law et al. 1991). To date five subtypes of human and rat SST-receptors and four of mouse have been cloned and it is assumed that the SST receptor subtypes (ssts) serve distinct biological functions. According to the IUPHAR nomenclature guidelines the receptors are named sst1, sst2, sst3, sst4, and sst5 (Hoyer et al. 1995). The ssts bind the two biologically occurring SSTs with high affinity and inhibit adenyl cyclase (AC) when they are expressed in appropriate cell lines. Although much effort has been undertaken to elucidate the function of these receptors several drawbacks such as the lack of selective ligands, specific antibodies, the presence of several receptors in the same tissue or even cells have hampered the identification of a distinct function for a particular receptor subtype. However, the cloning of the cDNAs and genes encoding sst subtypes facilitated the development of new tools for further biochemical and molecular characterizations of SST-receptor functions. In situ hybridization using subtype-specific cDNA and cRNA probes is being carried out for the construction of detailed maps of sst mRNA presence. The first specific antibodies are available and being used to localize the receptor proteins and study their coupling to effectors,

while new ligands are being tested in transfected cell lines and mutational analysis of sst subtypes promotes a rational design for the synthesis of novel SST agonists and antagonists. This review will focus on the molecular biology of the receptor subtypes and the advances in understanding their physiological importance through the use of these novel experimental tools.

2 Molecular Cloning of Somatostatin Receptors

Most sequences of the genes and cDNAs coding for SST receptors were published between 1992 and 1994. The first cDNA of an sst was described to encode a novel putative G protein-coupled receptor in brain (Meyerhof et al. 1991). It was later identified as the rat sst1 (rsst1) by sequence homology to the human sst1 (hsst1) and mouse sst1 (msst1) genes (Yamada et al. 1992). The cloning of the cDNA for rsst1 and hsst1 was based on polymerase chain reaction (PCR) fragments that were amplified with degenerate primers. The primers were deduced from conserved sequences of the third and sixth transmembrane domains of G protein-coupled seven transmembrane helix receptors (Libert et al. 1989). Using the PCR fragments as probes, clones specifying the complete amino acid sequences were isolated from rat cDNA – and human and mouse genomic libraries, respectively. hsst1 and msst1 were identified as SST receptors by expression of the genes in cultured mammalian cells, which resulted in the appearance of high-affinity binding sites for ^{125}I-[Tyr^{11}]-SST (Yamada et al. 1992). By using essentially this strategy rsst3 (Meyerhof et al. 1992) and rsst5 cDNAs have been isolated (O'Carroll et al. 1992). Rat sst2 cDNA was isolated by expression cloning in COS-1 cells (cells of CV-1 origin, SV40 transformed; Kluxen et al. 1992). The genes for hsst2, msst2 (Yamada et al. 1992), pig sst2 (Matsumoto et al. 1994), msst3 (Yasuda et al. 1992), rsst4 (Bruno et al. 1992), hsst4 (Demchyshyn et al. 1993; Rohrer et al. 1993; Xu et al. 1993; Yamada et al. 1993), msst4 (Schwabe et al. 1996), and hsst5 (Yamada et al. 1993; Panetta et al. 1994) have been subsequently isolated by cross-hybridization of genomic libraries using heterologous probes. In most of the cloning experiments functional expression of genomic DNA has been performed and was possible because the ssts are, with one exception known so far, devoid of introns within their coding region. Two variants have been described for mouse sst2, msst2A and msst2B (Vanetti

et al. 1992). The sequences are identical for the N-terminal 331 amino acid residues. However, both splice variants differ between transmembrane domain VII and the carboxyl-terminus. The sst2B comprises 346 amino acids and is therefore 23 amino acids shorter than the 369 amino acid receptor sst2A and it differs from the long form by the 15 C-terminal amino acids. These two msst2 variants arise by splicing a cryptic intron in the msst2 gene which generates msst2B mRNA of reduced length, while sst2A mRNA represents the unspliced form (Vanetti et al. 1993). At present sst2B mRNA has not been isolated from other species. However, the presence of conserved exon/intron boundaries in the human SST2 gene and the detection of sst2 transcripts of different sizes suggest the existence of spliced forms of sst2 mRNA also in other species (Patel et al. 1993; Kong et al. 1994). In addition to the amino acid sequences that have been deduced from cDNA clones, a partial amino acid sequence of the rsst2 was published by Hulmes et al. (1992), who purified and sequenced the SST receptor protein. Furthermore, a bovine sst2 sequence has been deposited in DNA databases (Xin et al. 1992).

3
Molecular Biology

3.1
Primary Structures

Comparisons of the amino acid sequences of the particular receptor subtypes from human, rat, and mouse revealed only 2%–14% sequence divergence, except for rat and human sst5 which display 19% divergence (Table 1). The divergence between the different receptor subtypes within a given species vary from 40% for rsst1 and rsst4 to 60% for msst3 and msst4 (Table 1). Hydrophobicity analyses have indicated that the ssts contain seven hydrophobic segments of about 25 amino acids that likely form transmembrane spanning α-helices (Meyerhof et al. 1991). Comparisons of the amino acid sequences with those contained in GenBank and EMBL databases clearly showed that the ssts form a small subfamily of receptors that is closest related to the subfamily of opioid receptors (Fig. 2). This structural relation is underscored by the observed pharmacological relationship showing that μ-receptor-acting opioids such as morphine and morphinomimetic peptide bind to SST receptors (Hatzogolu et al. 1995).

Table 1. Sequence divergence (%) of cloned ssts calculated with *DIVERGE* (Genetics Computer Group, Madison, USA)

hsst1	msst1	rsst1	msst4	rsst4	hsst4	msst3	rsst3	hsst3	msst2A	rsst2	psst	hsst2	bsst	hsst5	rsst5	
0.00	1.28	2.56	40.91	40.37	40.48	57.37	56.57	56.13	53.78	53.50	54.62	54.62	55.06	54.67	55.11	**hsst1**
	0.00	1.53	40.91	40.37	41.01	57.37	56.84	56.40	53.78	53.50	54.62	54.62	55.06	54.67	55.11	**msst1**
		0.00	40.91	40.37	41.01	57.37	57.10	56.40	53.50	53.22	54.34	54.34	54.78	54.96	55.40	**rsst1**
			0.00	4.17	13.02	60.37	59.84	58.38	55.06	54.78	55.62	55.62	54.65	50.14	51.43	**msst4**
				0.00	11.46	60.11	59.57	58.38	54.78	54.49	55.34	55.34	54.37	50.14	51.14	**rsst4**
					0.00	59.74	58.95	57.22	55.00	54.44	55.00	55.83	55.15	50.42	51.69	**hsst4**
						0.00	3.74	15.38	54.12	53.85	53.85	54.40	53.99	47.22	43.73	**msst3**
							0.00	13.94	53.85	53.57	53.85	53.57	53.44	46.39	42.62	**rsst3**
								0.00	53.06	53.33	52.50	52.78	52.65	44.10	41.41	**hsst3**
									0.00	1.90	4.61	6.23	5.71	46.80	45.96	**msst2A**
										0.00	5.42	7.05	5.71	46.80	46.24	**rsst2**
											0.00	3.52	3.26	47.35	46.52	**psst**
												0.00	5.16	46.80	45.68	**hsst2**
													0.00	47.21	46.65	**bsst**
														0.00	18.61	**hsst5**
															0.00	**rsst5**

bsst, bovine somatostatin receptor subtype; hsst, human somatostatin receptor subtype; msst, mouse somatostatin receptor subtype; rsst, rat somatostatin receptor subtype; psst, porcine somastatin receptor subtype.

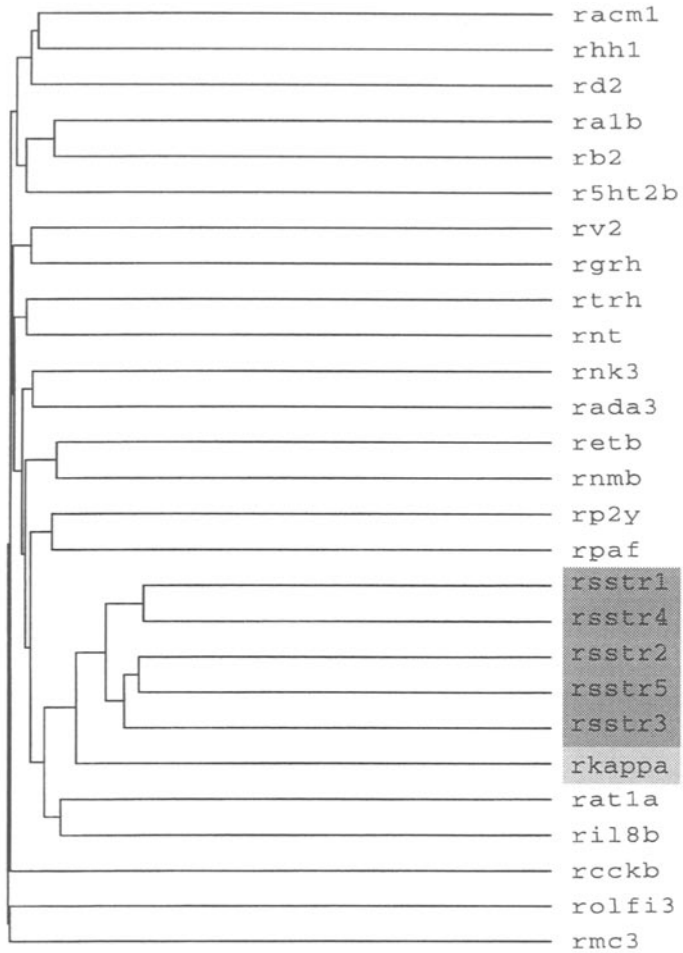

Fig. 2. Sequence relationship of various heptahelical receptors depicted in a dendrogram. The sequences of the rat muscarinic acetylcholine (*racm1*), histamine H1 (*rhh1*), dopamine D2 (*rd2*), α1b adrenergic (*ra1b*), β2 adrenergic (*rb2*), serotonin 5-HT2b (*r5ht2b*), vasopressin V2 (*rv2*), gastrin-releasing hormone (*rgrh*), thyrotropin-releasing hormone (*rtrh*), neurotensin (*rnt*), neurokinin 3 (*rnk3*), adenosine A3 (*rada3*), endothelin B (*retb*), neuromedin B (*rnmb*), purine p2Y (*rp2y*), platelet-activating factor (*rpaf*), sst1-sst5 (*rsstr1–rsstr5*), κ opioid (*rkappa*), angiotensin II AT1a (*rat1a*), interleukin 8b (*ril8b*), cholecystokinin B (*rcckb*), olfactory i3 (*rolfi3*), and melanocortin 3 (*rmc3*) have been compared using the pile-up program (Genetics Computer Group, Madison, Wisconsin, USA). The length of the lines corresponds to the degree of sequence divergence. The somatostatin receptor subtypes form a subfamily of receptors related to the opioid receptors. Sequences have been taken from GenBank, release 97

As observed for other G protein-coupled receptors, the sequences of the putative membrane-spanning domains (TM) and the intracellular connecting loops are more highly conserved among the five ssts than the extracellular N-terminal and the intracellular C-terminal domains. Furthermore, the ssts display most of the conserved sequence motifs common to class I of the heptahelical receptors such as the conserved GNXXV, LAXAD, SX_9DRY, $WXXSX_5P$, $FXXPX_7Y$, FXXCWXP, and NSXXNPXXY motifs in TM1–7, which likely contribute to the receptor topology (Figs. 3, 4). As other G protein-coupled receptors the sst subtypes contain between one and four consensus sequences for Asn-linked glycosylation sites in their N-terminal domains (Fig. 3). Noteworthy is that sst5 displays another glycosylation site in the second extracellular loop and sst2 in the upper part of TM6. Glycosylation was in fact demonstrated for rsst2 which had been purified from pituitary GH4C1 cells (Eppler et al. 1992). The 85-kDa glycoprotein was reduced in size to about 38 kDa by endoglycosidase F. Sequence comparisons further indicate that the five receptors can be distinguished into two subgroups: one comprising sst1 and sst4, the other sst2, sst3, and sst5 (see Fig. 2). This classification is supported by the pharmacological properties of the ssts (see below, and Hoyer et al. 1994). Two conserved cysteine residues in extracellular loops 1 and 2 may form a disulfide bond as is known for the β2-adrenergic receptor (Dohlmann et al. 1990). In the C-terminal domain following TM7 all ssts, except for sst3 (Fig. 3), contain an amino acid sequence motif (leucine, cysteine, leucine; LCL) that is palmitoylated in the β2- and α2-adrenergic receptors (O'Dowd et al. 1989; Kennedy and Limbird 1993). In these receptors the palmitoylation residue anchors the receptor to the membrane as might also be the case for the ssts, except for sst3. Modifications by fatty acids might well be of functional significance since it has been shown that palmitoylation affects agonist-dependent activation of the cellular effec-

Fig. 3. Alignment of the amino acid sequence of the cloned somatostatin receptor subtypes. Transmembrane segments were assigned following instructions of the SwissProt modeling interface and are *boxed*. Conserved cysteines are shown in *light gray*, the region of charged amino acids in sst3 in *intermediate gray*, N-linked glycosylation sites in *dark gray*. Phosphorylation consensus sequences for protein kinase A, protein kinase C, and casein kinase II are indicated by *dark gray fields* and *white letters*, *fat* and *bold letters* and *small letters* in *broken-line boxes*. Amino acid residues that have been analyzed by mutational analyses are indicated by *bold white letters* on *black background*

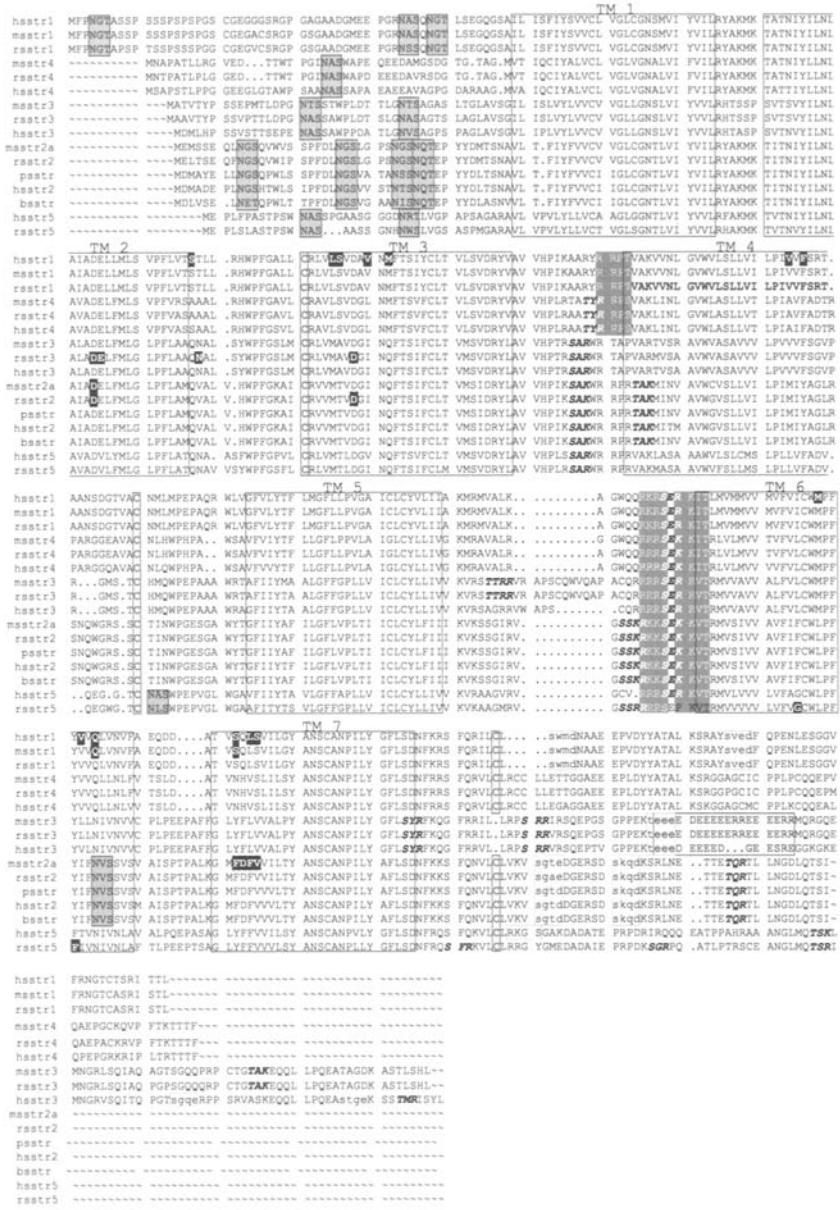
TM 1
TM 2
TM 3
TM 4
TM 5
TM 6
TM 7

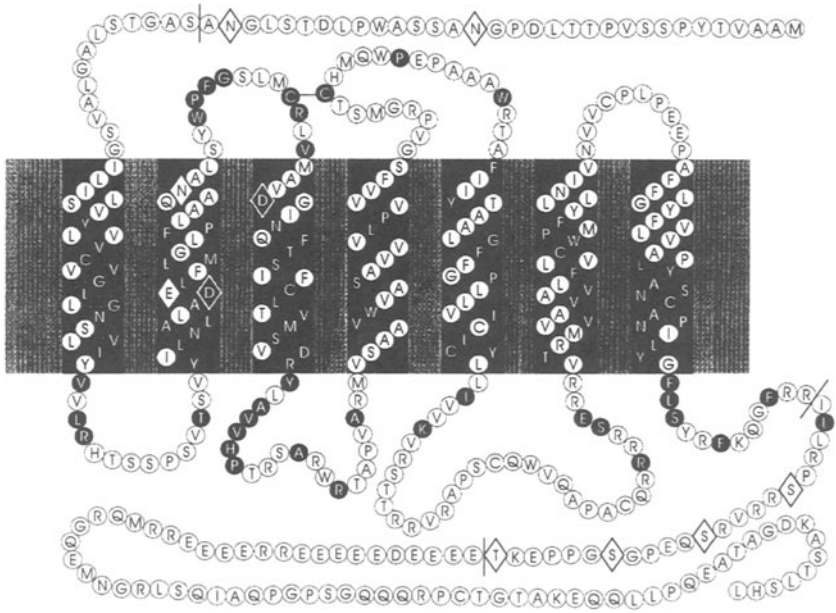

Fig. 4. Schematic representation of rat somatostatin receptor subtype (sst)3. Residues conserved in all ssts are indicated in *black*. Deletion mutants referred to in the text are marked by *lines* through the polypeptide chain. Amino acids that have been analyzed by point mutations are shown as *diamonds*

tors of the human endothelin A receptor (Horstmeyer et al. 1996). In addition to the sequence motifs that are also preserved in other seven helix receptors several motifs are unique to the ssts. Within TM7 the motif YANSCANP is found which may identify ssts. The sst1-4 display a glutamate residue in the unusual position adjacent to the conserved LAXAD motif in TM2, i.e., LAXADE. The sst3 contains a region of 18 consecutive amino acids rich in glutamic acid residues in its C-terminus of unknown significance. Scanning the PROSITE sequence motif database identified a number of consensus sequences for phosphorylation by protein kinase A, protein kinase C, and casein kinase II in the C-terminal regions and intracellular loops of all ssts (Fig. 3). Moreover, the presence of various serine and threonine residues in their intracellular loops and C-terminal domains suggests that the ssts may serve as substrates for other kinases such as receptor-specific kinases.

3.2
Chromosomal Location, Gene Structure, and Regulation

The chromosomal locations of the human sst subtypes have been determined. The five sst genes are scattered on different chromosomes, the genes for sst1-5 being located at 14q13, 17q24, 22q13.1, 20p11.2, and 16p13.3, respectively (Corness et al. 1993; Demchyshyn et al. 1993; Yamada et al. 1993; Yasuda et al. 1993; Panetta et al. 1994). The detection of highly informative simple tandem repeat polymorphisms in the sst1 and sst2 genes could facilitate genetic analyses of the corresponding loci (Yamada et al. 1993).

The observation of tissue and cell-type-specific distribution of sst1-5 mRNAs and of variations in sst mRNA levels during ontogenesis (see below) indicated that the sst genes are regulated in a spatial and temporal manner (Wulfsen et al. 1993; Hartmann et al. 1995; Thoss et al. 1995, 1996). Moreover, numerous reports demonstrate changes in the density of binding sites for SST and in sst mRNA levels in response to various extracellular stimuli. Kainic acid-induced limbic seizures led to decreased sst3 and sst4 mRNA levels specifically in the CA1 subfield, but not in other regions of the hippocampus, while sst1 and sst2 mRNAs were unaffected (Perez et al. 1995). Likewise, fasting/feeding affects sst1-3 mRNA but not sst4-5 mRNA levels in the rat pituitary and sst2 mRNA levels in the stomach (Bruno et al. 1994a; Sandvik et al. 1995). Steroids regulate sst gene expression in a complex manner in pituitary GH4C1 cells depending on the hormone used and the sst mRNA studied (Xu et al. 1995). The application of SST to GH_3 anterior pituitary cells or of epidermal growth factor or gastrin to pancreatic AR42 J cells caused an increase in SST binding sites which could be explained by elevated sst1-5 mRNA levels in the former system and by elevated sst2 and sst3 levels in the latter (Bruno et al. 1994b; Vidal et al. 1994). While in AR42 J cells the increase in sst levels were mediated by protein kinase C- and A-independent mechanisms, induction of cyclic adenosine monophosphate (cAMP) concentrations by forskolin increased sst2 mRNA levels in mouse AtT-20 pituitary cells (Patel et al. 1993). These observations indicate complex genetic regulation of the sst subtypes and have prompted the analyses of the structure and function of their genes.

As mentioned above, the sst genes are devoid of introns within their protein coding regions, with the exception of a cryptic intron in the msst2 gene (Vanetti et al. 1993). The presence of introns outside the coding

regions of the sst genes, however, has been observed. A comparison of the cDNA and gene sequences revealed that two introns of 3.1 kb and 0.19 kb are located between nucleotide positions -39 and -40, and positions -185 and -186, respectively, relative to the translational initiator codon of the rat sst3 gene (M. Gloos et al., manuscript in preparation). Both introns are flanked by the conserved nucleotide sequence motif GT/AG characteristic of splice donor and acceptor sites, respectively. Similarly, introns have been detected in the 5'-untranslated region of the mouse sst2 gene (V. Höllt, Magdeburg, personal communication), while introns have so far not been found in the corresponding regions of rat sst1 (Hauser et al. 1994) and sst4 (Xu et al. 1995) genes and the human sst2 (Greenwood et al. 1995) and sst5 genes (Greenwood et al. 1994).

Sequencing the putative promoter regions of rsst1 (Hauser et al. 1994), hsst2 (Greenwood et al. 1995), rsst3 (M. Gloos et al., manuscript in preparation), rsst4 (Xu et al. 1995), hsst5 (Greenwood et al. 1994), and msst5 (H. Baumeister et al., manuscript in preparation) revealed the lack of canonical TATA and CCAAT boxes 30 bp and 70 bp upstream of the initiation sites, respectively, and a high GC content in all subtype genes, which is quite common to genes of seven helix receptors. Searching for consensus sequences for binding sites of transcriptional activators identified various such sequence motifs. While most of these are unique to particular sst subtype genes, putative AP2 and GCF (factor binding to guanine- and cytosine-rich sequences) binding sites are common to all sst genes sequenced to date. Interestingly, in the case of the rsst1 gene two binding sites for the pituitary-specific transcription factor Pit-1 have been observed among others (Hauser et al. 1994). Pit-1 is known to control the expression of the prolactin-, growth hormone-, and thyroid-stimulating hormone (TSH)-β genes (reviewed in Anderson and Rosenfeld 1994). Binding of proteins in anterior pituitary GH_3-cell nuclear extracts to oligonucleotides containing these sequences has been demonstrated by electrophoretic mobility shift assays (Schäfer et al. 1996). These observations favor the attractive idea that a hormone and the receptors that control its release may be under common genetic control.

Functional studies that have been carried out using the hsst5 gene promoter showed that 0.9 kb DNA upstream of the initiator codon directed the expression of a reporter gene construct following transfection in GH_3 pituitary cells but not in Chinese hamster ovary (CHO) cells (Greenwood et al. 1994). Expression of the reporter gene was further increased by dibutyryl-cAMP. In the absence of the cAMP response ele-

ment (CRE) this effect has been attributed to mediation by activator protein (AP)1 and/or AP2 via their binding sites. Characterization of the hsst2 gene revealed that the minimal region necessary for transcriptional activity, in various neuronal cell lines, of its promoter is located between +4 and −22 of the transcription initiation site (Pscherer et al. 1996). Within this region the novel initiator element SSTR2inr has been identified. Transcriptional activity of this element is dependent on the presence of a binding site, termed E-box, for basic helix-loop-helix transcription factors. A member of this class of transcription factors, SEF-2, has been demonstrated to bind to the E-box of SSTR2inr and activate transcription from SSTR2inr. The observed specific interaction of SEF-2 with transcription factor IIB suggests that SEF-2 might activate transcription by recruiting the basal transcription machinery onto the SSTR2inr (Pscherer et al. 1996). However, the observation that the SSTR2inr is transcriptionally inactive in HeLa cells even when cotransfected with SEF-2-encoding constructs suggests that additional factors are required for full transcriptional activation of the SSTR2inr.

4 Pharmacology

4.1 Ligand Binding Studies

All sst receptors bind SST-14 and SST-28 with high affinity and little selectivity, although preferential binding of SST-28 has initially been reported for rsst5 (O'Carroll et al. 1992). However, reevaluation of rat sst5 could only demonstrate a very slight, fourfold preference of this receptor for SST-28 (Coy et al. 1998), which is comparable to that observed for rsst3 (Meyerhof et al. 1992). Thus it is clear that the development of receptor-selective ligands offers a valuable approach to establishing the physiological roles of the sst subtypes. In fact, large numbers of linear and cyclic peptide analogs that are metabolically stabilized by the introduction of d-amino acids have been synthesized. Some of the analogs contain tyrosine residues which, following iodination, can be used for radioligand binding studies. Since structure-function studies have shown that the two amino acids Trp8 and Lys9 in the natural SST peptides are necessary for high-affinity SST receptor binding (reviewed by Brazeau et al. 1972; Epelbaum 1986),

Table 2. Ligand binding properties of various cloned ssts for selected ligands. Data are taken from Coy et al. (1997), Viollet et al. (1997), and Liapakis et al. (1996a). In the case of CH-275 IC50 values are shown, for the other compounds Ki values are given (nM)

Peptide	Sequence[a]	hsst1	msst2	rsst2	msst2	rsst3	hsst4	hsst5	rsst5
SRIF	AG[CKNFFWKTFTSC]-OH	2.25	0.23	1.43	1.43	1.33	1.76	1.41	4.46
SRIF-28	HSANSNPAMAPRYRKAG[CKNFFWKTFTSC]-OH	2.38	0.29	1.78	1.02	0.81	7.93	0.38	1.02
SMS-201-995	**F**[CFWKTC]Tol	875	0.57	2.0	35	14.0	>1000	6.78	17.0
MK-678	[WKVFNMeAY]	>1000	0.13	0.48	88	45.0	>1000	15.5	72.0
RC-160	**F**[CYWKVC]W-NH2	481	0.57	0.85	795	87.0	351	7.53	6.8
BIM-23014	**Nal**[CYWKVC]T-NH2	2414	0.75	1.47	121	115	1826	5.21	23.0
BIM-23023	**F**[CYWKAbuC]T-NH2	6610	0.42	0.57	89	92.0	2700	4.18	14.0
BIM-23052	**FFF**WKTFT-NH2	97	11.9	69.0	5.58	3.5	126	1.22	2.4
BIM-23056	**FFY**WKVF**Nal**-NH2	692	132	3400	177	272	174	12	536
BIM-23268	[CFFWKTFC]-NH2	582	1.49	101	11	4.1	174	2.18	3.4
BIM-23295	[CFYWKTFC]-NH2	86.8	6.19	57.0	318	5.7	3.36	0.34	0.65
BIM-23313	[CFIYWKTFC]-NH2	151	4.78	45.0	115	11.2	55.3	0.27	9.88
L-362,855	[AhepFWWKTF]	993	2.96	12.0	98	33.0	467	0.76	51.0
		hsst1[b]	hsst2	rsst2	msst2	rsst3	hsst4	hsst5	rsst5c
CH-275	[CKFFWIAmpTFTSC]	1.8; 4.9	>1000	>1000	>1000	577	874	--	632; 279

hsst, Human somatostatin receptor subtype; msst, mouse somatostatin receptor subtype; rsst, rat somatostatin receptor subtype.
[a]Amino acid residues shown in bold denote d-amino acids.
[b]The values of 1.8 and 4.9 nM have been derived following transfection of hsst1 cDNA into COS and CHO cells, respectively.
[c]The values of 632 and 279 nM have been derived following transfection of rsst5 cDNA into CHO and HEK cells, respectively.

this motif is also present in almost all synthetic SST analogs (Table 2). Two of the synthetic analogs, MK678 (seglitide), a cyclic hexapeptide analog, and SMS 201–995 (octreotide, sandostatin), a cyclic octapeptide, have been used to distinguish between two types of binding sites for SST in native membranes, SS_A and SS_B, or $SRIF_1$ and $SRIF_2$ sites of high or low affinity for the two peptides, respectively (Reubi 1984; Tran et al. 1985; Martin et al. 1991). Following cloning of the five ssts, the synthetic analogs have been employed in binding to cells transfected with individual sst subtypes (Raynor et al. 1993b). However, the use of different cell lines, sst cDNAs from different species, and different radiolabeled reference peptides, as well as different binding assays in these studies, has caused problems in the reconciliation of data from different laboratories (Bruns et al. 1996). For instance IC_{50} values for BIM 23056 that have been reported vary from 0.02 nM to 100 nM and 380 nM for mouse, human, and rat sst3, respectively (Reisine and Bell 1995; Bruns et al. 1996; Viollet et al. 1997).

However, a critical reevaluation of the binding properties of a number of key agonists using ssts from different species carried out in one laboratory is now being accomplished (Coy et al. 1998). The data show (see Table 2) that there are in fact marked species differences. Notably L-362,855 displays an approximately 70-fold higher affinity for rsst5 than for hsst5. Moreover, it is also clear from the table that most compounds are only of limited selectivity for an individual sst subtype being of reasonably high affinity for sst2, sst3 and sst5 and of low affinity for sst1 and sst4. BIM23295 may be an interesting and exceptional compound that has high affinity for sst4, sst2, and sst5, but not for sst1 and sst3. Recently a compound, des-$AA^{1,2,5}$[D-Trp^8, $IAMP^9$, D-Ser^{13}]SST-14 was described with higher affinity for hsst1 than other cloned ssts (Liapakis et al. 1996a). However, the selectivity of this compound for rsst1 was less pronounced (Viollet et al. 1997). As a consequence compounds with (limited) selectivity for sst1, sst2, and sst5 are available and there is still a complete lack of sst3 and sst4 selective agonists.

The identification of distinct functions of the ssts has also been hampered by the lack of high-affinity antagonists. Recently the identification of novel disulfide-linked cyclic octapeptide antagonists of SST was described that contain a core structure of a DL-cysteine pair at positions 2 and 7 of the peptides (Bass et al. 1996). One of these peptide antagonists, [Ac-4-NO2-Phe-c(D-Cys-Tyr-D-Trp-Lys-Thr-Cys)-D-Tyr-NH2], displays a binding affinity to SST2 comparable with that observed for the native hormone and reverses SST-mediated inhibition of cAMP in cells transfected with

the sst2 and sst5 cDNAs, as well as SST-stimulated growth of yeast cells expressing the sst2 subtype. This novel class of SST antagonists will probably be useful for determining the individual physiological functions of the ssts.

Besides the peptide analogs, synthesis of the first nonpeptide analog has been reported recently by Papageorgiou and Borer (1996). They describe a new ligand with a benzodiazepinone structure and high affinity to sst receptors. The complete displacement of radioiodinated octreotide with this new ligand from its receptor occurred at 4–10 μM. The calculated IC_{50} value for this new ligand is about 7 μM. Also, three alkaloids isolated from two marine sponges have been found to exhibit quite high affinity for SST receptors (Vassas et al. 1995). Xestospongine B, sceptrine, and ageliferine have a high affinity for sst (IC_{50}=12 μM, 0.27 μM, and 2.2 μM, respectively). Due to the interaction between these nonpeptidic compounds and SST receptors, these three alkaloids might become promising agents in the research into natural nonpeptidic compounds for therapeutic interventions.

4.2 Mutational Analyses

Stable analogs of SST, such as octreotide, are widely being used in the diagnosis and symptomatic therapy of several neuroendocrine tumors (Lamberts et al. 1995). However, octreotide does not act on all ssts, but instead displays a clear subtype selectivity (Coy et al. 1998). Thus, for a rational design of new selective ligands also for the other sst subtypes a detailed understanding of receptor-ligand interactions of the ssts has been approached by mutational analyses (see Fig. 3; the mutated residues are indicated in white letters on black background).

The functional importance of the carbohydrate components of SST receptors has been analyzed by lectin-affinity chromatography and digestion with glycosidases of receptor preparations solubilized from rat brain and mouse pituitary AtT-20 cell membranes (Rens-Domiano and Reisine 1991). These experiments suggested that sialic acid residues, but not high mannose, N-acetylgalactosamine, fucose, and O-linked carbohydrates, were associated with SST receptors. Enzymatically desialylated SST receptors remained functionally active and coupled to guanosine triphosphate (GTP)-binding proteins, but exhibited a reduced affinity for agonists. Receptor glycosylation was recently supported by experiments with antibod-

ies directed against the cloned sst2A and sst3. In Western blot experiments using membranes of transfected cell lines the antibodies stained bands that displayed the typical broad shape of glycosylated proteins (Nehring et al. 1995; Dournaud et al. 1996). However, the sst3 antibody detected sharp bands when a mutant of rsst3 (see Fig. 4) was used for transfection in which the two consensus sequences for Asn-linked glycosylation were abolished (R.B. Nehring et al., unpublished observation). Moreover, this mutant displayed a fourfold reduced affinity for radiolabeled SST-14 while it remained functionally coupled to AC.

Structure-function studies have shown that the two amino acids Trp8 and Lys9 in the SST peptide are necessary for high-affinity SST receptor binding (reviewed by Brazeau et al. 1972; Epelbaum 1986). This motif is also present in almost all SST analogs (Trp as d-amino acid; see also Table 2). As outlined above, sequence comparisons have shown that the highest similarities between the ssts occur within the putative transmembrane domains. The aspartic acid residue which is highly conserved in TM3 of the G protein-coupled receptors appears to be directly involved in ligand binding. In adrenergic and muscarinic receptors it interacts with the cationic ammonium groups of agonists (Frazer et al. 1989; Strader et al. 1988; Curtis et al. 1989; Kurtenbach et al. 1990). Site-directed mutagenesis (Nehring et al. 1995) presented evidence that Asp124 is directly involved in the binding of SST-14 by rsst3, probably by forming an ion pair bond with the positively charged amino acid residues Lys4 or 9 of SST-14. By restoring high-affinity binding of radiolabeled Asp9-Tyr11-SST-14 to the msst2 mutant Asp122Lys, Strnad and Hadcock (1995) showed that Asp122 in TM3 of rsst2 represents one contact site between this receptor subtype and SST-14. These data are supported by a molecular model of the SST receptor-ligand interaction (Kaupmann et al. 1995) which predicts that the corresponding residue Asp137 of human sst1 forms an ion pair bond with Lys9 of SST-14. Thus, forming an ion pair bond between the conserved Asp in TM3 and Lys9 in SST-14 (or the corresponding Lys in the analogs) probably constitutes an important initial step in the binding of all SST peptides to all sst subtypes.

As mentioned above, sst2, sst3, and sst5 display high affinities for octapeptides and hexapeptides, while sst1 and sst4 do not. Peptide-selective binding to ssts is probably determined by the extracellular loops and the upper parts of transmembrane domains. Chimeras of msst1 and msst2 revealed the presence of determinants in a region encompassing the second and third extracellular loops that are responsible for selective binding

of the hexapeptide MK678 (Fitzpatrick and Vandlen 1994). Further studies delineated the region conferring selective binding of the octapeptides such as NC4–2B and octreotide and hexapeptides such as MK678 and BIM23027 to msst2 to the third extracellular loop and its surrounding transmembrane regions (Liapakis et al. 1996b). Within this region exchange of Phe-Asp-Phe-Val (294–297) by the corresponding residues of msst1 Ser-Gln-Leu-Ser (305–308) abolished high affinity binding of several synthetic peptides to the mutant (Liapakis et al. 1996b). Moreover, when in hsst1 and msst1 Ser305 of this motif is replaced by Phe, the corresponding amino acid of sst2, the affinities for octapeptides were enhanced in the mutant (Kaupmann et al. 1995; Liapakis et al. 1996b), while the effect on binding of hexapeptides was less clear. Binding of only some but not all analogs that have been tested was improved. It turned out that only hexapeptides with a phenylalanine adjacent to the D-Trp appear to interact with Phe294 of sst2. Hexapeptides with a tyrosine in that position, such as MK678 and BIM23027, did not interact with this Phe residue in the receptor molecule (Liapakis et al. 1996b). This finding implies that different residues in the receptor molecule mediate the binding of the individual ligands. A double mutant of hsst1 that in addition contained a glutamine-asparagine exchange in TM6 in position 291 further enhanced octreotide binding. In contrast, binding of the sst1 selective peptide des-$AA^{1,2,5}$-[D-Trp^{8}, $IAMP^{9}$]SST-14 is greatly determined by extracellular loop 2 since transplantation of this loop from msst1 to msst2 results in an over 100-fold enhanced affinity (Liapakis et al. 1996b). The importance of the second and third extracellular loop for the binding of octapeptide and hexapeptide analogs, but not of SST-14, to the sst subtypes is also supported by rsst3 mutants in which Asn105 on top of TM2 has been replaced by a serine or threonine. These mutants display reduced affinity for SST-14, while binding of octreotide and MK678 is not affected (R.B. Nehring et al., manuscript in preparation).

The region encompassing TM6 through the C-terminus in sst5 may also be critical for the lower binding affinity of SST-14 in comparison to SST-28. Exchange of this region with the corresponding region of sst2 produced chimeric receptors with high affinity for both SST-28 and SST-14. On substitution of Phe265 on top of TM6 in sst5 with a tyrosine, the corresponding residue of the other ssts improved the binding of SST-14 to an affinity comparable to that observed for sst2 (Ozenberger and Hadcock 1995). These findings suggest that the tyrosine in TM6 may be an important contact point between SST-14 and sst subtypes.

Agonist binding to various receptors including SST receptors is modulated by sodium ions (Reubi and Maurer 1986). Experiments with cloned ssts revealed that agonist binding to sst1 and sst4 is not sensitive to Na^+, while it is sensitive in the cases of sst2, sst3, and sst5 (Raynor et al. 1993a,b). All ssts exhibit a conserved aspartate residue in TM2. Exchange of these residues, Asp89 and Asp91, to Asn in msst2A and rsst3, respectively, caused the loss of Na^+ inhibition of agonist binding to this receptor. While the characteristics of ligand binding and G protein-coupling remained unchanged in the case of msst2 (Kong et al. 1993), in rsst3 the affinities to the natural peptides SST-14 and SST-28 decreased tenfold and to octreotide and MK678 about 20-fold. Likewise, G protein-coupling and inhibition of AC were impaired (R.B. Nehring et al., manuscript in preparation). All ssts, except for sst5, display a glutamate in TM2 adjacent to the conserved aspartate. Exchange of this residue Glu92 in rsst3 to Gln, Val or Leu increased Na^+ sensitivity of agonist binding in the order wild-type lu92Leulu92Glnlu92Val, while only little effect was seen on G protein-coupling and inhibition of AC (Nehring et al. 1996).

5
Signal Transduction Mechanisms

5.1
G Protein- and Effector-Coupling in Native Membranes

It is well established that the binding of SST to its receptors in native membranes results, indirectly, in the modulation of various cellular effector proteins such as AC (Jakobs et al. 1983; Koch and Schonbrunn 1984), potassium channels (Wang et al. 1987, 1989; Yatani et al. 1987), and calcium channels (Rosenthal et al. 1988; Ikeda and Schofield 1989; Wang et al. 1990a). It has also been reported that SST influences a Na^+/H^+ exchanger (Barber et al. 1989), cGMP-dependent protein kinases (Meriney et al. 1994), and tyrosine phosphatases (Viguerie et al. 1988; Colas et al. 1992; Pan et al. 1992). SST receptors mediate their effects by coupling to and activation of heterotrimeric G proteins which, among other things, is indicated by the observations that GTP decreases their affinity to the peptide (Koch and Schonbrunn 1984). Pertussis toxin (PTX)-sensitive and -insensitive G proteins or pathways have been reported to couple SST receptors to their cellular effectors (Koch and Schonbrunn 1984; Koch et al. 1985; Barber et

al. 1989; Viguere et al. 1989; Twery et al. 1991; Feniuk and Humphrey 1994). These observations suggested that the SST receptors are coupled to distinct effectors via specific signaling mechanisms. For a comprehensive understanding of the cellular mechanisms induced by SST, various attempts are being made to link the SST receptors to specific G proteins and these, in turn, to specific cellular effector molecules. Antibodies, antisense constructs, or antisense oligonucleotides directed against G protein subunits were used to demonstrate that G_o-, G_{i1}-, G_{i2}-, and G_{i3}-type proteins interact with native SST receptors in membranes of different organs or cell lines (Law et al. 1991; Murray-Whelen and Schlegel 1992; Tallent and Reisine 1992; Brown and Schonbrunn 1993; Luthin et al. 1993; Seaquist et al. 1995; Degtiar et al. 1996). In combination with functional studies native SST receptors were linked via $G\alpha_{i1}$, $G\alpha_{i2}$, and $G\alpha_{i3}$ to the inhibition of AC in mouse AtT-20 and rat GH_4C_1 cells (Tallent and Reisine 1992; Liu et al. 1994; Senogles 1994) and $G\alpha_{i3}$ to an inwardly rectifying 55 pS (picoSiemens) potassium channel in GH_3 cells (Yatani et al. 1987). In an elegant series of studies microinjection of antisense oligonucleotides specific for individual G protein subunits has been used to target the exact G protein heterotrimer that couples SST responses to the inhibition of calcium channels. Surprisingly, a specific triplet, $G\alpha_{o2}/\beta_1/\gamma_3$, was identified to mediate this effect in GH_3 anterior pituitary cells (Kleuss et al. 1991–1993) and also in rat insulinoma RINm5F cells (Degtiar et al. 1996).

5.2 Signal Transduction Mediated by Somatostatin Receptors in Transfected Cell Lines

These investigations did not identify the individual SST receptor subtypes that were involved in a particular signal transduction pathway. The cloned ssts have been analyzed for their ability to modulate cellular effector molecules following transfection in various cell lines devoid of endogenous SST receptors. The use of sst cDNAs from different species, of different cell lines, and different assay conditions in different laboratories made it difficult to reconcile all the results. Moreover, the high amounts of receptors that are usually present in transfected cells may favor a less selective G protein-coupling as it occurs in vivo which complicates the interpretation of the results. In general these studies revealed that ssts may be coupled to multiple cellular effectors (a summary of the data is shown in Table 3). The initial observation that agonist binding to sst1 is insensi-

Table 3. Summary of the suggested G protein/effector coupling of cloned somatostatin receptor subtypes (sst)

Receptor subtype	Transducer		Effector	
sst1	PTX insensitive		Na^+/H^+ exchange –	
	PTX sensitive		PLC+	
			PTP	
	$G\alpha_{i3}$		AC–	
sst2	PTX sensitive		PTP, PLC	
	$G\alpha_{i1}$		AC–	
	$G\alpha_{i2}$		?	
	$G\alpha_{i3}$		K^+ channel	
	$G\alpha_{o(2\beta1/\gamma2)}$		Ca^{++} channels	
sst3	$G\alpha_{i1}$	β/γ	AC–	PLC-β3+
	$G\alpha_o$	β/γ	AC–	PLC-β3+
	$G\alpha_{14}$, $G\alpha_{16}$		PLC+	
sst4	PTX sensitive		AC–, MAP kinase cascade	
sst5	PTX sensitive		AC–, PLC+	
			Serine/threonine phosphatase + protein	

PTX, pertussis toxin; PLC, phospholipase C; PTP, phosphotyrosine phosphatase; AC, adenyl cyclase; MAP, mitogen-activated protein (kinase).
+, Effector stimulation; –, effector inhibition.

tive to guanine nucleotides and PTX treatment and does not result in inhibition of forskolin-stimulated AC (Rens-Domiano et al. 1992; Raynor et al. 1993b) has only been confirmed since by some reports (Buscail et al. 1994; Tomura et al. 1994; Castro et al. 1996), but the majority of investigations showed inhibition of AC in a PTX-sensitive manner (Kaupmann et al. 1993; Garcia and Myers 1994; Hadcock et al. 1994; Hershberger et al. 1994; Hou et al. 1994; Kubota et al. 1994; Patel et al. 1994a). The sst1-mediated inhibition of AC may be transduced via $G\alpha_{i3}$ (Kubota et al. 1994). The sst1 transfected in CHO cells has also been shown to stimulate inositol-phosphate formation (Kubota et al. 1994) and phosphotyrosine phosphatase activity in a PTX-sensitive fashion (Buscail et al. 1994; Florio et al. 1994).

sst1 also mediated SST inhibition of Na^+/H^+ exchange activity in transfected human embryonic kidney HEK293 cells or mouse fibroblast Ltk^- cells and this action was insensitive to PTX (Hou et al. 1994). Two chimeric receptors have been used to identify molecular determinants unique to sst1 that may confer coupling to the exchanger. A sst2/sst1 chimera contained a sst1 segment encompassing determinants within the fifth and sixth hydrophobic domains and the entire third cytoplasmic loop. The other chimeric sst2/sst1 receptor contained a sst1 segment spanning the second through sixth hydrophobic domains, including the second and third cytoplasmic loops. Although both chimeric receptors mediated SST inhibition of cAMP accumulation, only the latter mediated the PTX-insensitive inhibition of Na^+/H^+ exchange. Therefore, the ability of sst1 to selectively attenuate Na^+/H^+ exchange activity requires determinants outside the third cytoplasmic domain. Most studies have indicated that seven helix receptors, including ssts, couple to G proteins through determinants in the third cytoplasmic loop (Kobilka et al. 1988; Reisine et al. 1994). However, it has also been observed that intracellular loop 2 contains determinants that specify G protein coupling. For instance, in chimeras of β_1-adrenergic and muscarinic cholinergic receptors m1 or m2, the intracellular loops 2 and 3 of the parent receptor is required for a specific G protein-coupling, while chimeras that contain only the third intracellular loop from a parent receptor coupled promiscuously (Wong and Ross 1994).

Binding of agonists to sst2 is reduced by GTP and PTX treatment (Rens-Domiano et al. 1992). Also, in the case of sst2 efficient coupling to AC of this subtype could (Kaupmann et al. 1993; Strnad et al. 1993; Garcia and Myers 1994; Hershberger et al. 1994; Hou et al. 1994; Patel et al. 1994; Tomura et al. 1994; Roosterman et al. 1997) or could not be demonstrated (Reisine et al. 1993; Castro et al. 1996). In part these discrepancies may be explained by the existence of the two sst2 isoforms, sst2A and sst2B, which differ in their coupling efficiency to AC (Reisine et al. 1993; Vanetti et al. 1993). The contradiction may also be explained by the presence of different G protein subunits in the various cell lines used for transfection and by the sst2/G protein-coupling specificity. An sst2A-specific antiserum and antisera directed against specific G protein subunits were used to immunoprecipitate the receptor/G protein complexes from transfected cells that contained the sst2A receptor. These studies showed an association of sst2A with $G\alpha_{o2}$, $G\alpha_{i1}$, $G\alpha_{i2}$ and $G\alpha_{i3}$ (Law et al. 1993; Gu and Schonbrunn 1997). In CHO cells with low levels of $G\alpha_{i1}$ and $G\alpha_{i2}$, sst2A strongly and selectively associates with $G\alpha_{i3}$ and $G\alpha_{o2}$ and its activation by SST-14 did not

inhibit AC activity (Rens-Domiano et al. 1992; Law et al. 1993). However, when exogenous $G\alpha_{i1}$ was coexpressed with sst2A in the same cell line this receptor subtype efficiently inhibited AC (Kagimoto et al. 1994), suggesting that G_{i1} coupled sst2A to AC under these conditions. Moreover, in view of the observed ability of sst2B to inhibit AC in CHO cells (Vanetti et al. 1993), it may be concluded that the short splice variant, sst2B, couples to G_{i1}. The association of sst2A with $G\alpha_{i3}$ and $G\alpha_{o2}$ suggests a linkage of this receptor subtype to potassium and calcium channels (Yatani et al. 1987; Kleuss et al. 1991). These experiments identified only the G protein α subunits that associate with sst2A and not the exact G protein triplets, raising the possibility that complexes with particular $\beta\gamma$ complexes may determine the exact nature of receptor/effector coupling and thereby resolve the apparent contradiction. In sst2-expressing cells, SST not only inhibited forskolin-induced cAMP accumulation but also stimulated phospholipase C (PLC) activity and calcium mobilization. While the former response was fully sensitive to PTX the latter was only partially sensitive (Tomura et al. 1994). Consistent with the coupling to $G\alpha_{o2}$, sst2 also induces the inhibition of high-voltage-activated calcium channels in transfected RINm5F cells (Fujii et al. 1994), and in RINm5F and AtT-20 cells that endogenously contain this subtype (Degtiar et al. 1996; Tallent et al. 1996a). The observed inhibition of cell proliferation by the SST analog RC-160 is, at least in part, mediated by sst2 via phosphotyrosine phosphatase activity (Buscail et al. 1994, 1995).

It is undisputed that agonist binding to sst3 is sensitive to GTP and results, in a PTX-sensitive manner, in the inhibition of AC (Yamada et al. 1992; Yasuda et al. 1992; Kaupmannn et al. 1993; Law et al. 1994; Rooosterman et al. 1997), an effect that seems to be mediated by $G\alpha_{i1}$ (Law et al. 1994). The G protein-coupling ability of sst3 has recently been examined in an alternative approach using chimeric G protein α subunits (Komatsuzaki et al. 1997). In the chimeras the C-terminal 5 residues of $G\alpha_s$,which are known to be involved in receptor binding, were replaced by the corresponding C-terminal region of each known $G\alpha$ subunit. Testing the constructs for their ability to confer sst3-mediated activation of AC revealed that this receptor subtype recognized the termini of $G\alpha_{i1/2}$, $G\alpha_{14}$, and $G\alpha_{16}$, but not that of $G\alpha_o$, $G\alpha_z$, $G\alpha_q$, and $G\alpha_{11}$. In line with this prediction activated sst3 stimulated polyphosphoinositide hydrolysis only when $G\alpha_{14}$ and $G\alpha_{16}$ were coexpressed (Komatsuzaki et al. 1997). Activation of PLC and calcium mobilization by all cloned human ssts transfected in COS-7 cells was described by Akbar et al. (1994), although the isoenzymes in-

volved have not been identified. In intestinal smooth muscle cells that endogenously express only sst3, SST inhibited AC and stimulated inositol-trisphosphate formation, calcium release, and contraction (Murthy et al. 1996). The latter effects were inhibited by pretreatment with antibodies to PLC-β3 but not with antibodies to other PLC-β isoezymes. They were also diminished by antibodies to the G protein β subunit but not to G protein α_i and α_o subunits. These results are in line with the observation that efforts to identify PTX-sensitive G protein α subunits that activate phosphatidylinositol-phospholipase C isoenzymes have generally been unsuccessful. It is now considered that stimulation of phosphatidylinositol biphosphate hydrolysis by the PTX-sensitive G proteins, G_i and G_o, involves their βγ subunits (Exton 1996). Inhibition of cAMP formation was partially blocked by $G\alpha_{i1}$ and $G\alpha_o$ antibodies and additively blocked by a combination of both antibodies. SST-induced ^{35}S-GTPγS-Gα complexes in plasma membranes were bound selectively by $G\alpha_{i1}$ and $G\alpha_o$ antibodies (Murthy et al. 1996). The authors concluded from these results that in smooth muscle sst3 is coupled to G_{i1} and G_o. Their α subunits mediate the inhibition of AC, while the βγ subunits mediate activation of PLC-β3. Both $G\alpha_i$ and $G\alpha_o$ subunits are known to be moderately effective inhibitors of Ca^{2+} – calmodulin-stimulated AC type I. $G\alpha_i$, in addition, also inhibits type V and VI AC (for review see Sunahara et al. 1996).

As in the case of sst1, agonist binding to sst4 has and has not been shown to be sensitive to GTP and PTX; similarly, inhibition of AC was and was not observed (Demchyshyn et al. 1993; Raynor et al. 1993a; Kaupmann et al. 1994; Roosterman et al. 1997). In transfected cells, sst4 was functionally coupled, in a PTX-sensitive fashion, not only to inhibition of AC, but also to activation of arachidonate release and mitogen-activated protein kinase cascade (Bito et al. 1994; Shimizu et al. 1996). These effects were accompanied by the phosphorylation of 85-kDa cytosolic phospholipase A_2 and were inhibited by the phosphatidylinositol-3-phosphate kinase inhibitor wortmannin.

Activation of sst5 is sensitive to GTP and PTX and results in the inhibition of AC (O'Carroll et al. 1992, 1994; Raynor et al. 1993a; Panetta et al. 1994). Native sst5 also inhibits L-type Ca^{2+} current in pituitary AtT-20 cells (Tallent et al. 1996a). In addition, sst5 is involved in the inhibition of cell proliferation by the analog RC-160 (Buscail et al. 1995). This action, however, is mediated via a different pathway than that observed for sst2 and does not involve phosphotyrosine phosphatase activity. The observation that RC-160 inhibited cholecystokinin-stimulated intracellular calcium

mobilization and cell proliferation in cells expressing sst5 but not in cells expressing sst1, sst2, sst3, or sst4 suggested that the inositol phospholipid/calcium pathway could be involved in the antiproliferative effect of sst5 (Buscail et al. 1995). Further support for this assumption comes from studies in GH_3 cells which express, endogenously, multiple sst subtypes (Bruno et al. 1993; Hauser et al. 1994). In these cells phorbol ester treatment resulted in cellular proliferation, binding of transcription factor AP-1 to DNA, and transcriptional activity (Todisco et al. 1995). These effects were inhibited in a PTX-sensitive manner by the sst2- and sst5-specific SST analog octreotide. In the presence of two different phosphatase inhibitors sodium orthovanadate, an inhibitor of phosphotyrosine phosphatases, or okadaic acid, an inhibitor of serine/threonine protein phosphatases 1 and 2A, the ability of SST to inhibit AP-1 binding and transcriptional activity was abolished. However, only the serine/threonine phosphatase inhibitor blocked the antiproliferative effect of SST (Todisco et al. 1995). Since sst2 has been shown to inhibit proliferation via phosphotyrosine phosphatases (Buscail et al. 1994, 1995), it may be assumed that the sst5 pathway involves serine/threonine protein phosphatases.

The patterns of effector modulation by the six sst variants are complex, at present not fully understood, and partially contradictory. Only certain aspects such as the coupling of sst2 and sst5 via G_o to calcium channels seems to be quite evident. Clarification of the signal transduction components will certainly require further studies using cloned, recombinant ssts in transfected cell lines, specific antibodies, and strictly subtype-specific agonists and antagonists for analyzing sst receptor action in native membranes, tools which are restricted at present. To date many of the disputed signal pathways have not even been fully characterized. In all studies using cloned ssts the participating $\beta\gamma$ complexes are not yet identified, although their importance in coupling specificity has been recognized (Kleuss et al. 1991, 1992, 1993). Furthermore, the sst-mediated inhibition of the AC system was only analyzed by measuring the reduction in forskolin-stimulated cAMP levels, although nine different AC variants (AC type I to AC type IX) are known so far (Sunahara et al. 1996). These comprise at least three different classes that are differently regulated, positively and negatively, in response to various G protein α or $\beta\gamma$ subunits, calcium/calmodulin, and protein kinases (Sunahara et al. 1996). It has been shown that the calcium stimulation of AC type I is inhibited by activation of G_i-coupled SST receptors. This inhibition was due primarily to $G\alpha_i$ and not $\beta\gamma$ subunits. Interestingly, AC type VIII, another calcium-stimulated AC, was

not inhibited by the G_i-coupled receptors. These data indicate that AC type I and AC type VIII are differentially regulated by G_i-coupled receptors and hence are of relevance for understanding sst signaling. It also has to be considered that the G proteins activated by the ssts at the same time also stimulate other effectors. In particular, all ssts affect phospholipase C, an enzyme family comprising at least four mammalian β forms, two γ variants and three δ isoforms (Exton 1996). The β enzymes are regulated by G proteins in both a PTX-sensitive and -insensitive fashion. The βγ complexes released from G_i and G_o proteins probably mediate the PTX-sensitive response and stimulate PLC-β2 and PLC-β3, while the PTX-insensitive responses are mediated, via PLC-β1 and PLCβ-3, by α subunits of the G_q family, G_q, G_{11}, G_{16} (Exton 1996). G_{11} and G_{16} have been identified as associating with sst3 (see above). Therefore, these pathways are important for interactions between the calcium and cAMP signal transduction systems activated by the SST receptors.

5.3 Desensitization and Internalization of Somatostatin Receptors

As outlined above, the five ssts display similar affinities for the two naturally occurring peptides but differ for the synthetic ligand octreotide. This compound is being used in the symptomatic therapy of several neuroendocrine tumors and in SST receptor scintigraphy (Lamberts et al. 1987; Weckbecker et al 1993; Lamberts et al. 1995). Octreotide binds only to sst2 and sst5 with high affinity and to sst3 with lower affinity. The analog does not bind to sst1 and sst4 (Hoyer et al. 1994; Reisine and Bell 1995). Two observations suggest that not only receptor-agonist interactions might be of clinical relevance but also receptor internalization, desensitization and/or down-regulation. Firstly, receptor scintigraphy is performed 24–48 h following injection of the radiolabeled SST analog (Baker et al. 1991) and hence probably detects not only receptor-ligand interactions but also internalized ligands. Secondly, most patients with neuroendocrine tumors of the pituitary and gastroenteropancreatic tissues do respond effectively to octreotide. However, in few cases the response is diminished in the course of the therapy due, at least in part, to downregulation of receptors (Bertherat et al. 1992; Haraguchi et al. 1995). In fact, uptake of radiolabeled octreotide and fluorescence-labeled BIM-23027 was observed in mouse and human pituitary tumor cells and in Neuro2A

neuroblastoma cells, respectively (Hofland et al. 1995; Koenig et al. 1997), suggesting a receptor-dependent internalization of the agonists.

Previous electrophysiological studies on CNS neurons and investigations of the inhibition of hormone release from anterior pituitary AtT-20 cells have revealed that SST signaling desensitizes in response to prolonged agonist stimulation (Reisine 1984; Wang et al. 1990b; Reisine and Axelrod 1993). In contrast, desensitization of SST signaling has not been observed in GH4C1 cells, another pituitary cell line (Presky and Schonbrunn 1988). These differences may be attributed to the expression of different sst genes, since reduction of high-affinity agonist binding has been shown for cloned sst2, sst3, sst4, and sst5 and uncoupling from AC for sst2B, 3, and 5, while sst1 did not show either response (Rens-Domiano et al. 1992; Yasuda et al. 1992; Raynor et al. 1993a,b; Reisine et al. 1993; Vanetti et al. 1993). When expressed in CHO-K1 cells, human sst2, sst3, sst4 and sst5 mediated internalization of a radiolabeled SST-28 analog, while human sst1 did not (Hukovic et al. 1996). Similarly, in COS-7 cells human sst1 mediated only little internalization of ^{125}I-SST-14 or of a fluorescent SST-14 analog quite in contrast to mouse sst2A (Nouel et al. 1996). Two recent studies compared the endocytosis of all five cloned ssts with or without epitope tags at their carboxyl termini following expression in human embryonic kidney (HEK) and neuroendocrine rat insulinoma 1046–38 cells (Roosterman et al. 1997; Roth et al. 1997a). Application of various SST peptides to the transfected cells interestingly resulted in an agonist and receptor subtype-specific decrease of cell surface binding sites in both systems. Whereas sst1, sst2, and sst3 internalized in response to both SST peptides, sst5 did so only following stimulation with SST-28 but not SST-14. Moreover, sst4 did not internalize at all (Fig. 5a). Confocal microscopy and the use of inhibitors (Fig. 5b) suggested that the tagged sst1, sst2, and sst3 were internalized via the clathrin-dependent pathway into perinuclear sorting vesicles (Roosterman et al. 1997; Roth et al. 1997a). In sst1-, sst2-, and sst3-expressing cells the receptors recycled to the plasma membrane while the peptide was sorted in sst3-expressing cells into a degradation pathway. Receptor recycling was not sensitive to cycloheximide, indicating that it did not depend on de novo protein synthesis. It was, however, sensitive to acidotropic agents and brefeldin A suggesting that recycling proceeded through vesicular traffic of acidified compartments (Roosterman et al. 1997). Endocytosis and recycling of SST receptors 1 and 3 was not affected by activation of protein kinases A and C and was accompanied by desensitization of AC cyclase inhibition in HEK cells (Roosterman et al.

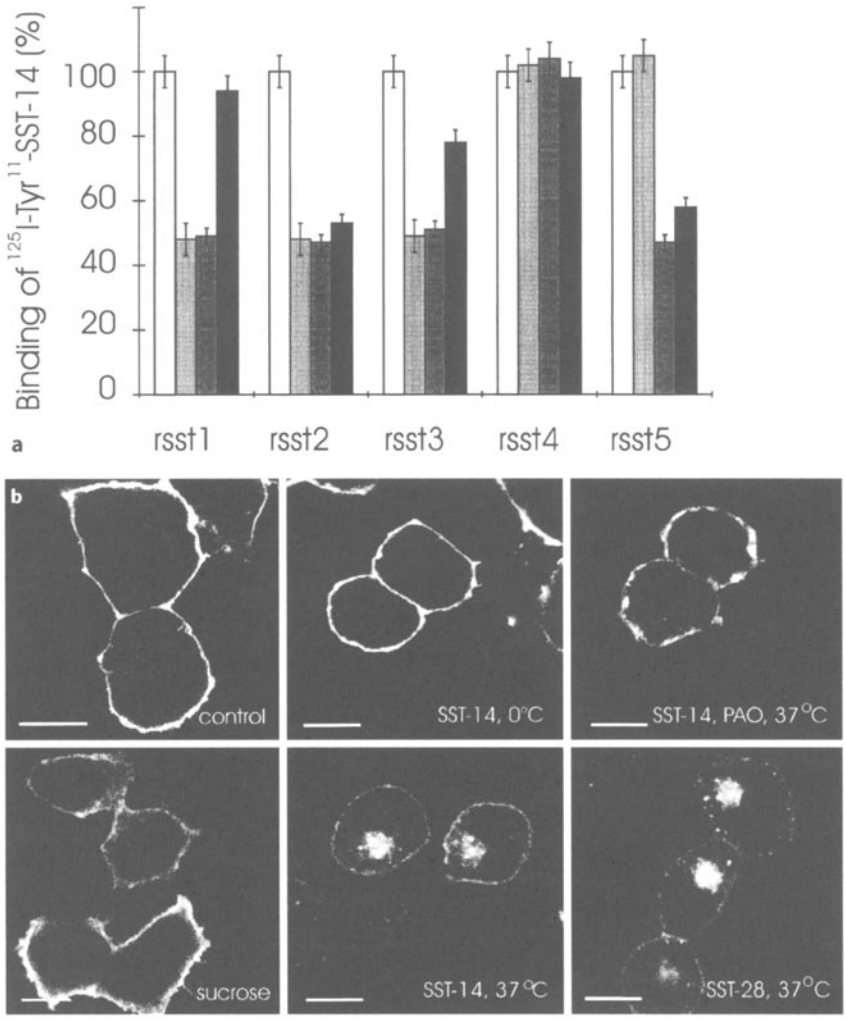

Fig. 5. a Agonist-mediated reduction of cell surface binding of ^{125}I-Tyr^{11}-SST-14. Rat insulinoma RIN1046–38 cells were transfected with rat somatostatin receptor subtype (sst)1–5 cDNAs. Transfected cells were exposed for 45 min to 1 μM somatostatin (SST)-14 (*light gray bars*), SST-28 (*intermediate gray bars*), or octreotide (*dark gray bars*) at 37°C or to 1 μM SST-14 at 4°C (*white bars*). Thereafter unlabeled peptides have been removed from the cell surface by cold acidic washing (removing receptor-bound ligand) and the remaining cell surface binding was determined using ^{125}I-Tyr^{11}-SST-14 at 4°C. Residual cell surface binding is presented relative to the binding of control cells that have not been pre-exposed to peptides. The results represent the standard error of mean of three independent experiments. Note that exposure to agonist in the cold did

1997). Mutational analysis of sst3 identified positive determinants in the C-terminal domain of this subtype that are critical for internalization (see Fig. 4). Mutation of three serine residues and one threonine residue (S314, S346, S351, T357) in sst3 near TM7 to alanine abolished agonist-mediated reduction of cell surface binding and the appearance of intracellular receptors (Roth et al. 1997a). Moreover, it could be shown that phosphorylation of these residues is crucial for internalization and desensitization of sst3 (Roth et al. 1997b). Agonist-dependent desensitization, internalization, and phosphorylation has also been observed for the native sst2A receptor in pituitary tumor GH-R2 cell membranes (Hipkin et al. 1997). Deletions introduced into the C-terminal domain into rat sst4 identified a motif of three amino acids, Glu-Thr-Thr (position 330–331). Removal of this motif from sst4 now conferred agonist-dependent regulation of cell surface binding and receptor internalization to this receptor subtype (Roth et al. 1997a). The importance of this motif is underscored by the finding that transplantation of a corresponding part of the sst4 tail to the C-terminus of sst3 prevented agonist regulation of surface binding and receptor internalization in cells expressing the chimera. These results established clear differences in the cellular regulation of cloned ssts and support the assumption that receptor-mediated internalization may be important for tumor diagnosis and therapy. They also suggest a manifold control in cellular signaling by SST receptors.

not reduce surface binding (*white bars*). Regulation of agonist binding clearly depends on the particular sst subtype, as well as on the peptide. **b** Internalization of sst3 in transfected RIN cells. RIN cells expressing epitope-tagged rat sst3 were analyzed by confocal microscopy. Cells were either not exposed to peptides (control) or to 1 μM SST-14 or SST-28 at 37°C to induce internalization. As a control cells were also incubated with peptide agonist at 0°C, with phenylarsine oxide, or with high sucrose concentrations (0.4 M). All treatments are known to prevent receptor-mediated endocytosis. Following treatment cells were fixed and subsequently incubated with the primary anti-epitope antibody and the secondary Cy3-conjugated antisera. Optical sections were taken every 0.3 μm and sections through the center of the cells are shown. Bar=10 μm. In the absence of agonist all fluorescence is seen at the cell surface. Control treatments prevented internalization of the epitope-tagged sst3. Agonist treatment at 37°C resulted in a cellular redistribution of the receptor to intracellular vesicles that accumulate in a perinuclear location and probably represent sorting compartments

6
Tissue Distribution

6.1
Somatostatin Receptors in the CNS

By receptor autoradiography binding sites for SST have been identified in brain, pituitary, adrenal gland, endocrine and exocrine pancreas, and the gastrointestinal tract, as well as in a large number of cultured cell lines (reviewed by Epelbaum 1986; Raynor and Reisine 1992; Epelbaum et al. 1994). Different binding affinities to ligands such as octreotide and MK678 indicated the presence of different SST receptor subtypes in different brain regions. Through the cloning of the five sst genes it has been possible to study the tissue distribution of sst mRNAs by in situ hybridization (Breder et al. 1992; Meyerhof et al. 1992; Kaupmann et al. 1993; Kong et al. 1994; Perez et al. 1994), Northern blotting (Meyerhof et al. 1991; Kluxen et al. 1992; Yamada et al. 1992; Yasuda et al. 1992), sensitive reverse transcriptase polymerase chain reaction (RT-PCR) (Wulfsen et al. 1993; Mori et al. 1997) and RNase protection assays (Bruno et al. 1993). Moreover, sst-specific antisera have been raised against fusion proteins or synthetic peptides and used for receptor subtype localization (Dournaud et al. 1996; Schindler et al. 1997). From these studies the size of sst mRNAs have been deduced which are generally much larger than about 1.0–1.3 kb, i.e., a size required to encode 346–428 amino acid proteins. The expression of several sst genes in individual organs was observed and in a number of cases like brain and pituitary the expression of all five genes was seen. In the CNS sst1-sst4 receptors are readily detected by blotting methods while the detection of sst5 requires more sensitive RT-PCR (Raulf et al. 1994; Viollet et al. 1995), or RNase protection methods (Bruno et al. 1993).

In rat brain sst1 mRNA was particularly concentrated in the cerebral and piriform cortex, magnocellular preoptic nucleus, hypothalamus, amygdala, hippocampus, and several nuclei of the brainstem (Meyerhof et al. 1992; Kong et al. 1994; Senaris et al. 1994; Beaudet et al. 1995). sst2 mRNA was observed in the medial habenular nucleus, claustrum, endopiriform nucleus, hippocampus, amygdala, cerebral cortex, hypothalamus, pons, and medulla (Bruno et al. 1993; Kong et al. 1994; Senaris et al. 1994; Beaudet et al. 1995). msst2A and msst2B were similarly distributed in mouse brain with, however, different ratios. The cerebral cortex contained the highest amounts of msst2A mRNA and only little sst2B mRNA, while

pons and medulla expressed both isoforms to an equal extent (Vanetti et al. 1994). sst3 mRNA was comparably abundant in the cerebellum and it was also found in hippocampus, amygdala, hypothalamus, in motor nuclei of the brainstem, and in motoneurons of the spinal chord (Meyerhof et al. 1992; Senaris et al. 1994). Adult rat cerebellum contains only a low density of binding sites for SST (Martin et al. 1991). In the molecular layer of the rat cerebellar cortex these are probably translated from sst2 mRNA as suggested by in situ hybridization and pharmacological characterization (Piwko et al. 1995). The fairly high levels of sst3 mRNA in the cerebellar cortex (Meyerhof et al. 1991; Kong et al. 1994) suggests that this mRNA species may not be translated appropriately, or that the sst3 protein is not processed correctly, or that the sst3 in the cerebellum may be in a low-affinity state preventing its specific labeling by radioligands. Alternatively, sst3 may be present on axons of neurons projecting to other brain regions. sst4 mRNA was found primarily in the hippocampus, striatum, cerebral cortex, hypothalamus, thalamus and iris/ciliary body (Wulfsen et al. 1993; Bito et al. 1994; Harrington et al. 1995; Perez and Hoyer 1995; Mori et al. 1997). The sst5 mRNA was primarily detected in the preoptic area and the hypothalamus (Raulf et al. 1994). Comparisons of the expression of sst1-5 genes in human, mouse, and rat brain revealed similar distribution patterns (Breder et al. 1992; Schindler et al. 1995; Thoss et al. 1996a). However, some variations such as differences in sst1 mRNA levels between mouse and human cerebrum (Li et al. 1992; Yamada et al. 1992) indicate species-specific differences in sst gene expression.

The overlapping patterns of sst mRNAs raise the interesting possibility that several sst genes are expressed in the same cell. This question has been addressed directly by using in situ hybridization with digoxygenin-labeled sst3 and isotope-labeled sst4 oligonucleotide probes (Perez and Hoyer 1995). The study revealed that sst3 and sst4 mRNAs are indeed colocalized in neurons of CA1 and CA2 hippocampal regions, subiculum, and layer IV of the cerebral cortex. These observations raise interesting questions about what might be the consequences of a simultaneous activation of these receptors by cognate peptides or whether these receptors are separated at a subcellular level, i.e., axonal vs dendritic localization.

Specific antibodies have been used to analyze the distribution of the sst2A protein in the rat brain (Dournaud et al. 1996; Schindler et al. 1997). Somatodendritic labeling was most prominent in the olfactory tubercle, layers II–III of the cerebral cortex, nucleus accumbens, stratum pyramidale of CA1 and CA2 areas of the hippocampus, central and cortical

amygdaloid nuclei, and locus ceruleus, while labeled terminals were found in the endopiriform cortex, layers V–VI of the cerebral cortex, claustrum, substantia innominata, subiculum, basolateral amygdaloid nucleus, medial habenula, and periaqueductal gray. The regional distribution of sst2A immunoreactivity closely paralleled that of binding sites for the SST analogs octreotide and MK678 (Martin et al. 1991; Krantic et al. 1992) which are of high affinity for rsst2 and rsst5 and of moderate affinity for rsst3 (see Table 2). Surprisingly, it also resembles closely the distribution of binding sites for the unselective ligand SST-14 (Martin et al. 1991; Krantic et al. 1992; Moyse et al. 1992). This suggests either that ssts other than sst2A are contained in subpopulations of the same cells or in subsets of neurons in the same area. Probably both assumptions complement one another; the observed colocalization of different sst mRNAs in the same cells supports the former and the observed distinct expression patterns of different sst genes supports the latter assumption. Importantly, the subcellular localization on dendrites/somata or on axons detected in this study also favors the idea that SST mediates both post- and presynaptic effects.

At present no precise conclusion about specific functions of individual ssts can be drawn from the observed widespread and overlapping distribution of their mRNAs. However, the presence of sst1-4 mRNA in the neocortex, hippocampus, and amygdala suggests roles for these subtypes in the regulation of complex integrative functions such as locomotor activity, learning, and memory, while the presence of sst1-4 mRNA in the olfactory system and in the retina is consistent with functions of SST in sensory processing. The presence of all five sst mRNAs in the hypothalamus suggests an involvement in the regulation of autonomic and neuroendocrine function (Breder et al. 1992; Meyerhof et al. 1992; Kaupmann et al. 1993; Wulfsen et al. 1993; Kong et al. 1994; Perez et al. 1994; Beaudet et al. 1995).

6.2 Hypothalamic/Pituitary Axis

Regulation of hypophyseal growth hormone secretion, but also regulation of the release of other pituitary hormones, is one of the prominent functions of SST. Binding sites for SST have been identified by receptor autoradiography on somatotrophs, lactotrophs, and thyrotrophs (Morel et al. 1985). In rat pituitary mRNAs for sst1-5 have recently been detected at different amounts by RNA blotting, RT-PCR, RNase protection, and in situ

hybridization (Bruno et al. 1993; Wulfsen et al. 1993; Kong et al. 1994; O'Carroll et al. 1994; Raulf et al. 1994; Senaris et al. 1994). Generally, sst1, sst2, and sst5 mRNA appear to be more abundant than sst3 and sst4 mRNAs (Wulfsen et al. 1993; Kong et al. 1994; Raulf et al. 1994). More detailed studies revealed the presence of all five sst mRNAs in the anterior pituitary, while sst1, sst2, and sst4 were also detected in the intermediate lobe melanotrophs and sst2 and sst3 mRNA probably in pituicytes in the neural lobe (O'Carroll and Krempels 1995). Colocalization studies revealed that all of the endocrine cell types within the anterior pituitary, corticotrophs, lactotrophs, somatotrophs, thyrotrophs, and gonadotrophs contained varying amounts of mRNAs for all five ssts (Day et al. 1995; O'Carroll and Krempels 1995), somatotrophs being rich in sst3-5, thyrotrophs in sst1 and sst2, lactotrophs and follicotrophs in sst3, luteotrophs in sst2 mRNA, respectively, while corticotrophs displayed approximately equal amounts of sst1-5 mRNA (O'Carroll and Krempels 1995). SST is also known to regulate growth hormone-releasing hormone neurons in the arcuate nucleus of the hypothalamus (Epelbaum et al. 1994). Within this nucleus the distribution of sst1 and sst2 mRNAs resembles that of neurons previously shown to bind SST (Beaudet et al. 1995). The observation that about 30% of these cells contain growth hormone-releasing factor suggests that both sst1 and sst2 participate in the central regulation of growth hormone-releasing hormone secretion through SST. Hypophysectomy reduced the level and number of cells containing sst1 and sst2 mRNAs specifically in the arcuate nucleus (Guo et al. 1996). Administration of recombinant growth hormone reversed this effect in the cases of sst1 mRNA and sst1 mRNA-containing cells, but did not significantly alter sst2 mRNA levels. These results suggest that the expression of both sst1 and sst2 genes in the hypothalamic arcuate nucleus is under the control of pituitary hormones and that growth hormone may influence its own secretion through the regulation of the sst1 gene in arcuate neurons (Guo et al. 1996).

6.3 Peripheral Tissues

An overlapping pattern of sst1-5 mRNAs has also been observed in many peripheral tissues. It should be noted that these are relatively rare and have usually been detected using sensitive RT-PCR methods. In the rat certain tissues such as small intestine and spleen contain all five sst mRNAs while

others contain subsets of them (Bruno et al. 1993). In general, sst1 and sst2 mRNAs display a broad anatomical distribution and are comparably abundant, while sst3 and sst5 mRNAs are less abundantly represented and sst4 mRNA has been detected in a restricted number of tissues (Bruno et al. 1993; Hauser et al. 1994; Kong et al. 1994; Raulf et al. 1994). In rat adrenals sst2 mRNA seems to be the major species, while in the ovary sst1, in pancreatic islets, prostate and muscle sst3, in heart and lung sst4 mRNAs dominate. The sst5 mRNA is found in eye and liver (Bruno et al. 1993; Yamada et al. 1993; Raulf et al. 1994). In line with the presence of sst4 mRNA in the rat heart coronary artery smooth muscle cells specific binding sites for SST-14 have been detected. Interestingly, these display higher affinity for SST-14 than for the analog angiopeptin. Both peptides caused the inhibition of smooth muscle cell proliferation and decreased levels of phosphorylated tyrosine residues (Leszczynski et al. 1993). In contrast, in guinea pig heart SST-28 has a negative inotropic effect which may be mediated by a pharmacologically characterized sst5-like receptor (Feniuk et al. 1993), and this finding corresponds to the presence of sst5 mRNA in the human heart (O'Carroll et al. 1994). This and several other differences in the tissue-specific expression of sst genes have been observed, such as for instance a lack of sst2 mRNA in the rat but not in human kidney (Yamada et al. 1992). The physiological consequences of these findings are unclear but might point to physiological differences of the ssts in different species. sst mRNAs have also been localized in a number of endocrine or neuroendocrine cell lines. Here again it has been observed that in some instances, such as the anterior pituitary GH_3 cells, all five sst mRNAs are present (Bruno et al. 1994b), while in AtT-20 cells a subset of sst1, sst2, sst4, and sst5 mRNAs was observed (Patel et al. 1994b), and in rat insulinoma RIN1046–38 cells only sst1 mRNA and marginal amounts of sst2 mRNA have been detected (Roosterman et al., unpublished observation).

6.4 Ontogenesis

The observed transient maximal levels of SST immunoreactivity and SST binding sites during ontogenesis have suggested that this neuropeptide may play a role within the developing nervous system (Shiokasa et al. 1981; Inagaki et al. 1982; Leroux et al. 1985; Heimann et al. 1987; Gonzalez 1989; Kimura 1989). Thus, SST is expressed by preplate cells preceding cortical development (Chun et al. 1987) in transient neuron populations in sympa-

thetic ganglia (New et al. 1986), brain stem nuclei (Morley et al. 1985), and the cortical anlage proper (Cavanagh et al. 1988). Likewise, SST binding sites have been detected in various brain areas such as in immature areas of the neural tube and sensory ganglia (Maubert et al. 1995), the intermediate zone of the cerebral cortex (Gonzalez et al. 1991; Leroux et al. 1995), the retina (Bodenant et al. 1991), and the external granule cell layer of the cerebellum (Gonzalez et al. 1988, 1989). These maxima in the densities of SST binding sites may be explained by corresponding sst mRNA levels. Initially, by RNA blotting experiments a decrease in sst1 mRNA from birth to adulthood has been observed in the cerebellum, while sst3 mRNA was first detected at postnatal day 7 (P7) and reached a constant maximum from day 14 onwards (Meyerhof et al. 1992). By semiquantitative RT-PCR analyses sst1-4 mRNA levels were found to reach transient maxima during postnatal development in various brain regions such as the cortex, hippocampus, hypothalamus, and also in the pituitary about 7 days after birth (Wulfsen et al. 1993). During this time span in other parts of the brain, such as the nucleus accumbens, a general decline in sst1-4 mRNA amounts were observed, while in the cerebellum, for instance, a complex pattern of the sst mRNA abundance was seen, i.e., a gradual decrease in sst1 and sst4 mRNAs, an increase in sst3 mRNA, and fairly constant amounts of sst2 mRNA.

By in situ hybridization the distribution of sst mRNAs in the CNS of rats from embryonic day 14 (E14) onwards has been analyzed at greater anatomic resolution (Wulfsen et al. 1993; Hartmann et al. 1995; Thoss et al. 1995). In these studies a widespread distribution was observed for sst1-4 mRNAs at E17 and E18 and P5 in the telencephalon, diencephalon, mesencephalon, and metencephalon. In contrast, at E18 sst5 mRNAs were found at very low levels only in the olfactory system and retinal neuroepithelium and the cerebral cortex. At P5 the sst5 mRNA levels had increased significantly in the cortex and this species was also seen in the anterior olfactory nuclei, lateral ventricle neuroepithelium, the CA1 and CA3 area of Ammon's horn, the medial habenula, the hypothalamic arcuate and anterior nuclei, and the superior cerebellar peduncle, while it is absent from the other CNS regions (Thoss et al. 1995, 1996b).

Expression of the sst1 gene during development has been followed in detail (Hartmann et al. 1995). Preceding the development of the cortical anlage proper which, in the rat, starts with the formation of the cortical plate shortly before E17, sst1 mRNA has been seen as early as E14 in the marginal zone of the hemispheral wall. Although the definitive cells of the

cortex have not yet been produced, there are peptidergic neurons in the marginal zone, a subpopulation of which contain SST (Chun et al. 1987), suggesting that a functional peptide-receptor system may operate at this early embryonic day. Within the cortical plate expression of the sst1 gene was first detected in a narrow band representing early deposited neurons in parallel to the establishment of the deep laminae V/VI at E16. This has not been observed in the proliferative zones adjacent to the ventricle or migratory neuroblasts in the intermediate zone. With subsequent addition of the supragranular neurons beyond E18 the location of sst mRNA spreads over the entire cortical plate. Similar developmental gradients were seen along the lateromedial and fronto-occipital dimension. sst1 transcripts have been detected about 2 days earlier near the frontal pole and the lateral cortical areas than in the occipital and medial cortical region. From the homogenous distribution sst mRNAs were restricted to laminae V/VI and II/III, sparing lamina IV during the first postnatal week. In the hippocampus sst1 gene expression proceeds from the subicular complex at E18 to the neighboring CA1 region after birth and to CA2 and CA3 regions and dentate gyrus during the first and second postnatal weeks. In both the hippocampal and cortical regions sst gene expression drops significantly during further development. Based on the transient peak in sst1 transcript levels in the cortex and the corresponding transient presence of somatostatinergic interneurons it has been suggested that the elimination of afferent cells may be an important aspect of the early postnatal reduction in sst1 gene expression (Hartmann et al. 1995).

Despite these efforts, an exact correlation of the individual sst subtypes with the maps of pharmacologically identified binding sites has not yet been achieved and only approached in the developing cerebellum (Viollet et al. 1997). Adult rat cerebellum contains virtually no SST (Vincent et al. 1985; Epelbaum et al. 1986) and SST receptors (Leroux et al. 1985; Reubi and Maurer 1985; Uhl et al. 1985; Epelbaum et al. 1986). SST immunoreactivity and mRNA have, however, been observed in various cerebellar cell types during the postnatal weeks (Inagaki et al. 1982; Villar et al. 1989). During this period SST receptors are abundant in the external granule cell layer, the germinative epithelium (EGC) in which cerebellar interneurons are generated, and also in the internal granule cell layer (GCL) (Gonzalez et al. 1988). Combined RT-PCR analyses and binding studies with various sst subtype-preferring analogs using brain sections and cultured cells have clearly identified sst2 as the major receptor subtype in immature granule cells in the proliferative and postmitotic regions of EGC at all developmen-

tal stages (Viollet et al. 1997). In addition, comparably low levels of sst1 have been detected. The observation that sst1 and sst2 receptors, but not their mRNAs, have been detected in the GCL indicated that these cells probably represent neurons that just arrived from the EGC. The presence of sst4 and sst3 mRNAs has been observed in both EGC and GCL. However, the lack of appropriate analogs has hampered the definite identification of respective receptor subtypes. Despite high sst3 mRNA amounts, the observed decline in binding of SST analogs in parallel with the decrease in sst1 and sst2 mRNA levels has supported the assumption that sst3 mRNA may not result in functional receptors (Viollet et al. 1997). To date the functional consequences of the developmental variation in sst gene expression are far from being understood. SST does not affect proliferation of granule cells in culture and cerebellar explants, while it stimulates neurofilament synthesis and neurite outgrowth in cultured cerebellar granule cells (Taniwaki and Schwartz 1995; Bodenant et al. 1997). Whether this observation is relevant in vivo and which receptor subtype may trigger these events in EGC or GCL neurons is not yet known.

7 Physiology

Analyses of the tissue distribution and cellular expression of ssts in combination with functional studies and the employment of selective ligands have mediated first insights into their peripheral physiological functions while their role in the CNS is still not known. These studies suggested that sst2 could be the major subtype involved in the inhibition of growth hormone release from the anterior pituitary (Raynor et al. 1993b), glucagon release from pancreatic α cells (Rossowski and Coy 1994; Coy and Taylor 1996), histamine release from the antrum (Zaki et al. 1996), gastrin release from enterochromaffin-like cells in the mucosa (Prinz et al. 1994), acid secretion (Rossowski et al. 1994; Lloyd et al. 1995), and ion secretion in the colon (Warhurst et al. 1996). sst3 probably mediates the inhibitory action of SST on gastric smooth muscle cells (ZF Gu et al. 1995) and could also participate in inhibition of insulin release (Coy et al. 1998). sst5 has been shown to mediate the inhibition of amylase release from the exocrine and insulin release from the endocrine pancreas (Rossowski et al. 1994; Coy and Taylor 1996, Coy et al. 1998).

8
Future Perspectives

The cloning of the five SST receptor subtypes was the prerequisite for the development of experimental tools that are being used to establish the biological functions for each receptor subtype. Although far from being complete these tools have yielded first ideas about the roles of some of the ssts. Certain useful selective agonists are available for the receptor sst2 and sst5, as well as a sst2A-specific antibody, and have identified some gastrointestinal functions for these receptor types. Although a sst1-selective agonist has been synthesized it has so far not been used in the identification of sst1 functions and there is a complete lack of sst3- and sst4-selective compounds. Accordingly, the biological roles for sst1, sst3, and sst4 are completely unknown. Priority goals for the future would be the development of specific antibodies, agonists, and antagonists for each subtype for studies at the molecular, cellular, and tissue levels and the construction of gene knock-outs for studies at the level of tissues, organs, and organisms. Particular emphasis will also have to be given to the elucidation of the role of cortistatin. Recently, in addition to the identification of rat cortistatin mRNA (de Lecea et al. 1996), expressed sequence tags were found in a human fetal brain cDNA library that showed significant homology to rat cortistatin (Fukusumi et al. 1997). These could give rise to at least two different mature peptides of 29 and 17 amino acid residues. Chemically synthesized human cortistatin-17 bound to all human SST receptor subtypes in almost the same manner as the rat peptide and inhibited forskolin-stimulated cAMP production. Thus it might be concluded that a family of statins, somatostatins, and cortistatins, signal through a common family of receptors which, to date, include sst1, sst2, sst3, sst4, and sst5. However, there are indications that the statin receptor family could further expand. Firstly, separate cortistatin receptors may exist, but have not yet been identified. Secondly, the presence of a putative novel SST receptor in AtT-20 cells has recently been described. The novel receptor couples to an inward rectifier potassium current and is sensitive to hexapeptide analogs of SST but insensitive to octapeptide analogs. This pharmacological profile is distinct from any of the cloned SST receptors (Patel et al. 1994b; Tallent et al. 1996b). However, final proof of this assumption has to await the cloning of this receptor and the cloning and pharmacological characterization of the mouse sst5.

Acknowledgements. Original research carried out in the author's laboratory and referred to in this article was supported by grants from the Deutsche Forschungsgemeinschaft (SFB232/B4) and Fonds der Chemischen Industrie.

References

Akbar M, Okajima F, Tomura H, Majid M, Yamada Y, Seino S, Kondo Y (1994) Phospholipase C activation and Ca^{2+} mobilization by cloned human somatostatin receptor subtypes 1–5, in transfected COS-7 cells. FEBS Lett 348:192–196

Andersen B, Rosenfeld MG (1994) Pit-1 determines cell types during development of the anterior pituitary gland. A model for transcriptional regulation of cell phenotypes in mammalian organogenesis. J Biol Chem 269:29335–29338

Bakker WH, Albert R, Bruns C et al. (1991) [111In-DTPA-D-Phe1]-octreotide, a potential radiopharmaceutical for imaging of somatostatin receptor-positive tumors: synthesis, radiolabeling and in vitro validation. Life Sci 49:1583–1591

Barber D, McGuire M, Ganz M (1989) Beta-adrenergic and somatostatin receptor regulate Na^+–H^+ exchange independent of cAMP. J Biol Chem 264:21038–21042

Bass RT, Buckwalter BL, Patel BP, Pausch MH, Price LA, Strnad J, Hadcock JR (1996) Identification and characterization of novel somatostatin antagonists. Mol Pharmacol 50:709–715

Beaudet A, Greenspun D, Raelson J, Tannenbaum GS (1995) Patterns of expression of SSTR1 and SSTR2 somatostatin receptor subtypes in the hypothalamus of the adult rat: relationship to neuroendocrine function. Neuroscience 65:551–561

Bertherat J, Chanson P, Dewailly D, Enjalbert A, Jaquet P, Kordon C, Peillon F, Timsit J, Epelbaum J (1992) Resistance to somatostatin (SRIH) analog therapy in acromegaly. Re-evaluation of the correlation between the SRIH receptor status of the pituitary tumor and the in vivo inhibition of GH secretion in response to SRIH analog. Horm Res 38:94–99

Bito H, Mori M, Sakanaka C, Takano T, Honda Z, Gotoh Y, Nishida E, Shimizu T (1994) Functional coupling of SSTR4, a major hippocampal somatostatin receptor, to adenylate cyclase inhibition, arachidonate release, and activation of the mitogen-activated protein kinase cascade. J Biol Chem 269:12722–12730

Bodenant C, Leroux P, Gonzalez BJ, Vaudry H (1991) Transient expression of somatostatin receptors in the rat visual system during development. Neuroscience 41:595–606

Bodenant C, Laquerrière A, Paresy M, Hemet J, Vaudry H, Leroux P (1997) Somatostatin does not affect multiplication of granule cells in the rat cerebellum. Peptides 18:257–262

Brazeau P, Vale W, Burgus R, Ling N, Rivier J, Guillemin R (1972) Hypothalamic polypeptide that inhibits the secretion of immunoreactive pituitary growth hormone. Science 129:77–79

Breder CD, Yamada Y, Yasuda K, Seino S, Saper CB, Bell GI (1992) Differential expression of somatostatin receptor subtypes in brain. J Neurosci 12:3920–3934

Brown M, Rivier J, Vale W (1977) Somatostatin analogs with selected biological activities. Science 196:1467–1468

Brown PJ, Schonbrunn A (1993) Affinity purification of a somatostatin receptor–G-protein complex demonstrates specificity in receptor–G-protein coupling. J Biol Chem 268:6668–6676

Bruno JF, Xu Y, Song J, Berelowitz M (1992) Molecular cloning and functional expression of a brain-specific somatostatin receptor. Proc Natl Acad Sci USA 89:11151–11155

Bruno JF, Xu Y, Song J, Berelowitz M (1993) Tissue distribution of somatostatin receptor subtype messenger ribonucleic acid in the rat. Endocrinology 133:2561–2567

Bruno JF, Xu Y, Song J, Berelowitz M (1994a) Pituitary and hypothalamic somatostatin receptor subtype messenger ribonucleic acid expression in the food-deprived and diabetic rat. Endocrinology 135:1787–1792

Bruno JF, Xu Y, Berelowitz M (1994b) Somatostatin regulates somatostatin receptor subtype mRNA expression in GH_3 cells. Biochem Biophys Res Commun 202:1738–1743

Bruns C, Raulf F, Hoyer D, Schloos J, Lübbert H, Wackbecker G (1996) Binding properties of somatostatin receptor subtypes. Metabolism 45:17–20

Buscail L, Delesque N, Esteve J-P, Saint-Laurent N, Prats H, Clerc P, Robberecht P, Bell GI, Liebow C, Schally AV, Vayisse N, Susini C (1994) Stimulation of tyrosine phosphatase and inhibition of cell proliferation by somatostatin analogues: mediation by human somatostatin receptor subtypes SSTR1 and SSTR2. Proc Natl Acad Sci USA 91:2315–2319

Buscail L, Esteve JP, Saint-Laurent N, Bertrand V, Reisine T, O'Carroll AM, Bell GI, Schally AV, Vaysse N, Susini C (1995) Inhibition of cell proliferation by the somatostatin analogue RC-160 is mediated by somatostatin receptor subtypes SSTR2 and SSTR5 through different mechanisms. Proc Natl Acad Sci USA 92:1580–1584

Castro SW, Buell G, Feniuk W, Humphrey PP (1996) Differences in the operational characteristics of the human recombinant somatostatin receptor types, sst1 and sst2, in mouse fibroblast Ltk^-. cells. Br J Pharmacol 117:639–646

Cavanagh ME, Parnavelas JG (1988) Development of somatostatin-immunoreactive neurons in the rat occipital cortex: a combined immunocytochemical-autoradiographic study. J Comp Neurol 268:1–12

Chun J, Nakamura M, Shatz CJ (1987) Transient cells of the mammalian telencephalon are peptide-immunoreactive neurons. Nature 325:617–620

Colas B, Cambillau C, Buscail L, Zeggari M, Esteve JP, Lautre V, Thomas F, Vaysse N, Susini C (1992) Stimulation of a membrane tyrosine phosphatase activity by somatostatin analogues in rat pancreatic acinar cells. Eur J Biochem 207:1017–1024

Corness JD, Demchyshyn LL, Seeman P, Van Tol HH, Srikant CB, Kent G, Patel YC, Niznik HB (1993) A human somatostatin receptor (SSTR3), located on chromosome 22, displays preferential affinity for somatostatin-14-like peptides. FEBS Lett 321:279–284

Coy DH, Taylor JE (1996) Receptor-specific somatostatin analogs: correlation with biological activity. Metabolism 34[Suppl 1]:21–23

Coy DH, Taylor JE, Rossowski WJ (1998) Biological properties of old and new human and rat receptor specific somatostatin analogs. Yale J Biol Med (in press)

Curtis CAM, Wheatley M, Bansall S, Birdsall NJM, Eveleigh P, Pedder EK, Poyner D, Hulme EC (1989) Probylbenzilycholine mustard labels an acidic residue in transmembrane helix 3 of the muscarinic receptor. J Biol Chem 264:489–495

Day R, Dong W, Panetta R, Kraicer J, Greenwood MT, Patel YC (1995) Expression of mRNA for somatostatin receptor (sstr) types 2 and 5 in individual rat pituitary cells. A double labeling in situ hybridization analysis. Endocrinology 136:5232–5235

de Lecea L, Criado JR, Prosperogarcia O, Gautvik KM, Schweitzer P, Danielson PE, Dunlop CLM, Siggins GR, Henriksen SJ, Sutcliffe JG (1996) A cortical neuropeptide with neuronal depressant and sleep-modulating properties. Nature 381:242–245

Degtiar VE, Wittig B, Schultz G, Kalkbrenner F (1996) A specific G(o) heterotrimer couples somatostatin receptors to voltage-gated calcium channels in RINm5F cells. FEBS Lett 380:137–141

Demchyshyn LL, Srikant CB, Sunahara RK, Kent G, Seeman P, Van Tol HHM, Panetta R, Patel YC, Niznik HB (1993) Cloning and expression of a human somatostatin-14-selective receptor variant (somatostatin receptor 4) located on chromosome 20. Mol Pharmacol 43:894–901

Dohlmann HG, Caron MG, Deblasi A, Frielle T, Lefkowitz RJ (1990) Role of extracellular disulfide-bonded cysteines in the ligand binding function of the β2-adrenergic receptor. Biochemistry 29:2335–2342

Dournaud P, Gu YZ, Schonbrunn A, Mazella J, Tannenbaum GS, Beaudet A (1996) Localization of the somatostatin receptor SST2A in rat brain using a specific anti-peptide antibody. J Neurosci 16:4468–4478

Epelbaum J (1986) Somatostatin in the central nervous system: physiology and pathological modifications. Prog Neurobiol 27:63–100

Epelbaum J, Dussaillant M, Enjalbert A, Kordon C, Rostene W (1986) Autoradiographic localization of a non-reducible somatostatin analog (125I-CGP 23996) binding sites in the rat brain: comparison with membrane binding. Peptides 6:713–719

Epelbaum J, Dournaud P, Fodor M, Viollet C (1994) The neurobiology of somatostatin. Crit Rev Neurobiol 8:25–44

Eppler CM, Zysk JR, Corbett M, Shieh HM (1992) The utility of biotinylated somatostatin analogs. J Biol Chem 267:15603–15612

Exton JH (1996) Regulation of phosphosinositide phospholipases by hormones, neurotransmitters and other agonists linked to G proteins. Annu Rev Pharmacol Toxicol 36:481–510

Feniuk W, Humphrey PPA (1994) Somatostatin-induced inhibition of neurotransmission in the mouse isolated vas deferens is resistant to pertussis toxin. Eur J Pharmacol 261:333–337

Feniuk W, Dimech J, Humphrey PPA (1993) Characterization of somatostatin receptors in guinea-pig isolated ileum, vas deferens and right atrium. Br J Pharmacol 110:1156–1164

Fitzpatrick V, Vandlen R (1994) Agonist selectivity determinants in SRIF receptor subtypes I and II. J Biol Chem 269:24621–24626

Florio T, Rim C, Hershberger RE, Loda M, Stork PJ (1994) The somatostatin receptor SSTR1 is coupled to phosphotyrosine phosphatase activity in CHO-K1 cells. Mol Endocrinol 8:1289–1297

Frazer CM, Wang CD, Robinson DA, Gocayne JD, Venter JC (1989) Site-directed mutagenesis of m1 muscarinic acetylcholine receptors: conserved aspartic acids play important roles in receptor functions. Mol Pharmacol 36:840–847

Fujii Y, Gonoi T, Yamada Y, Chihara K, Inagaki N, Seino S (1994) Somatostatin receptor subtype SSTR2 mediates the inhibition of high-voltage-activated calcium channels by somatostatin and its analogue SMS 201–995. FEBS Lett 355:117–120

Fukusumi S, Kitada C, Takekawa S, Sakamoto J, Miyamoto M, Hinuma S, Kitano K, Fujino M (1997) Identification and characterization of a novel human cortistatin-like peptide. Biochem Biophys Res Commun 232:157–163

Garcia PD, Myers RM (1994) Pituitary cell line GH_3 expresses two somatostatin receptor subtypes that inhibit adenyl cyclase: functional expression of rat somatostatin receptor subtypes 1 and 2 in human embryonic kidney 293 cells. Mol Pharmacol 45:402–409

Gonzalez BJ, Leroux P, Laquerrière A, Coy DH, Bodenant C, Vaudry H (1988) Transient expression of somatostatin receptors in the rat cerebellum during development. Dev Brain Res 40:154–157

Gonzalez BJ, Leroux P, Laquerrière A, Coy DH, Bodenant C, Vaudry H (1989) Ontogeny of somatostatin receptors in the rat brain: biochemical and autoradiographic study. Neuroscience 29:629–644

Gonzalez BJ, Leroux P, Bodenant C, Vaudry H (1991) Ontogeny of somatostatin receptors in the rat somatosensory cortex. J Comp Neurol 305:177–188

Greenwood MT, Panetta R, Robertson LA, Liu JL, Patel YC (1994) Sequence analysis of the 5'-flanking promoter region of the human somatostatin receptor 5. Biochem Biophys Res Commun 205:1883–1890

Greenwood MT, Robertson LA, Patel YC (1995) Cloning of the gene encoding human somatostatin receptor 2: sequence analysis of the 5'-flanking promoter region. Gene 159:291–292

Gu YZ, Schonbrunn A (1997) Coupling specificity between somatostatin receptor 2A and G proteins – isolation of the receptor G protein complex with a receptor antibody. Mol Endocrinol 11:527–537

Gu YZ, Brown PJ, Loose-Mitchell DS, Stork PJS, Schonbrunn A (1995) Development and use of a receptor antibody to characterize the interaction between somatostatin receptor subtype 1 and G proteins. Mol Pharmacol 48:1004–1014

Gu ZF, Corleto VD, Mantey SA, Coy DH, Maton PN, Jensi RT (1995) Somatostatin receptor subtype 3 mediates the inhibitory action of somatostatin on gastric smooth muscle cells. Am J Physiol 268(5 Pt 1):G739–G748

Guo F, Beaudet A, Tannenbaum GS (1996) The effect of hypophysectomy and growth hormone replacement on sst1 and sst2 somatostatin receptor subtype messenger ribonucleic acids in the arcuate nucleus. Endocrinology 137:3928–3935

Hadcock JR, Strnad J, Eppler CM (1994) Rat somatostatin receptor type 1 couples to G proteins and inhibition of cyclic AMP accumulation. Mol Pharmacol 45:410–416

Haraguchi K, Ohtaka M, Takazawa K, Endo T, Onaya T (1995) Desensitization to somatostatin analogue (Octreotide) observed in a patient with acromegaly. Endocr J 42:295–300

Harrington KA, Schindler M, Humphrey PP, Emson PC (1995) Expression of messenger RNA for somatostatin receptor subtype 4 in adult rat brain. Neurosci Lett 188:17–20

Hartmann D, Fehr S, Meyerhof W, Richter D (1995) Distribution of somatostatin receptor subtype 1 mRNA in the developing cerebral hemispheres of the rat. Dev Neurosci 17:246–525

Hatzoglou A, Ouafik L, Bakogeorgou E, Thermos K, Castanas E (1995) Morphine cross-reacts with somatostatin receptor SSTR2 in the T47D human breast cancer cell line and decreases cell growth. Cancer Res 55:5632–5636

Hauser F, Meyerhof W, Wulfsen I, Schonrock C, Richter D (1994) Sequence analysis of the promoter region of the rat somatostatin receptor subtype 1 gene. FEBS Lett 345:225–228

Hershberger RE, Newman BL, Florio T, Bunzow J, Civelli O, Li X-J, Forte M, Stork PJS (1994) The somatostatin receptors SSTR1 and SSTR2 are coupled to inhibition of adenyl cyclase in Chinese hamster ovary cells via pertussis toxin-sensitive pathways. Endocrinology 134:1277–1285

Hipkin RW, Friedman J, Clark RB, Eppler CM, Schonbrunn A (1997) Agonist-induced desensitization, internalization and phosphorylation of the sst2A somatostatin receptor. J Biol Chem 272:13869–13876

Hofland LJ, Koetsveld V, PM, Waaijers M, Zuyderwijk J, Breeman WAP, Lamberts SWJ (1995) Internalization of the radioiodinated somatostatin analog (^{125}I-Tyr^{3}) octreotide by mouse and human pituitary tumor cells: increase by unlabeled octreotide. Endocrinology 136:3698–3706

Horstmeyer A, Henning C, Sauer T, Müller-Esterl W, Schroeder C (1996) Palmitoylation of endothelin receptor A. J Biol Chem 271:20811–20819

Hou C, Gilbert RL, Barber DL (1994) Subtype-specific signalling mechanisms of somatostatin receptors SSTR1 and SSTR2. J Biol Chem 269:10357–10362

Hoyer D, Lübbert H, Bruns C (1994) Molecular pharmacology of somatostatin receptors. N S Arch Pharmacol 350:441–453

Hoyer D, Bell GI, Berelowitz M, Epelbaum J, Feniuk W, Humphrey PPA, O'Carroll A-M, Patel YC, Schonbrunn A, Taylor J, Reisine T (1995) Classification and nomenclature of somatostatin receptors. Trends Pharmacol Sci 16:86–88

Hukovic N, Panetta R, Kumar U, Patel YC (1996) Agonist-dependent regulation of cloned human somatostatin receptor types 1–5 (hSSTR1–5): subtype selective internalization or upregulation. Endocrinology 137:4046–4049

Hulmes JD, Corbett M, Zysk JR, Bohlen P, Eppler CM (1992) Partial amino acid sequence of a somatostatin receptor isolated from GH4C1 pituitary cells. Biochem Biophys Res Commun 184:131–136

Ikeda S, Schofield G (1989) Somatostatin blocks a Ca^{++} current in rat sympathetic ganglion neurons. J Physiol 409:221–240

Inagaki S, Shiosaka S, Takatsuki K, Iida H, Sakanaka M, Senba E, Hara Y, Matsuzaki T, Kawai Y, Tohyama M (1982) Ontogeny of somatostatin-containing neuron system of the rat cerebellum including its fiber connections: an experimental and immunohistochemical analysis. Dev Brain Res 3:509–527

Jakobs K, Aktories K, Schultz G (1983) A nucleotide regulatory site for somatostatin inhibition of adenyl cyclase in S49 lymphoma cells. Nature 303:177–178

Kagimoto S, Yamada Y, Kubota A, Someya Y, Ihara Y, Yasuda K, Kozasa T, Imura H, Seino S, Seino Y (1994) Human somatostatin receptor, SSTR2, is coupled to adenyl cyclase in the presence of G_i alpha 1 protein. Biochem Biophys Res Commun 202:1188–1195

Kaupmann K, Bruns C, Hoyer D, Seuwen K, Lübbert H (1993) mRNA distribution and second messenger coupling of four somatostatin receptors expressed in brain. FEBS Lett 331:53–59

Kaupmann K, Bruns C, Raulf F, Weber HP, Mattes H, Lübbert H (1995) Two amino acids, located in transmembrane domains VI and VII, determine the selectivity of the peptide agonist SMS 201-995 for the SSTR2 somatostatin receptor. EMBO J 14:727–735

Kennedy ME, Limbird LE (1993) Mutations of the α_{2A}-adrenergic receptor that eliminate detectable palmitoylation do not perturb receptor/G protein coupling. J Biol Chem 268:8003–8011

Kimura N (1989) Developmental change and molecular properties of somatostatin receptors in the rat cerebral cortex. Biochem Biophys Res Commun 160:72–78

Kleuss C, Hescheler J, Ewel C, Rosenthal W, Schultz G, Wittig B (1991) Assignment of G-protein subtypes to specific receptors inducing inhibition of calcium currents. Nature 353:43–48

Kleuss C, Scherübl H, Hescheler J, Schultz G, Wittig B (1992) Different β-subunits determine G-protein interaction with transmembrane receptors. Nature 358:424–426

Kleuss C, Scherübl H, Hescheler J, Schultz G, Wittig B (1993) Selectivity in signal transduction determined by γ subunits of heterotrimeric G proteins. Science 259:832–834

Kluxen FW, Bruns C, Lubbert H (1992) Expression cloning of a rat brain somatostatin receptor cDNA. Proc Natl Acad Sci USA 89:4618–4622

Kobilka BK, Kobilka TS, Daniel K, Regan JW, Caron MG, Lefkowitz RJ (1988) Chimeric α_2-, β_2-adrenergic receptors: delineation of domains involved in effector coupling and ligand binding specificity. Science 240:1310–1316

Koch B, Schonbrunn A (1984) The somatostatin receptor is directly coupled to adenylate cyclase in GH_4C_1 pituitary cell membranes. Endocrinology 114:1784–1790

Koch BD, Dorflinger LJ, Schonbrunn A (1985) Pertussis toxin blocks both cyclic AMP-mediated and cyclic AMP-independent actions of somatostatin: evidence for coupling of Ni to decreases in intracellular free calcium. J Biol Chem 260:13138–13145

Koenig JA, Edwardson JM, Humphrey PPA (1997) Somatostatin receptors in Neuro2A neuroblastoma cells – ligand internalization. Br J Pharmacol 120:52–59

Komatsuzaki K, Murayama Y, Giambarella U, Ogata E, Seino S, Nishimoto I (1997) A novel system that reports the G-proteins linked to a given receptor – a study of type 3 somatostatin receptor. FEBS Lett 406:165–170

Kong H, Raynor K, Yasuda K, Bell GI, Reisine T (1993) Mutation of aspartate residue 79 in the SRIF receptor subtype SSTR2 prevents Na^+ regulation of agonist binding but does not affect apparent receptor/G protein association. Mol Pharmacol 44:380–384

Kong H, DePaoli AM, Breder CD, Yasuda K, Bell GI, Reisine T (1994) Differential expression of messenger RNAs for somatostatin receptor subtypes SSTR1, SSTR2 and SSTR3 in adult rat brain: analysis by RNA blotting and in situ hybridization histochemistry. Neuroscience 59:175–184

Krantic S, Quirion R, Uhl G (1992) Somatostatin receptors. In: Björklund A, Hökfelt T, Kuhar MJ (eds) Neuropeptide receptors in the CNS. Elsevier, Amsterdam, pp 321–346 (Handbook of chemical neuroanatomy, vol 2)

Krulich L, Dhariwal APS, McCann SM (1968) Stimulatory and inhibitory effects of purified hypothalamic extracts on growth hormone release from rat pituitary in vitro. Endocrinology 83:787–790

Kubota A, Yamada Y, Kagimoto S, Yasuda K, Someya Y, Ihara Y, Okamoto Y, Kozasa T, Seino S, Seino Y (1994) Multiple effector coupling of somatostatin receptor subtype SSTR1. Biochem Biophys Res Commun 204:176–186

Kurtenbach E, Curits CAM, Pedder EK, Aitken A, Harris ACM, Hulme EC (1990) Muscarinic acetylcholine receptors. J Biol Chem 265:13702–13708

Lamberts SWJ, Koper JW, Reubi J-C (1987) Potential role of somatostatin analogues in the treatment of cancer. Eur J Clin Invest 17:281–287

Lamberts SWJ, de Herder WW, van Koetsveld PM, Koper JW, van der Lely AJ, Visser-Wisselaar HA, Hofland LJ (1995) Somatostatin receptors: clinical implications for endocrinology and oncology. Ciba Found Symp 190:222–236

Law S, Manning, Reisine T (1991) Identification of the subunits of GTP binding proteins coupled to somatostatin receptors. J Biol Chem 266:17885–17897

Law SF, Yasuda K, Bell GI, Reisine T (1993) G_i alpha 3 and G(o) alpha selectively associate with the cloned somatostatin receptor subtype SSTR2. J Biol Chem 268:10721–10727

Law SF, Zaina S, Sweet R, Yasuda K, Bell GI, Stadel J, Reisine T (1994) G_i alpha 1 selectively couples somatostatin receptor subtype 3 to adenyl cyclase: identification of the functional domains of this alpha subunit necessary for mediating the inhibition by somatostatin of cAMP formation. Mol Pharmacol 45:587–590

Leroux P, Querion R, Pelletier G (1985) Localization and characterization of brain somatostatin receptors as studied with somatostatin-14 and somatostatin-28 receptor radioautography. Brain Res 347:74–84

Leroux P, Bodenant C, Bologna E, Gonzalez BJ, Vaudry H (1995) Transient expression of somatostatin receptors in the brain during development. In: Somatostatin and ist receptors. Wiley, Chichester, pp 127–141

Leszczynski D, Zhao Y, Cathapermal S, Nilsson J, Foegh ML (1993) Rat heart smooth muscle cells express high and low affinity receptors for somatostatin-14, which are involved in regulation of cell proliferation. Life Sci 53:1663–1674

Li XJ, Forte M, North RA, Ross CA, Snyder SH (1992) Cloning and expression of a rat somatostatin receptor enriched in brain. J Biol Chem 267:21307–21312

Liapakis G, Hoeger C, Rivier J, Reisine T (1996a) Development of a selective agonist at the somatostatin receptor subtype SSTR1. J Pharmacol Exp Ther 276:1089–1094

Liapakis G, Fitzpatrick D, Hoeger C, Rivier J, Vandlen R, Reisine T (1996b) Identification of ligand binding determinants in the somatostatin receptor subtypes 1 and 2. J Biol Chem 271:20331–20339

Liapakis G, Tallent M, Reisine T (1996c) Molecular and functional properties of somatostatin receptor subtypes. Metabolism 1:12–13

Libert F, Parmentier M, Lefort A, Dinsart C, Wan Sande J, Maenhaut C, Simons M-J, DuMont JE, Vassart G (1989) Selective amplification and cloning of four new members of the G protein-coupled receptor family. Science 244:569–572

Liu YF, Jakobs KH, Rasenick MM, Albert PR (1994) G protein specificity in receptor–effector coupling. Analysis of the roles of G_o and G_{i2} in GH4C1 pituitary cells. J Biol Chem 269:13880–13886

Lloyd KC, Wang J, Aurang K, Gronhed P, Coy DH, Walsh JH (1995) Activation of somatostatin receptor subtype 2 inhibits acid secretion in rats. Am J Physiol 268(1 Pt 1):G102–G106

Luthin D, Eppler C, Linden J (1993) Identification and quantification of G_i-type GTP-binding proteins that copurify with a pituitary somatostatin receptor. J Biol Chem 268:5990–5996

Mandarino L, Stenner D, Blanchard W, Nissen S, Gerich J, Ling N, Brazeau P, Bohlen P, Esch F, Guillemin R (1981) Selective effects of somatostatin-14, -25, and -28 on in vitro insulin and glucagon secretion. Nature 291:76–77

Martin J-L, Chesselet M-F, Raynor K, Gonzales C, Reisine T (1991) Differential distribution of somatostatin receptor subtypes in rat brain revealed by newly developed somatostatin analogs. Neuroscience 41:581–593

Matsumoto K, Yokogoshi Y, Fujinaka Y, Zhang C, Saito S (1994) Molecular cloning and sequencing of porcine somatostatin receptor 2. Biochem Biophys Res Commun. 199:298–305

Maubert E, Ciofi P, Tramu G, Mazzuca M, Dupouy JP (1995) Early transient expression of somatostatin (SRIF) immunoreactivity in dorsal root ganglia during ontogenesis in the rat. Brain Res 573:153–156

Meriney SD, Gray DB, Pilar R (1994) Somatostatin-induced inhibition of neuronal Ca^{2+} current modulated by cGMP-dependent protein kinase. Nature 369:336–339

Meyerhof W, Paust H-J, Schönrock C, Richter D (1991) Cloning of a cDNA encoding a novel putative G-protein-coupled receptor expressed in specific rat brain regions. DNA Cell Biol 10:689–694

Meyerhof W, Wulfsen I, Schönrock C, Fehr S, Richter D (1992) Molecular cloning of a somatostatin-28 receptor and comparison of its expression pattern with that of a somatostatin-14 receptor in rat brain. Proc Natl Acad Sci USA 89:10267–10271

Morel G, Leroux P, Pelletier G (1985) Ultrastructural autoradiographic localization of somatostatin-28 in the rat pituitary gland. Endocrinology 116:1015–1020

Mori M, Aihara M, Shimizu T (1997) Differential expression of somatostatin receptors in the rat eye – SSTR4 is intensely expressed in the iris/ciliary body. Neurosci Lett 223:185–188

Morley B, Spengler K, Javel E (1985) The development of somatostatin immunoreactivity in the interpeduncular nucleus of the cat. Dev Brain Res 20:241–248

Moyse E, Beaudet A, Bertherat J, Epelbaum J (1992) Light microscopic radioautographic localization of somatostatin binding sites in the brain stem of the rat. J Chem Neuroanat 5:75–84

Murray-Whelan R, Schlegel W (1992) Brain somatostatin receptor–G protein interaction. J Biol Chem 267:2960–2965

Murthy KS, Coy DH, Makhlouf GM (1996) Somatostatin receptor-mediated signaling in smooth muscle. Activation of phospholipase C-beta3 by G beta gamma and inhibition of adenyl cyclase by G $alpha_{i1}$ and G $alpha_o$. J Biol Chem 271:23458–23463

Nehring RB, Meyerhof W, Richter D (1995) Aspartic acid residue 124 in the third transmembrane domain of the somatostatin receptor subtype 3 is essential for somatostatin-14 binding DNA. Cell Biol 14:939–944

Nehring R, Meyerhof W, Richter D (1996) Mutation of glutamate residue 92 of the rat somatostatin receptor subtype 3 enhances sodium regulation of sst-14 binding. In: Krisch B, Mentlein R (eds) The peptidergic neuron. Birkhäuser, Basel, pp 135–140

New H, Mudge A (1986) Distribution and ontogeny of SP, CGRP, SOM and VIP in chick sensory and sympathetic ganglia. Dev Biol 116:337–346

Nielsen MD, Chan GCK, Poser SW, Storm DR (1996) Differential regulation of type I and Type VIII Ca^{2+} stimulated adenyl cyclases by G(I)-coupled receptors in vivo. J Biol Chem 271:33308–33316

Nouel D, Gaudriault G, Houle M, Reisine T, Vincent JP, Mazaella J, Beaudet A (1996) Differential internalization of somatostatin in COS-7 cells transfected with SST1 and

SST2 receptor subtypes: a confocal microscopic study using novel fluorescent somatostatin derivatives. Endocrinology 188:1–11

O'Carroll AM, Krempels K (1995) Widespread distribution of somatostatin receptor messenger ribonucleic acids in rat pituitary. Endocrinology 136:5224–5227

O'Carroll AM, Lolait SJ, König M, Mahan LC (1992) Molecular cloning and expression of a pituitary somatostatin receptor with preferential affinity for somatostatin-28. Mol Pharmacol 42:939–946

O'Carroll AM, Raynor K, Lolait SJ, Reisine T (1994) Characterization of cloned human SRIF receptor SSTR5. Mol Pharmacol 48:291–298

O´Dowd BF, Hnatowich M, Caron MG, Lefkowitz RJ, Bouvier M (1989) Palmitoylation of the human beta2-adrenergic receptor: mutation of Cys341 in the carboxyl tail leads to an uncoupled nonpalmitoylated form of the receptor. J Biol Chem 264:7564–7569

Ozenberger BA, Hadcock JR (1995) A single amino acid substitution in somatostatin receptor subtype 5 increases affinity for somatostatin-14. Mol-Pharmacol 47:82–827

Pan MG, Florio T, Stork PJ (1992) G protein activation of a hormone-stimulated phosphatase in human tumor cells. Science 256:1215–217

Panetta R, Greenwood MT, Warszynska A, Demchyshyn LL, Day R, Niznik HB, Srikant, CB, Patel YC (1994) Molecular cloning, functional characterization and chromosomal localization of a human somatostatin receptor (somatostatin receptor type 5) with preferential affinity for somatostatin 28. Mol Pharmacol 45:417–427

Papageorgiou C, Borer X (1996) A non peptide ligand for the somatostatin receptor having a benzodiazepinone structure. Bioorg Med Chem Lett 6:267–272

Patel Y, Greenwood M, Kent G, Panetta R, Srikant CB (1993) Multiple gene transcripts of the somatostatin receptor SSTR2: tissue selective distribution and cAMP regulation. Biochem Biophys Res Commun 192:288–294

Patel YC, Galanopoulou A (1995) Processing and intracellular targeting of prosomatostatin-derived peptides: the role of mammalian endoproteases. Ciba Found Symp 190:26–40

Patel YC, Greenwood M, Warszynska A, Panetta R, Srikant CB (1994a) All five human somatostatin receptors (hSSTR1–5) are functionally coupled to adenyl cyclase. Biochem Biophys Res Commun 198:605–612

Patel YC, Panetta R, Escher E, Greenwood M, Srikant CB (1994b) Expression of multiple somatostatin receptor genes in AtT-20 cells. Evidence for a novel somatostatin-28 selective receptor subtype. J Biol Chem 269:1506–1509

Perez J, Hoyer D (1995) Coexpression of somatostatin SSTR-4 and SSTR-3 receptor mRNAs in the rat central nervous system. Neuroscience 64:241–253

Perez J, Rigo M, Kaupmann C, Bruns C, Yasuda K, Bell GI, Lübbert H, Hoyer D (1994) Localization of somatostatin (SRIF) SSTR-1, SSTR-2 and SSTR-3 receptor RNA in rat brain by in situ hybridization. N S Arch Pharmacol 349:145–160

Perez J, Vezzani A, Civenni G, Tutka P, Rizzi M, Schupbach E, Hoyer D (1995) Functional effects of D-Phe-c[Cys-Tyr-D-Trp-Lys-Val-Cys]-Trp-NH2 and differen-

tial changes in somatostatin receptor messenger RNAs, binding sites and somatostatin release in kainic acid-treated rats. Neuroscience 65:1087–1097

Piwko C, Thoss VS, Hoyer D (1995) Localization and pharmacological characterization of somatostatin sst2 sites in the rat cerebellum. N S Arch Pharmacol 352:607–613

Pradayrol L, Jornvall H, Mutt V, Ribet A (1980) N-terminally expended somatostatin: the primary structure of somatostatin-28. FEBS Lett 109:55–58

Presky D, Schonbrunn A (1988) Somatostatin pretreatment increases the number of somatostatin receptors in GH_4C_1 pituitary cells and does not reduce cellular responsiveness to somatostatin. J Biol Chem 263:714–723

Prinz C, Sachs G, Walsh JH, Coy DH, Wu SV (1994) The somatostatin receptor subtype on rat enterochromaffin-like cells. Gastroenterology 107:1067–1074

Pscherer A, Dorflinger U, Kirfel J, Gawlas K, Ruschoff J, Buettner R, Schule R (1996) The helix-loop-helix transcription factor SEF-2 regulates the activity of a novel initiator element in the promoter of the human somatostatin receptor II. EMBO J 15:6680–6690

Raulf F, Perez J, Hoyer D, Bruns C (1994) Differential expression of five somatostatin receptor subtypes, SSTR1–5, in the CNS and peripheral tissue. Digestion 55:46–53

Raynor K, Reisine T (1992) Somatostatin receptors. Crit Rev Neurobiol 16:273–289

Raynor K, O'Carroll AM, Kong H, Yasuda K, Mahan LC, Bell GI, Reisine T (1993a) Characterization of cloned somatostatin receptors SSTR4 and SSTR5. Mol Pharmacol 44:385–392

Raynor K, Murphy W, Coy D, Taylor J, Moreau J-P, Yasuda K, Bell GI, Reisine T (1993b) Cloned somatostatin receptors: identification of subtype selective peptides and demonstration of high affinity binding of linear peptides. Mol Pharmacol 43:838–844

Reichlin S (1983) Somatostatin. In: Krieger DT, Brownstein MJ, Martin JB (eds) Brain peptides. Wiley, New York, pp 711–752

Reisine T (1984) Somatostatin desensitization: loss of the ability of somatostatin to inhibit cAMP accumulation and adrenocorticotropin release. J Pharmacol Exp Ther 229:14–20

Reisine T, Axelrod J (1983) Prolonged somatostatin pretreatment desensitizes somatostatin inhibition of receptor-mediated release of adrenocorticotropin and sensitizes adenyl cyclase. Endocrinology 113:811–813

Reisine T, Bell GI (1995) Molecular biology of somatostatin receptors. Endocr Rev 16:427–442

Reisine T, Kong H, Raynor K, Yanao H, Takeda J, Yasuda K, Bell GI (1993) Splice variant of the somatostatin receptor 2 subtype, somatostatin receptor 2B, couples to adenyl cyclase. Mol Pharmacol 44:1016-1020

Reisine T, Heerding J, Raynor K (1994) The third intracellular loop of the delta receptor is necessary for coupling to adenyl cyclase and receptor desensitization. Regul Pept 54:241–242

Rens-Domiano S, Reisine T (1991) Structural analysis and functional role of the carbohydrate component of somatostatin receptors. J Biol Chem 266:20094–20102

Rens-Domiano S, Reisine T (1992) Biochemical and functional properties of somatostatin receptors. J Neurochem 58:1987–1996

Rens-Domiano S, Law S, Yamada Y, Seino S, Bell GI, Reisine T (1992) Pharmacological properties of two cloned somatostatin receptors. Mol Pharmacol 42:28–34

Reubi JC (1984) Evidence for two somatostatin-14 receptor types in rat brain cortex. Neurosci Lett 49:259–263

Reubi JC, Maurer R (1985) Autoradiographic mapping of somatostatin receptors in the rat central nervous system and pituitary. Neuroscience 15:1183–1193

Reubi JC, Kvols L, Krenning E, Lamberts SWJ (1990) Distribution of somatostatin receptors in normal and tumor tissue. Metabolism 39:78–81

Rohrer L, Raulf F, Bruns C, Buettner R, Hofstaedter F, Schuele R (1993) Cloning and characterization of a novel human somatostatin receptor. Proc Natl Acad Sci USA 90:4196–4200

Roosterman D, Roth A, Kreienkamp H-J, Richter D, Meyerhof W (1997) Distinct agonist-mediated endocytosis of cloned rat somatostatin receptor subtypes expressed in insulinoma cells. J Neuroendocrinol 9:741–751

Rosenthal W, Hescheler J, Hinsch K-D, Spicher K, Trautwein W, Schultz G (1988) Cyclic AMP-independent, dual regulation of voltage-dependent Ca^{++} currents by LHRH and somatostatin in a pituitary cell line. EMBO J 7:1627–1633

Rossowski WJ, Coy DH (1994) Specific inhibition of rat pancreatic insulin or glucagon release by receptor-selective somatostatin analogues. Biochem Biophys Res Commun 206:341–346

Rossowski WJ, Gu ZF, Akarca US, Jensen RT, Coy DH (1994) Characterization of somatostatin receptor subtypes controlling rat gastric acid and pancreatic amylase release. Peptides 15:1421–1424

Roth A, Kreienkamp H-J, Nehring RB, Roosterman D, Meyerhof W, Richter D (1997a) Endocytosis of the rat somatostatin receptors: subtype discrimination, ligand specificity, and delineation of carboxyl terminal positive and negative sequence motifs. DNA Cell Biol 16:111–119

Roth A, Kreienkamp, H-J, Meyerhof W, Richter D (1997b) Phosphorylation of four amino acid residues in the carboxyl terminus of the rat somatostatin receptor subtype 3 is crucial for its desensitization and internalization. J Biol Chem 272:23769–23774

Sakanaka C, Ferby I, Waga I, Bito H, Shimizu T (1994) On the mechanism of cytosolic phospholipase A2 activation in CHO cells carrying somatostatin receptor: wortmannin-sensitive pathway to activate mitogen-activated protein kinase. Biochem Biophys Res Commun 205:18–23

Sandvik AK, Dimaline R, Brenna E, Waldum HL (1995) Differential expression and regulation of SSTR2 messenger RNA in rat gastric antrum and corpus. Am J Physiol 269:G542-G547

Schäfer J, Baumeister H, Lorenz A, Meyerhof W (1997) Localization of somatostatin receptor subtype mRNA in the rat gastrointestinal tract and regulation of SSTR1 gene expression. Z Ernährungswiss 36[Suppl 1] (in press)

Schindler M, Harrington KA, Humphrey PP, Emson PC (1995) Cellular localisation and co-expression of somatostatin receptor messenger RNAs in the human brain. Mol Brain Res 34:321–326

Schindler M, Sellers LA, Humphrey PPA, Emson PC (1997) Immunohistochemical localization of the somatostatin SST2(A) receptor in the rat brain and spinal cord. Neuroscience 76:225–240

Schwabe W, Brennan MB, Hochgeschwender U (1996) Isolation and characterization of the mouse (Mus musculus) somatostatin receptor type-4-encoding gene (mSSTR4). Gene 168:233–235

Seaquist ER, Armstrong MB, Gettys TW, Walseth TF (1995) Somatostatin selectively couples to G(o) alpha in HIT-T15 cells. Diabetes 44:85–89

Senaris RM, Humphrey PP, Emson PC (1994) Distribution of somatostatin receptors 1, 2 and 3 mRNA in rat brain and pituitary. Eur J Neurosci 6:1883–1896

Senogles SE (1994) The D2 dopamine receptor isoforms signal through distinct $G_i\alpha$ proteins to inhibit adenyl cyclase: a study with site-directed mutant $G_i\alpha$ proteins. J Biol Chem 269:23120–23127

Shimizu T, Mori M, Bito H, Sakanaka C, Tabuchi S, Aihara M, Kume K (1996) Platelet-activating factor and somatostatin activate mitogen-activated protein kinase (MAP kinase) and arachidonate release. J Lipid Mediat Cell Signal 14:103–108

Shiosaka S, Takatsuki K, Sakanaka M, Inagaki S, Takagi H, Senba E, Kawai Y, Tohyama M (1981) Ontogeny of somatostatin-containing neuron system of the rat: immunohistochemical observations. I. Lower brainstem. J Comp Neurol 203:173–188

Strader DD, Sigal IS, Candelore MR, Rands E, Hill WS, Dixon RAF (1988) Conserved aspartic acid residues 79 and 113 of the β-adrenergic receptor have different roles in receptor function. J Biol Chem 263:10267–10271

Strnad J, Hadcock JR (1995) Identification of a critical aspartate residue in transmembrane domain three necessary for the binding of somatostatin to the somatostatin receptor SSTR2. Biochem Biophys Res Commun 216:913–921

Strnad J, Eppler CM, Corbett M, Hadcock JR (1993) The rat SSTR2 somatostatin receptor subtype is coupled to inhibition of cyclic AMP accumulation. Biochem Biophys Res Commun 191:968–976

Sunahara RK, Dessauer CW, Gilman AG (1996) Complexity and diversity of mammalian adenyl cyclases. Annu Rev Pharmacol Toxicol 36:461–480

Tahiri-Jouti N, Cambillau C, Viguerie N, Vidal C, Buscail L, Saint-Laurent N, Vaysse N, Susini C (1992) Characterization of a membrane tyrosine phosphatase in AR42 J cells: regulation by somatostatin. Am J Physiol 262:G1007-G1014

Tallent M, Reisine T (1992) G_i alpha 1 selectively couples somatostatin receptors to adenyl cyclase in pituitary-derived AtT-20 cells. Mol Pharmacol 41:452–455

Tallent M, Liapakis G, O'Carroll AM, Lolait SJ, Dichter M, Reisine T (1996a) Somatostatin receptor subtypes SSTR2 and SSTR5 couple negatively to an L-type Ca^{2+} current in the pituitary cell line AtT-20. Neuroscience 71:1073–1081

Tallent M, Dichter MA, Reisine T (1996b) Evidence that a novel somatostatin receptor couples to an inward rectifier potassium current in AtT-20 cells. Neuroscience 73:855–864

Taniwaki T, Schwartz JP (1995) Somatostatin enhances neurofilament expression and neurite outgrowth in cultured rat cerebellar granule cells. Dev Brain Res 88:109–116

Thoss VS, Perez J, Duc D, Hoyer D (1995) Embryonic and postnatal mRNA distribution of five somatostatin receptor subtypes in the rat brain. Neuropharmacology 34:1673–1688

Thoss VS, Perez J, Probst A, Hoyer D (1996a) Expression of five somatostatin receptor mRNAs in the human brain and pituitary. N S Arch Pharmacol 354:411–419

Thoss VS, Duc D, Hoyer D (1996b) Somatostatin receptors in the developing rat brain. Eur J Pharmacol 297:145–155

Todisco A, Seva C, Takeuchi Y, Dickinson CJ, Yamada T (1995) Somatostatin inhibits AP-1 function via multiple protein phosphatases. Am J Physiol 269:G160–G166

Tomura H, Okajima F, Akbar M, Abdul-Majid M, Sho K, Kondo Y (1994) Transfected human somatostatin receptor type 2, SSTR2, not only inhibits adenylate cyclase but also stimulates phospholipase C and Ca^{2+} mobilization. Biochem Biophys Res Commun 200:986–992

Tran VT, Beal MF, Martin JB (1985) Two types of somatostatin receptors differentiated by cyclic somatostatin analogs. Science 228:492–495

Twery MJ, Wong LA, Gallagher JP (1991) Somatostatin induced hyperpolarization of septal neurons is not blocked by pertussis toxin. Eur J Pharmacol 192:287–291

Uhl GR, Tran V, Snyder SH, Martin JB (1985) Somatostatin receptors: distribution in the rat central nervous system and human frontal cortex. J Comp Neurol 240:288–304

Vanetti M, Kouba M, Wang X, Vogt G, Hollt V (1992) Cloning and expression of a novel mouse somatostatin receptor. FEBS Lett 311:290–294

Vanetti M, Vogt G, Hollt V (1993) The two isoforms of the mouse somatostatin receptor (mSSTR2A and mSSTR2B) differ in coupling efficiency to adenylate cyclase and in agonist-induced receptor desensitization. FEBS Lett 331:260–266

Vanetti M, Ziolkowska B, Wang X, Horn G, Hollt V (1994) mRNA distribution of two isoforms of somatostatin receptor 2 (mSSTR2A and mSSTR2B) in mouse brain. Mol Brain Res 27:45–50

Vassas A, Bourdy G, Paillard JJ, Lavayre J, Pais M, Quirion JC, Debitus C (1996) Naturally occurring somatostatin and vasoactive intestinal peptide inhibitors. Isolation of alkaloids from two marine sponges. Planta Med 62:28–30

Vidal C, Rauly I, Zeggari M, Delesque N, Esteve JP, Saint-Laurent N, Vaysse N, Susini C (1994) Up-regulation of somatostatin receptors by epidermal growth factor and gastrin in pancreatic cancer cells. Mol Pharmacol 46:97–104

Viguerie N, Tahiri-Jouti N, Esteve J, Clerc P, Logsdon C, Svoboda M, Susini C, Vaysse N, Ribet A (1988) Functional somatostatin receptors on rat pancreatic acinar cell line. Am J Physiol 255:G113–G120

Villar MJ, Hökfelt T, Brown JC (1989) Somatostatin expression in the cerebellar cortex during post-natal development; an immunohistochemical study in the rat. Anat Embryol 179:257–267

Vincent SR, McIntosh CHS, Buchan AMJ, Brown JC (1985) Central somatostatin systems revealed with monoclonal antibodies. J Comp Neurol 238:169–186

Viollet C, Faivre-Bauman A, Zhang J, Llorens-Cortes C, Loudes C, Kordon C, Epelbaum J (1995) Differential expression of somatostatin receptors by quantitative PCR in the rat brain. C R Acad Sci III 318:851–857

Viollet C, Bodenant C, Prunotto C, Roosterman D, Schäfer J, Meyerhof W, Epelbaum J Vaudry H, Leroux P (1997) Differential expression of multiple somatostatin receptors in the rat cerebellum during development. J Neurochem 68:2378–2272

Wang H, Bogen C, Reisine T, Dichter M (1989) Somatostatin-14 and somatostatin-28 induce opposite effects on potassium currents in rat neocortical neurons. Proc Natl Acad Sci USA 86:9616–9620

Wang H, Reisine T, Dichter M (1990a) Somatostatin-14 and somatostatin-28 inhibit calcium currents in rat neocortical neurons. Neuroscience 38:335–342

Wang H, Dichter M, Reisine T (1990b) Lack of cross-desensitization of somatostatin-14 and somatostatin-28 receptors coupled to potassium channels in rat neocortical neurons. Mol Pharmacol 38:357–361

Warhurst G, Higgs NB, Fakhoury H, Warhurst AC, Garde J, Coy DH (1996) Somatostatin receptor subtype 2 mediates somatostatin inhibition of ion secretion in rat distal colon. Gastroenterology 111:325–333

Weckbecker G, Raulf F, Stolz B, Bruns C (1993) Somatostatin analogs for diagnosis and treatment of cancer. Pharmacol Ther 60:245–264

Wong SK, Ross EM (1994) Chimeric muscarinic cholinergic:beta-adrenergic receptors that are functionally promiscuous among G proteins. J Biol Chem 269:18968–18976

Wulfsen I, Meyerhof W, Fehr S, Richter D (1993) Expression patterns of rat somatostatin receptor genes in pre- and postnatal brain and pituitary. J Neurochem 61:1549–1552

Xu Y, Song J, Bruno JF, Berelowitz M (1993) Molecular cloning and sequencing of a human somatostatin receptor, hSSTR4. Biochem Biophys Res Commun 193:648–652

Xu Y, Berelowitz M, Bruno JF (1995) Dexamethasone regulates somatostatin receptor subtype messenger ribonucleic acid expression in rat pituitary GH4C1 cells. Endocrinology 136:5070–5075

Yamada Y, Post SR, Wang K, Tager HS, Bell GI, Seino S (1992) Cloning and functional characterization of a family of human and mouse somatostatin receptors expressed in brain, gastrointestinal tract and kidney. Proc Natl Acad Sci USA 89:251–255

Yamada Y, Kagimoto S, Kubota A, Yasuda K, Masuda K, Someya Y, Ihara Y, Li Q, Imura H, Seino S, Seino Y (1993) Cloning, functional expression and pharmacological characterization of a fourth (hSSTR4) and fifth (hSSTR5) human SRIF receptor subtype. Biochem Biophys Res Commun 195:844–852

Yasuda K, Rens-Domiano S, Breder CD, Law SF, Saper CB, Reisine T, Bell GI (1992) Cloning of a novel somatostatin receptor, SSTR3, coupled to adenyl cyclase. J Biol Chem 267:20422–20428

Yatani A, Codina J, Sekura R, Birnbaumer L, Brown A (1987) Reconstitution of somatostatin and muscarinic receptor mediated stimulation of K^+ channels by G_k protein in clonal rat anterior pituitary cell membrane. Mol Endocrinol 1:283–293

Zaki M, Harrington L, McCuen R, Coy DH, Arimura A, Schubert ML (1996) Somatostatin receptor subtype 2 mediates inhibition of gastrin and histamine secretion from human, dog, and rat antrum. Gastroenterology 111:919–924

Editor-in-charge: Professor G. Schultz

Cytokine-Mediated Hepatic Apoptosis

M. Leist[1], F. Gantner[2], G. Künstle[2], and A. Wendel[2]

[1]Chair of Molecular Toxicology, Faculty of Biology, University of Konstanz, POB X911, 78457 Konstanz, Germany
[2]Chair of Biochemical Pharmacology, Faculty of Biology, University of Konstanz

Contents

1 Introduction 110
2 Apoptosis vs Necrosis: Definitions and Delimitations 110
3 Evidence for Apoptosis in the Liver 114
3.1 Historical Aspects 114
3.2 Inflammation and Hepatic Apoptosis 115
3.3 Viral Disease and Apoptosis 116
3.4 Apoptosis Induced by Toxins and Organ Size Regression . . 118
4 Hepatic Apoptosis Elicited by Cytokine Signaling 118
4.1 Transforming Growth Factor-β 118
4.2 Tumor Necrosis Factor 119
4.2.1 Studies in Hepatocyte Cultures 120
4.2.2 In Vivo Studies in Mice 122
4.2.3 LPS-Induced Endogenous Production of TNF 123
4.2.4 Induction of Endogenous TNF by Stimuli Other Than LPS . 124
4.3 CD95 (fas/APO-1) 125
4.3.1 Studies in Hepatocyte Cultures 126
4.3.2 In Vivo Studies in Mice 126
4.4 Delimitation of the CD95/CD95L System and the TNF-R/TNF System 127
5 Mechanisms and Modulation of Hepatic Apoptosis 128
5.1 Key Mechanisms of Apoptosis 130
5.2 Pharmacological Prevention of Apoptosis 131
5.3 Immunological and Genetic Modulation of Apoptosis . . . 133
6 Apoptosis in Hepatotoxicology 134
6.1 Mediators Derived From Non-parenchymal Cells and Cytokines in Hepatotoxicology 135
6.2 Toxin-Induced Apoptosis 136
6.3 TNF as Mediator of Toxin-Induced Apoptosis 136
References 138

1 Introduction

Thirty years ago liver pathology defined apoptosis as a novel mode of cell death. Recently, experimental models of liver injury have been made available for examining the signaling molecules and receptors of apoptotic mechanisms as well as their pathological relevance. Experimental evidence suggests the involvement of apoptosis not only in various inflammatory liver disorders, but also in conditions of poisoning with xenobiotic hepatotoxins. The presence of several differentially regulated apoptosis-mediating receptors and their ligands on hepatocytes may explain the liver's susceptibility to autoimmune reactions, toxins, and viruses causing chronic liver disease, as well as the differential sensitivity of this system in various metabolic and pathologic conditions.

Tumor necrosis factor (TNF) and its receptors (TNF-R), as well as CD95L and its receptor (CD95), are well-known cytokine/cytokine receptor systems relevant to hepatic disease and to apoptosis. Neutralization of endogenously released TNF prevents hepatocyte apoptosis associated with inflammatory liver damage. Direct injection of TNF in sensitized mice results in large scale hepatocyte apoptosis which is exclusively and selectively mediated by the 55-kDa TNF-R. Fulminant apoptotic liver damage is also triggered upon stimulation of CD95. Possible triggering cells include hepatocytes that express CD95L under pathological conditions. Despite the lack of interaction between TNF-R and CD95 on the receptor level, their signal transduction inside the cell seems to involve common proteolytic steps since inhibition of proteases of the caspase family blocks hepatocyte death, liver damage, or lethality in mice signaled by either receptor.

2 Apoptosis vs Necrosis: Definitions and Delimitations

Despite early pioneering studies of pathologists and developmental biologists on programmed cell death in regressing organs and during development, up until the late 1960s cell death had been mostly regarded as a passive and barely regulated event that follows excessive disturbances of cellular homeostasis (see review in Majno and Joris 1995). Up to that time

mechanisms of cell death had been exclusively studied in tissues of multicellular organisms and the events following cell death on the tissue level were termed necrosis. Nowadays, cell death has become an important topic in biochemistry, cell biology, immunology, and molecular biology. In these fields the word necrosis is often used to describe a type of cell demise characterized by edema, swelling, and dysfunction of intracellular organelles, with rupture of the cell membrane and without precedent packaging and ordered fragmentation of the chromatin (for the purposes of this chapter we follow this definition). Since, strictly speaking, the term necrosis refers to post-mortem events in tissues, alternative terms such as oncosis or lytic cell death have been suggested for the description of the above mode of cell demise (Majno and Joris 1995). Although historically more correct these terms are generally less common.

A different form of cell death with a distinct morphology was first described more than 100 years ago (Flemming 1885; Councilman 1890; Nissen 1886; Pfitzner 1886). This form of cell death was finally classified as a morphological entity of its own (Table 1) with distinct conceptual implications by Kerr, Wyllie, and Currie, and eventually named apoptosis (Kerr et al. 1972). Its defining features include: shrinkage of the cell, detachment from neighboring cells, preservation of the morphological structure of intracellular organelles, packaging and specific fragmentation of the chromatin, and specific cell membrane alterations indicating the readiness to be phagocytosed. Apoptosis is an inconspicuous type of cell death, allowing rapid removal of the dying cell to prevent tissue damage and inflammation that would otherwise be caused by spilt cell contents (Gräper 1914; Savill et al. 1993). In addition, apoptosis favors rapid reorganization of the tissue to the original structure, and avoids leakiness of epithelia such as that formed by gut brush border cells. Accordingly, patients may recover from massive, probably apoptotic, hepatocyte loss during fulminant viral hepatitis without scarring (Karvountzis et al. 1974). In cell cultures exposed to apoptotic stimuli or in pathological situations associated with an extremely high rate of synchronized apoptosis, cells cannot be taken up by phagocytosis and eventually lyse. This process of secondary lysis of originally apoptotic cells is often confusingly called secondary necrosis or apoptotic necrosis. However, this post-mortem process does not seem to be related to necrotic/lytic/oncotic cell demise (which describes the transition of living to dead cells).

In parallel to the pathological characterization of apoptosis, developmental biologists discovered a form of "natural" cell death, occurring

Table 1. Distinguishing features of apoptosis and necrosis

	Apoptosis	Necrosis
Nucleus	Condensation and margination of chromatin, often to characteristic crescent-shaped figures. Very frequently disintegration into sharply delineated spherical chromatin masses that are eventually scattered throughout the cytosol	Occasionally condensation (pyknosis) at initial stages; later mostly disintegration (karyorrhexis) and dissolution (karyolysis). On light microscopic level, early pyknotic stages may sometimes resemble apoptosis
Cytoplasm	Condensation of cytosol. Dense packaging of relatively intact organelles. Occasional dilatation of endoplasmic reticulum. Occasionally pronounced autophagic vacuolization	Edematous swelling of organelles and rupture of intracellular membranes
Tissue distribution	Mostly affecting scattered single cells. Detachment of apoptotic cells from neighboring cells and rounding up	Often contiguous groups of cells are affected. Often, no retraction/ rounding up of affected cells, but rather closure of intercellular gaps due to edema
Plasma membrane	Loss of microvilli; blebbing (zeiosis) with maintenance of membrane integrity until cells are phagocytosed; display of phagocytosis signals; rapid active loss of lipid assymetry	Blebbing, leading eventually to rupture of plasma and spillage of intracellular contents
DNA fragmentation	Characteristic high molecular weight DNA fragmentation into 50-kbp and 300-kbp fragments. In many cases oligonucleosomal cleavage into n × 180-bp DNA-fragments	Sometimes random DNA degradation. Often little DNA degradation before lysis of the plasma membrane
Phagocytosis	Rapid removal by professional phagocytes and by neighboring cells	Clearance of necrotic tissue by infiltrating phagocytes after disintegration of cells
Tissue reaction	Mostly inconspicuous; mostly reconstitutio ad integrum; often apoptosis necessary for tissue organization	Often inflammatory response, leukocyte infiltration, production of immune mediators; often formation of scar tissue or disturbance of tissue organization

without severe external insult, but often involving de novo gene induction (Glücksmann 1951; Schwartz and Osborne 1993; Saunders 1966; Lockshin and Beaulaton 1974). Certain cells seemed to be destined (or "programmed") to die at a given stage of development at a given location. In fact, this process of creation of cells that would be eliminated according to a predetermined scheme had already been outlined in 1858 by Virchow in his lecture on atherosclerosis: "Thus, we have here an active process which really produces new tissue, but then hurries on to destruction in consequence of its own development" (Virchow 1858). It is now clear that most of this so-called programmed developmental cell death is characterized by apoptotic morphology. The terms apoptosis and programmed cell death are therefore currently used as synonyms, although forms of programmed cell death (especially in multinucleated muscle cells) without apoptotic morphology may exist (Schwartz et al. 1993; Lockshin and Williams 1965). Notably, it is now evident that there is no absolute requirement of gene induction for programmed cell death or apoptosis to occur. Transcription may be required in many instances in the signaling phase of apoptosis to create a metabolic situation in the cell that would cause a constitutively present core program to be executed (Weil et al. 1996). This core program may be conceived as the series of partially self-regulatory steps, beyond the signaling phase, that can lead to cell demise. Since the proper execution of these steps commonly results in apoptotic morphology, the term apoptosis has gained a conceptual aspect in addition to its original strictly morphological definition.

Recent observations suggest that apoptosis and necrosis present only the two extremes of a continuum of different modes of cell death. It has been experimentally shown that the same stimulus may either induce apoptosis or necrosis, depending on the metabolic situation or the intensity of the insult (Leist and Nicotera 1997; Nicotera and Leist 1997). This may be explained by some characteristics of the internal death program: this program does not seem to be strictly linear and sequential, but rather it involves various partially independent branches responsible for the different characteristic features of apoptotic cells (e.g., membrane changes and nuclear changes). The cell will die by pure apoptosis if this program can be run and terminated properly and undisturbed. In contrast, necrosis or intermediate forms are observed if the insult is so intense that only parts of the program can be executed before unspecific events (e.g., failure of ion pumps) lead to membrane rupture. Thus, many intermediate or even completely different morphological (Leist and Wendel 1996) variants

of cell death may exist. In experimental studies on liver cell death, a continuum of different modes of cell demise is often observed (Bohlinger et al. 1995; Leist et al. 1996a; Oberhammer et al. 1996; Zeid et al. 1997; Fukuda et al. 1993; Ledda-Columbano et al. 1991; Columbano 1995). This may be explained by the recruitment of different execution mechanisms in cells exposed to different concentrations of toxins. An alternative explanation has been derived from studies of lymphocyte and neuronal death (Nicotera and Leist 1997). The metabolic situation of the cell, in particular the ATP content, may determine the shape and mode of cell demise. For example, when ATP levels were experimentally reduced, typically apoptotic stimuli would result in necrosis (Leist et al. 1997b).

3
Evidence for Apoptosis in the Liver

Studies on the regressing or pathological liver and on isolated hepatocytes have initially contributed largely to the identification and characterization both of apoptosis and necrosis (Svoboda et al. 1962; Klion and Schaffner 1966; Levy et al. 1968; Kehrer et al. 1990; Orrenius et al. 1989; Kerr 1971). However, due to its inconspicuous characteristics the widespread occurrence and relevance of apoptosis for human pathology has been generally appreciated only recently (Que and Gores 1996; Schulte-Hermann et al. 1995), in contrast to the early recognition of ischemic or necrotic cell death.

3.1
Historical Aspects

Before the term apoptosis was coined (Kerr et al. 1972), the morphological appearance of this mode of cell death in the liver had been known as shrinkage necrosis, Councilman bodies, chromatolysis, acidophilic bodies, or eosinophilic single-cell necrosis, and apoptotic shrinkage of the chromatin was described as pyknosis (Biava and Mukhlova-Montiel 1965; Miyai et al. 1962; Moppert et al. 1967; Kerr 1971; Klion and Schaffner 1966; Svoboda et al. 1962; Child and Ruiz 1968). The earliest descriptions of hepatic apoptosis date back to 1890 with the characterization of histopathology due to yellow fever (Councilman 1890). Strong interest in hepatic apoptosis developed in the 1960s and the state of the art at that

time is compiled in the milestone review by Kerr et al. (1972). First evidence of intracellular mechanisms characteristic of apoptosis was found in 1970, when Williams described oligonucleosomal DNA fragmentation in embryonic liver (Williamson 1970). Despite the appearance of visionary and instructive reviews (Kerr et al. 1972; Wyllie et al. 1980; Searle et al. 1982, 1987), the field of apoptosis research hardly moved until the late 1980s, when new methodological approaches finally led to the explosive development seen today.

3.2 Inflammation and Hepatic Apoptosis

Apoptosis is a mode of cell death that does not generally favor ensuing inflammation. Accordingly, large numbers of hepatocytes may die by apoptosis without significant enzyme release or inflammation (Hully et al. 1994). On the other hand, inflammatory mediators often induce hepatocyte apoptosis. In the liver apoptosis and necrosis often occur simultaneously, especially with high intensity insults killing more than 20% of all hepatocytes within hours. Accordingly, apoptotic hepatocytes can be found simultaneously with typical signs of inflammation or hemorrhage.

The prototype of a general inflammatory stimulus is lipopolysaccharide (LPS). This substance has been demonstrated to induce murine hepatocyte apoptosis with concomitant necrosis upon injection of sublethal doses into mice (Levy et al. 1968). Upon injection of lethal doses, liver damage was predominantly necrotic (Bohlinger et al. 1996). In addition to LPS, hepatic inflammation may also be induced by injection of D-galactosamine (GalN). This prototype liver-specific toxin acts by sensitizing the liver towards the effects of endogenous or exogenously applied LPS (Galanos et al. 1979; review in Leist et al. 1995a) and has been shown to induce hepatocyte destruction and apoptosis (Reutter et al. 1968, 1970; Keppler et al. 1968).

In inflammatory conditions not directly induced by experimental inflammogens there is also evidence of hepatocyte apoptosis: Apoptosis is found during chronic active hepatitis (Kerr et al. 1979; Searle et al. 1982; Hiramatsu et al. 1994) and liver allograft rejection (Battersby et al. 1974; Searle and Balderson 1996; Krams et al. 1995; Searle et al. 1982). In addition, TNF is induced during acute hepatitis (Torre et al. 1994; Ding-feng et al. 1993) and type-2 autoimmune hepatitis is linked to CD95 mutation (Pensati et al. 1997). TNF is a powerful inflammogen and has been shown

to be a potent inducer of hepatocyte apoptosis in sensitized and non-sensitized mice (Gantner et al. 1995b; Leist et al. 1994).

3.3 Viral Disease and Apoptosis

There is ample evidence of hepatocyte apoptosis in mouse and man during viral infection (Hiramatsu et al. 1994; Klion and Schaffner 1966; Svoboda et al. 1962; Child and Ruiz 1968; Kerr et al. 1979; Searle et al. 1982). Additional evidence for induction of liver damage possibly by hepatocyte apoptosis comes from the findings that viral infection strongly sensitizes the liver towards LPS toxicity (Gut et al. 1984; Mori et al. 1981), and that under defined experimental conditions injection of viral antigens can cause fulminant liver failure (Mori et al. 1981). Viral infection may result in hepatocyte apoptosis by three conceptionally different mechanisms: (1) Viruses may directly induce apoptosis of cells; (2) hepatocytes presenting viral peptides may be attacked by cytotoxic lymphocytes that kill their target cell by apoptosis (Kondo et al. 1997). Accordingly, lymphocytes are found in close association with apoptotic hepatocytes (Bathal et al. 1982; Galle et al. 1995); and (3) upon viral infection hepatocytes may become sensitive towards certain apoptosis-inducing cytokines. This concept is based on the following lines of evidence: Firstly, viruses may elicit the production and upregulation of proapoptotic cytokines and their receptors even within hepatocytes (González-Amaro et al. 1994; Hiramatsu et al. 1994; Galle et al. 1995); secondly, viral infection generally sensitizes cells towards TNF toxicity or TNF-induced apoptosis (Ohno et al. 1993; review in Wong et al. 1992; Rubin 1992). Accordingly, TNF is frequently virustatic. The sensitization of cells may be explained by the transcriptional inhibition of cell-specific RNA by viruses (Huang and Wagner 1965). Under the metabolic condition of transcriptional block hepatocytes are sensitized more than 10 000-fold towards TNF-induced apoptosis (Leist et al. 1994). In particular, it has been shown that expression of hepatitis B virus (HBV) or HBx protein sensitized cells dose-dependently towards the induction of apoptosis by TNF (Guilhot et al. 1996; Su and Schneider 1997) and expression of HBV protein in transgenic mice sensitized hepatocytes towards TNF- and interferon (IFN)-γ-induced apoptosis and liver damage (Gilles et al. 1992).

Control of viral infection by apoptosis as opposed to necrosis would provide a considerable advantage to the body. Viral particles would not be

Table 2. Toxins, intercellular signaling, and hepatocyte apoptosis

Toxin	Immune mediators[a]	Synergy with LPS or TNF	Apoptosis	DNA-fragmentation	References
Paracetamol	+	np	+	+	Laskin et al. (1995); Ray et al. (1993, 1996); Blazka et al. (1995, 1996)
Cocaine	np	np	+	+	Cascales et al. (1994)
Nitrosamine	np	np	+	+	Pritchard and Butler (1989); Ray et al. (1992); Shikata et al. (1996)
Ethanol	+	+	+	np	Adachi et al. (1994); Goldin et al. (1993); Hansen et al. (1994); Koop et al. (1997); Higuchi et al. (1996)
D-Galactosamine	+	+	+	np	Czaja et al. (1994); Keppler et al. (1968); Galanos et al. (1979)
Pb^{2+} (withdrawal)	np	+	+	np	Honchel et al. (1991); Seyberth et al. (1972); Selye et al. (1966); Columbano et al. (1985)
Thioacetamide	np	np	+	np	Ledda-Columbano et al. (1991)
α-Amanitin	+	+	+	+	Leist et al. (1997a); Seyberth et al. (1972)
Actinomycin D	+	+	+	+	Leist et al. (1994, 1995a, 1997a)
Diethyldithiocarbamate	+	np	np	np	Ishiyama et al. (1995)
Phalloidin	+	np	np	np	Barriault et al. (1995)
CCl_4	+	+	+	np	Czaja et al. (1994, 1995); Leach and Forbes (1941); Nolan (1989); Shi et al. (1997)
Cyproteroneacetate	+	synergy with TGF-β	+	np	Oberhammer et al. (1996)
Heliotrine (pyrrolizidine)	np	np	+	np	Kerr (1969)
Ischemia-reperfusion	np	np	+	+	Sasaki et al. (1996); Shimizu et al. (1996)
Microcystine	+	np	np	np	Nakano et al. (1991)

[a]Non-parenchymal liver cells or immune mediators are involved in toxicity.
+, Positive evidence; np, no obvious evidence published in the cited reference.

released from dying cells, but rather be digested, after phagocytosis of the membrane-enclosed apoptotic bodies. In addition, viral DNA would be destroyed by the process of oligonucleosomal DNA-fragmentation, that is typically found in hepatocytes killed by TNF or CD95 (Leist et al. 1994, 1996a).

3.4
Apoptosis Induced by Toxins and Organ Size Regression

It was recognized (Kerr et al. 1972) very early that apoptosis is not only the physiological mode of cell death in tissue turnover and development, but it may also be induced by stressful stimuli, toxins, unfavorable environmental conditions, and organ size regression (Ledda-Columbano et al. 1996; Columbano et al. 1985; Kerr 1971; Bursch et al. 1992; Grasl Kraupp et al. 1994). Accordingly, a large number of toxins produce hepatocyte apoptosis (Table 2), often associated with concomitant necrosis. The significance of apoptosis has been little appreciated by many toxicologists in the past. However, in this field the distinction between apoptosis and necrosis may have major practical implications for the interpretation of tissue damage, of the mechanisms leading to cell death, and for the design of preventive therapies.

4
Hepatic Apoptosis Elicited by Cytokine Signaling

4.1
Transforming Growth Factor-β

Transforming growth factor (TGF)-β is involved in many inflammatory processes. However, it differs from classical proinflammatory cytokines since it may also have strong anti-inflammatory (Randow et al. 1995), cytoprotective (Prehn et al. 1994; Merrill and Zimmerman 1991), and growth regulatory functions (Bedossa et al. 1995). In the liver it acts as a negative regulator of hepatocyte growth (Bursch et al. 1992) and mediates collagen deposition by Ito cells and fibrosis (Weiner et al. 1990).

TGF-β was identified as the first defined mediator eliciting hepatocyte apoptosis (Oberhammer et al. 1991–1993a). It seems to be involved in the normal growth regulation of the liver rather than in inflammatory or

infectious hepatocyte apoptosis. In fact, TGF-β-induced hepatocyte apoptosis is counteracted by the inflammogen LPS (Martin-Sanz et al. 1996) possibly due to the induction of protective growth factors (Fabregat et al. 1996). Overexpression of TGF-β in transgenic mice leads to multiple tissue lesions, including hepatocyte apoptosis (Sanderson et al. 1995). The acute hepatocyte toxicity of TGF-β (≤16 h) is relatively low (Oberhammer et al. 1992, 1996) compared to that mediated by TNF or CD95L. However, the mechanism of apoptosis induction by the three cytokines may be similar as far as the activation of caspase-3-related proteases is concerned (Künstle et al. 1997; Rodriguez et al. 1996b; Rouquet et al. 1996b; Inayat-Hussain et al. 1997). The effects of TGF-β after prolonged exposure seem to depend on the metabolic situation of the liver, e.g., TGF-β-induced apoptosis is greatly enhanced in vivo and in vitro by tumor promoters, cyproterone acetate treatment, or conditions of liver size regression (Oberhammer and Qin 1995; Oberhammer et al. 1993a, 1996). A specific characteristic of TGF-β is the arrest of apoptotic DNA fragmentation at the level of 50-kbp fragments in rat liver (Oberhammer et al. 1993b). This is an important example showing that oligonucleosomal DNA fragmentation is not generally required for the apoptotic process. In various hepatoma cell lines TGF-β induces oligonucleosomal DNA fragmentation (Lin and Chou 1992), and the related protein activin induces murine hepatic apoptosis associated with oligonucleosomal DNA fragmentation (Hully et al. 1994).

4.2
Tumor Necrosis Factor

TNFs are cytokines produced mainly by macrophages and T-cells, but under certain metabolic conditions also by many other cell types. Soluble or membrane-bound (Ware et al. 1992) TNF-β (also known as lymphotoxin-α) acts on either TNF receptors (Stauber and Aggarwal 1989) or, in conjunction with lymphotoxin-β, on a specific lymphotoxin receptor (Crowe et al. 1994; Browning et al. 1993). TNF-α is initially expressed as a 26-kDa membrane protein. Alternatively, the extracellular 17-kDa part is released by a metalloproteinase (Mohler et al. 1994) into the circulation and acts as a trimer on TNF receptors. Both the membrane-bound form and the soluble form have been found to be involved in toxic and inflammatory processes. TNF-α (TNF) is an extremely pleiotropic mediator inducing hepatic acute phase response, hepatic regeneration and growth, stimulation of immune cells, upregulation of adhesion molecules, shock-

like conditions, lipolysis, cachexia, tissue destruction, and apoptotic or necrotic cell death in various cell types (Beutler 1992; Aggarwal and Vilcek 1992). Its cellular effects are mediated by two receptors, i.e., the 55-kDa TNF-RI and the 75-kDa TNF-RII (Lewis et al. 1991; Tartaglia and Goeddel 1992). Its signal transduction involves trimerization and consequent binding of intracellular proteins (Peter et al. 1996; Wallach et al. 1996; Wallach 1997; Darnay and Aggarwal 1997) to the cytoplasmic tail of the receptor. The coupling of TNF-RI by various adaptor proteins to distinct downstream signaling pathways has been characterized recently: One pathway ends with the activation of caspases, a second involves the generation of ceramide by neutral sphingomyelinase, a third involves Jun NH_2-terminal kinase (JNK) activation, and a further one leads to the activation of the apoptosis-preventing transcription factor nuclear factor (NF)-κB (Z.G. Liu et al. 1996; Adam-Klages et al. 1996). The most relevant pathway for the initiation of cell death is the activation of caspases with the cleavage of caspase-8 (FLICE) and caspase-10 possibly constituting the first steps in a protease cascade (Boldin et al. 1996; Muzio et al. 1996). This pathway seems to be autoinhibited by the presence of dominant negative variants of caspases in the cell (Wallach 1997; Irmler et al. 1997), that resemble the viral FLICE-inhibitory proteins (FLIPs) (Thome et al. 1997). In addition, mitochondrial alterations and signals are involved in the toxic effects of TNF in various cell types (Stadler et al. 1992; Higuchi et al. 1997; Lancaster et al. 1989; Pastorino et al. 1996). It is likely that the balance of all these pathways determines the cellular fate.

4.2.1
Studies in Hepatocyte Cultures

The study of TNF-induced apoptosis in isolated hepatocytes has been complicated by the fact that under standard short-term culture conditions, TNF alone induces no or only very a low percentage of hepatocyte death (Guilhot et al. 1996; Leist et al. 1994, 1995b; Stadler et al. 1992; Shinagawa et al. 1991). Cell death was only observed if TNF was present in excessively high concentrations in combination with IFN-γ (Adamson and Billings 1992, 1993). Under very specialized culture conditions direct hepatocyte apoptosis by TNF is observed (Bour et al. 1996; Ohno and Maier 1995). This difficulty in studying TNF toxicity in hepatocyte cultures is due to the fact that TNF transmits simultaneously possibly cytotoxic signals, and induces various cytoprotective mechanisms, such as the activation of NF-

κB (Z.G. Liu et al. 1996; Beutler 1992; Aggarwal and Vilcek 1992). When these effects are eliminated by blocking transcription, hepatocytes become extremely sensitive to TNF (Leist et al. 1994). Under these conditions ≥80% of all cells in culture were killed within 16 h as evidenced by enzyme leakage and loss of the ability to reduce tetrazolium salts. The typical features of cell death were chromatin condensation, budding of the cells, formation of crescent-shaped chromatin lumps and break-up of the chromatin in several apoptotic bodies. These structural changes occurred within hepatocytes which maintained their membrane integrity. In parallel to the structural changes and well before membrane lysis, the DNA fragments and a typical oligonucleosomal pattern of cleavage is observed. All these observations are characteristic of apoptotic cell death. Similar results, i.e., TNF-induced apoptotic cell death under the condition of transcriptional sensitization by actinomycin D (ActD) (Fig. 1), GalN, or α-amanitin, were obtained in cultures of HepG2 human hepatoma cells (Leist et al. 1994, 1997a). Examination of the signal transduction showed

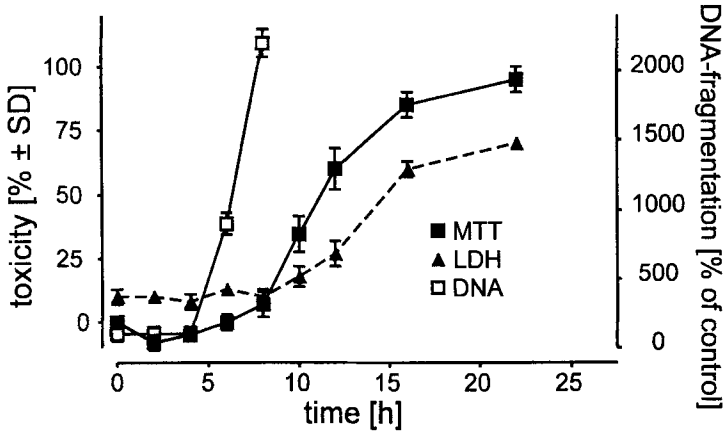

Fig. 1. Time course of cell death parameters in tumor necrosis factor (TNF)-induced apoptosis. Human hepatoma cells (HepG2) were incubated in the presence of 400 nM actinomycin D plus 1.6 ng/ml recombinant human TNF (rhTNF)-α. MTT-dye reduction (parameter of mitochondrial function), lactate dehydrogenase (*LDH*) release (parameter for cell membrane rupture), and DNA fragmentation (parameter associated with typically apoptotic nuclear changes) were determined over a time period of 24 h. As is characteristic of apoptotic cell death, DNA fragmentation always preceded the other death parameters. Similar findings have been obtained in primary hepatocyte cultures and murine livers

that neither reactive oxygen species (ROS) nor NO, nor any of the various other well-known classical second messengers played a significant role as mediator of apoptotic death (Leist et al. 1994).

4.2.2 In Vivo Studies in Mice

TNF has been shown to be hepatotoxic in man and mice (Jones and Selby 1989; Talmadge et al. 1987). Mice can be dramatically sensitized (up to 10 000-fold) by viral or bacterial infection or chemicals such as GalN. The aminosugar GalN is metabolized by enzymes of galactose metabolism that are only present in hepatocytes. High concentrations of GalN cause a selective depletion of uridine nucleotides in hepatocytes (Decker and Keppler 1974). Therefore, they cause a selective transcriptional inhibition in rat (Keppler et al. 1968) or murine (Leist et al. 1995a) liver. The mechanism of sensitization towards TNF by this substance is due to the selective facilitation of hepatocyte apoptosis caused by such a transcriptional block (Leist et al. 1994, 1995a). Accordingly, selective hepatocyte apoptosis in mice is also observed when GalN is substituted by the general and non-organ-specific transcriptional inhibitors ActD or α-amanitin (Leist et al. 1994, 1995a, 1997a). Hepatocyte apoptosis in vivo develops analogously to that observed in vitro. Condensation, margination, and fragmentation of the chromatin, associated with oligonucleosomal DNA fragmentation precedes the loss of intracellular enzymes or a drop of total glutathione levels as parameters for membrane lysis or oxidative stress, respectively (Leist et al. 1994, 1995a,b). Histological examination of the late phases of TNF-induced liver damage in mice sensitized either by GalN or ActD showed widespread necrosis, inflammation, and hemorrhage. Thus, there is a sequence of events characterized by initially pure hepatocyte apoptosis that is followed by the simultaneous occurrence of apoptosis and necrosis as the liver damage proceeds to virtually complete destruction of the organ. Similar events are observed if livers are not sensitized by transcriptional inhibitors, but by preceding infection with *Propionibacterium. acnes* (Tsuji et al. 1997). Due to the complexity of the in vivo approach, it is difficult to decide at this point: (1) whether the occurrence of necrosis is due to secondary actions of TNF, possibly involving other cell types (Sauer et al. 1996; Hewett et al. 1993), (2) whether this is due to an inherent, but direct, necrosis-inducing activity of TNF, or (3) whether this is due to an incompletely terminated apoptotic program in an overstressed or energy-de-

pleted tissue. There is some evidence for each of these possibilities. The last possibility is backed by findings (Leist and Nicotera 1997) that a variety of insults induce apoptosis at low intensities and cause necrosis if the intensity or duration of stress is increased (Dypbukt et al. 1994; Ankarcrona et al. 1995; Bonfoco et al. 1995; Shimizu et al. 1996; Oberhammer et al. 1996; Hartley et al. 1994; Lennon et al. 1991; Jensen et al. 1992; Corcoran and Ray 1992; Zeid et al. 1997; Fukuda et al. 1993; Ledda-Columbano et al. 1991). In addition, we found that typically apoptotic stimuli cause necrosis of T cells if their ATP levels are reduced (Leist et al. 1997b).

The large scale induction of hepatocyte apoptosis in vivo and in vitro suggests that a very effective endogenous death program is present in hepatocytes. This can be very easily triggered under certain metabolic conditions whereas it is efficiently repressed in others. When activated appropriately such a program may provide means to control viral infection and tumor growth in the organ that is most heavily exposed to toxins. If activated inappropriately, it may cause rapid destruction of the organ.

4.2.3 LPS-Induced Endogenous Production of TNF

In the studies described above, the actions of exogenously applied TNF were examined. Similar results were obtained in pathological model situations of endogenous TNF release. The liver harbors the largest pool of macrophages in the body and thus it is a potent TNF-producing organ (Leist et al. 1996b). Kupffer cells within the liver may produce TNF after direct stimulation, e.g., with LPS or after interaction with activated lymphocytes in a more complicated immunological setting (Gantner et al. 1996).

Accordingly, LPS injection into GalN-sensitized mice causes TNF release (Wendel 1990; Jilg et al. 1996) and the typical sequence of selective hepatocyte apoptosis followed by widespread necrosis and enzyme release from the liver (Leist et al. 1995a). Passive immunization of mice against TNF prevented apoptosis (Leist et al. 1995b), as well as transaminase release as a late sign of liver damage (Leist et al. 1995b; Tiegs et al. 1990). When doses of LPS 1000-fold higher than those given to sensitized animals were injected into non-sensitized mice the pathological findings were different (Bohlinger et al. 1996). Although a strictly TNF-dependent liver damage associated with DNA fragmentation was still observed, the incidence of hepatocyte apoptosis was very low. Liver cell types other than

hepatocytes were affected and organ damage was widespread and far from being selective for the liver. Under such an excessive intensity of insult the selective triggering of an apoptotic program may be overridden by many other processes (Gutierrez-Ramos and Bluethmann 1997), such as complement activation, neutrophil immigration and activation (Sauer et al. 1996), ROS generation, and many more. In addition, a possibly initiated apoptotic process may not be fully executed until the stage of chromatin condensation due to energy failure (Leist and Nicotera 1997).

4.2.4
Induction of Endogenous TNF by Stimuli Other Than LPS

LPS is an excellent model stimulus for the induction of circulating TNF in animals and also in man (Zabel et al. 1989). The levels of serum TNF reached in humans exposed to LPS are sufficient to induce liver toxicity (Otto et al. 1996). Besides LPS, there is a large variety of other stimuli that induce TNF and cause fulminant apoptotic liver failure in GalN-treated mice. For example, hepatic apoptosis is also observed in GalN-pretreated mice when T cells are polyclonally activated by stimulation of the T cell receptor with an anti-CD3 antibody or the superantigen *Staphylococcus aureus* enterotoxin B (Gantner et al. 1995a). Both stimuli strongly increase the serum TNF concentrations of mice, and passive immunization against TNF prevented this rise, as well as apoptosis and other signs of liver damage. Similar forms of liver damage are also induced by malarial antigens (Bate et al. 1989; Jakobsen et al. 1997; Taverne et al. 1990) or constituents of Gram-positive bacteria (Miethke et al. 1992, 1993; Sparwasser et al. 1997). Thus, it seems that whenever circulating TNF is induced in GalN-sensitized mice, liver apoptosis will be observed (Leist et al. 1995a).

Some animal models exist in which liver damage is induced by endogenous TNF in the absence of transcriptional inhibitors. In one of them, liver damage associated with hepatocyte apoptosis is induced by the polyclonal T cell stimulator concanavalin A (ConA) (Gantner et al. 1995b). Again the rise of serum TNF, of apoptosis, and other signs of damage were not present in mice immunized against TNF. However, mechanisms of liver damage seem to be different from those observed in GalN/TNF models, including those where primarily T cells are activated. For instance, TNF-α -/- mice are normally sensitive to ConA (Tagawa et al. 1997), whereas TNF-RI -/- mice are protected (Leist et al. 1995a, 1996a). Thus TNF-β may play an important role in this model, at least when it has to compensate for

lacking TNF-α. In addition, it has been found that inhibition of the processing of the 26-kDa membrane-bound TNF-α to its soluble form protected GalN-sensitized mice from LPS toxicity, but enhanced the liver damage in ConA-treated mice (Solorzano et al. 1997). Thus ConA hepatitis possibly involves signals of the membrane-bound form of TNF (Küsters et al. 1997) that preferentially activates TNF-RII (Grell et al. 1995). A further feature of ConA-induced liver damage is the dependence on IFN-γ (Tagawa et al. 1997; Küsters et al. 1996; Watanabe et al. 1996). IFN-γ may exert direct toxicity on hepatocytes (Morita et al. 1995). However, the more likely role of this cytokine is upregulation of CD95 or perforin-dependent pathways, which may both play some role in ConA-dependent hepatic apoptosis (Watanabe et al. 1996; Tagawa et al. 1997).

Another situation where TNF-dependent liver apoptosis is observed is in LPS-challenged mice pretreated with *P. acnes* (previously called *Corynebacterium parvum*) (Tsuji et al. 1997). The pretreatment strongly increases production of TNF (Moldawer et al. 1987) and of IFN-γ (Katschinski et al. 1992). In this complex model, hepatocyte apoptosis may be dependent on TNF-R and on CD95 since toxicity is considerably reduced in CD95-deficient mice or when the activation of CD95 is inhibited (Tsuji et al. 1997; Kondo et al. 1997).

4.3
CD95 (fas/APO-1)

CD95 (Nagata and Golstein 1995; Nagata 1997; Stanger 1996) is the nomenclature name for a cell surface receptor structurally homologous to TNF-RI that was initially identified under the names APO-1 (Oehm et al. 1992) and fas (Yonehara et al. 1989). It shares with TNF-RI a short intracellular domain called the "death domain" (Tartaglia et al. 1993; Itoh and Nagata 1993). Upon ligand binding and trimerization of the receptor a death-inducing signaling complex (DISC) is formed by association of several molecules to the death domain (Peter et al. 1996). Following DISC formation a protease cascade involving caspases is triggered (Boldin et al. 1996; Muzio et al. 1996). The CD95 system seems to be less pleiotropic than the TNF/TNF-R system and cell death mediated by CD95 is generally apoptotic.

4.3.1
Studies in Hepatocyte Cultures

It was shown that injection of an agonistic monoclonal antibody against CD95 (Jo-2) into mice was lethal and associated with fulminant hemorrhagic hepatic failure (Ogasawara et al. 1993). Histological examination of these livers showed apoptotic hepatocytes. In order to find out whether these effects of Jo-2 were mediated directly or via other cell types and/or mediators, the action of this antibody was examined directly on primary murine hepatocytes (Leist et al. 1996a). Analogously to the TNF model a typical sequence of apoptotic events was observed with chromatin and DNA changes preceding the loss of membrane integrity and mitochondrial function. Similar results were obtained in primary human hepatocytes (Galle et al. 1995). Notably, murine hepatocyte apoptosis induced by CD95 stimulation did not require any sensitization of the cells. CD95-induced apoptosis in HepG2 human hepatoma cells, however, required sensitization by ActD or bleomycin (Galle et al. 1995; Künstle et al. 1997). These studies suggest that hepatocytes express a second receptor that can directly trigger programmed cell death.

4.3.2
In Vivo Studies in Mice

RNAse protection assays showed that CD95 is highly expressed in murine livers starting at embryonic stages, whereas RNA for the CD95L was not detectable in untreated mice (French et al. 1996). There are situations when CD95L can be upregulated in the liver, e.g., after transformation to hepatocellular carcinoma (Strand et al. 1996). Upregulation may also occur during infection/inflammation in viral or alcoholic liver disease (Galle et al. 1995), or possibly near the central vein, a region that is thought to be specialized for elimination of aged hepatocytes and where the apoptotic index is increased compared to other liver regions (Benedetti et al. 1988). Correspondingly, mice with a CD95 null mutation show liver hyperplasia due to a lack of this death pathway (Adachi et al. 1995).

CD95 expressed in the liver is functional as an apoptosis-triggering-receptor, since the liver is the major target organ affected by systemic injection of Jo-2 (Ogasawara et al. 1993). It was shown that apoptotic liver damage also occurred after injection of the soluble CD95 ligand (CD95L) itself (Rensing-Ehl et al. 1995; Tanaka et al. 1997). The time course of

various cell death parameters, and the question of whether the liver could be sensitized to CD95 triggered apoptosis by GalN was also examined. Analogous to the in vitro situation, only a minor sensitizing effect of GalN towards CD95-mediated liver damage was found, but the sequence of events (chromatin changes, oligonucleosomal DNA fragmentation, and subsequent enzyme release) was similar to that seen with GalN *plus* TNF (Leist et al. 1996a). Strong evidence for endogenously formed CD95L in hepatitis comes from studies with models where IFN-γ is strongly induced. For example, liver damage due to *P. acnes* plus LPS seems to be mediated in part by CD95 (Kondo et al. 1997; Tagawa et al. 1997) and *P. acnes* infection strongly sensitizes the liver towards soluble CD95L (Tanaka et al. 1997). In addition it has been demonstrated that cytotoxic T cells specific for hepatitis B virus antigen killed infected hepatocytes in a CD95-dependent manner (Kondo et al. 1997).

4.4 Delimitation of the CD95/CD95L System and the TNF-R/TNF System

Due to the structural homology of CD95 with TNF-RI and CD95L with TNF and because of the functional redundancy there were early suggestions that these systems would not act independently. This question was examined by using mice or hepatocytes from mice (Fig. 2) that lacked either functional CD95 (lpr) or TNF-RI (tnf-1°) or TNF-RII (tnf-R2°) (Leist et al. 1996a).

- Hepatocytes from lpr mice reacted toward TNF just as wild-type (wt) mice, but were insensitive towards CD95 stimulation. Similar results were obtained in vivo: lpr mice reacted normally towards exogenously injected TNF or after endogenous TNF-induction due to ConA injection, whereas they were insensitive towards CD95 stimulation.
- In complementary experiments hepatocytes from tnf-r1° mice were used (Leist et al. 1995b, 1996a). They were completely insensitive towards TNF, but normally susceptible to CD95 stimulation. Similar results were obtained in vivo (Leist et al. 1995b, 1996a; Tsuji et al. 1997).
- In a third line of experiments, the role of TNF-RII was tested. Hepatocytes from tnf-r2° mice were normally sensitive towards CD95 stimulation and exposure to TNF in vivo or in vitro. In other words, TNF-RII does not seem to play a major role in the induction of apoptosis by TNF. The transmission of the TNF death signal in hepatocytes by TNF-RI

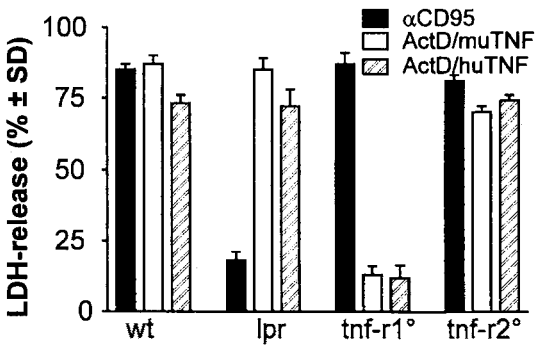

Fig. 2. Tumor necrosis factor (TNF)- or αCD95-induced cytotoxicity in hepatocyte cultures. Hepatocytes from genotypically different mice [*wt* (wild-type), *lpr* (mice lacking functional CD95), *tnf-r1°* (TNF-RI-deficient), *tnf-r2°* (TNF-RII-deficient)] were incubated with 333 nM actinomycin D (*ActD*) plus 100 ng/ml murine TNF-α (*ActD/muTNF*) or human TNF-α (*ActD/huTNF*) or 100 ng/ml agonistic anti-CD95 monoclonal antibody (*αCD95*). Cell death was determined 16 h after the start of the incubation by measurement of lactate dehydrogenase (*LDH*) release. LDH release of unstimulated cultures was 18%±2%

alone is further suggested by the fact that human TNF (which binds to the murine TNF-RI, but not to the murine TNF-RII) induces murine hepatocyte apoptosis in vivo and in vitro (Leist et al. 1995b) (Fig. 2).

These studies strongly suggest that two fully independent receptor-ligand systems control hepatocyte apoptosis (Fig. 3). Additional evidence is provided by the observations that TNF apoptosis is modulated by GalN or variable ambient oxygen tensions, whereas that induced by CD95 stimulation is not (Leist et al. 1996a). Furthermore, the inhibition profile upon immunological, pharmacological, or genetic intervention differs between the two stimuli.

5
Mechanisms and Modulation of Hepatic Apoptosis

Modulation of hepatic apoptosis is desirable in disease control. Conversely, important mechanistic information can be derived from genetic, pharmacological, and immunologic intervention studies in disease models.

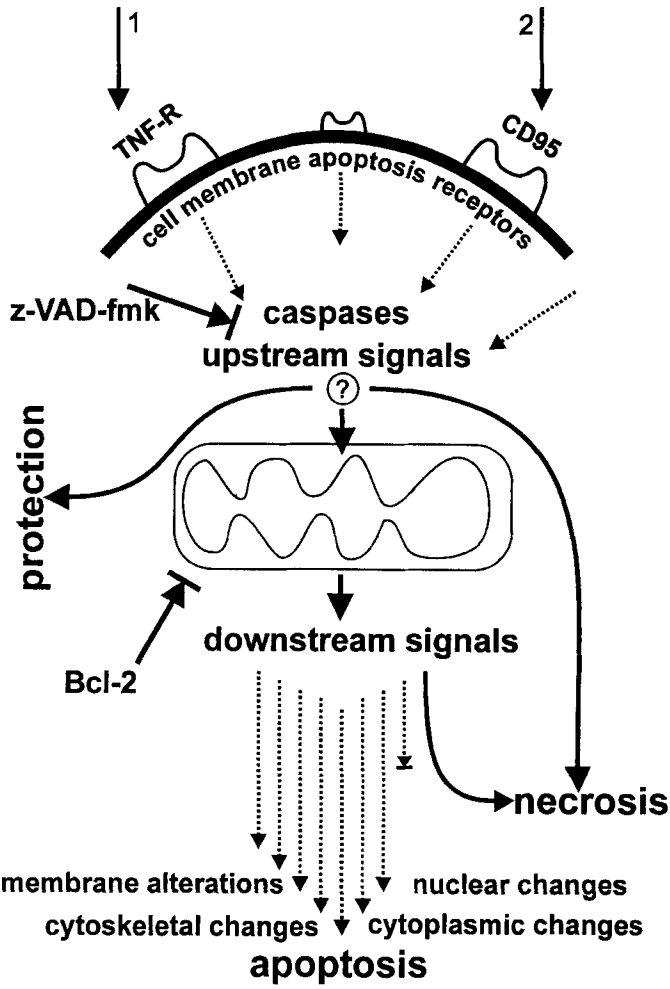

Fig. 3. Possible pathways of cytokine-induced hepatocyte death. Tumor necrosis factor receptor (*TNF-R*) and CD95 stimulated by independent signals (*1, 2*) activate signaling proteases such as caspase-8. This step is experimentally inhibited by caspase inhibitors such as z-VAD-fmk which protect hepatocytes. An irreversible step may include mitochondrial alterations and release of downstream signals such as cytochrome-c or apoptosis-inducing factor that would cause the activation of caspase-3 and/or other proteases. Completion of all downstream steps results in apoptosis and failure to do so would result in necrosis or in cell death of intermediate morphology

5.1
Key Mechanisms of Apoptosis

There is an overwhelming wealth of studies on either hepatocyte necrosis or on non-hepatocyte apoptosis. However, information on specific mechanisms of apoptosis in primary hepatocytes in vitro or in experimental animals in vivo is relatively sparse. Unlike the situation in many leukemic/tumor cell lines that mostly die by apoptosis, triggering of cell death in hepatocytes by a variety of stimuli often results in necrosis (Rosser and Gores 1995). This does not necessarily imply a different "death program" in hepatocytes, since apoptosis and necrosis are neither mechanisms of cell death nor do they allow conclusions on the mechanism having led to cell death. In fact, similar mechanisms seem to operate in hepatocytes as in many other well characterized cell types, although the final outcome may be apoptosis or necrosis.

The most critical event in apoptosis is currently thought to be the release of protein factors such as cytochrome c or apoptosis-inducing factor (AIF) from mitochondria (Krippner et al. 1996; Golstein 1997; Zamzami et al. 1996; Kluck et al. 1997; Susin et al. 1996, 1997; Yang et al. 1997; X. Liu et al. 1996; Kroemer et al. 1997). The released factors seem to play a role in the activation of cell death execution mechanisms (Liu et al. 1997; Chinnaiyan et al. 1997a; Susin et al. 1997). Possibly, they form part of a so-called apoptosome complex that joins caspase precursors and bcl-2 related molecules via a linking protein that is called ced-4 in *Caenorhabditis elegans* and APAF-1 in eukaryotic cells (Chinnaiyan et al. 1997b; Hengartner 1997; Zou et al. 1997). APAF-1 or ced-4 may be allosterically regulated by ATP (Chinnaiyan et al. 1997a). The key process associated with the release of AIF is mitochondrial permeability transition (MPT), i.e., a breakdown of the diffusion barrier normally formed by the inner mitochondrial membrane and a resulting exchange of solutes up to a size of 3–10 kDa (Kroemer 1997a,b). MPT was in fact observed in livers from GalN-/LPS-challenged mice (Zamzami et al. 1996); mitochondria from such livers were able to induce nuclear apoptotic changes (Zamzami et al. 1996), and TNF has been shown to induce MPT in cells (Pastorino et al. 1996). MPT has also been observed in hepatocyte necrosis (Pastorino et al. 1993; Aguilar et al. 1996; Rosser and Gores 1995; Nieminen et al. 1995; Arora et al. 1997) and therefore seems to be independent of a specific mode of cell death. Another event, which has been thought to be a universal feature in apoptosis, is caspase activation. In fact, caspases are activated

for example in CD95-triggered livers or primary hepatocytes (Rodriguez et al. 1996b; Leist et al. 1997c). However, both apoptosis and necrosis induced by CD95 in murine livers are inhibited by caspase inhibitors (Künstle et al. 1997). Moreover, there are also situations of hepatic apoptosis that do not involve caspase activation (Adjei et al. 1996). Possibly other proteases can substitute for caspases in the liver;. for example, MPT has been shown to be induced in liver by calpains (Aguilar et al. 1996). Although protease activation seems to be a general theme of hepatocyte death, this may apply to both apoptosis and necrosis (Bronk and Gores 1993; Kwo et al. 1995; Nicotera et al. 1986a,b).

The complex situation can be explained by the following concept (see Fig. 3): (a) Various stimuli may induce the activation of proteases or other disturbances of cellular homeostasis. In the case of TNF or CD95 caspases 8 and 10, for example, would be activated. (b) Depending on the metabolic situation, hepatocytes would compensate the noxious insult, die rapidly by necrosis, or proceed to the next step of the death program. (c) MPT would mark the irreversible step in the sequence leading to cell death. (d) The metabolic situation of the cell and on additional effects of the death-inducing stimulus would then decide on the mode/shape of cell death. In the case of TNF/CD95 caspase-3-related proteases would be activated and usually apoptosis would ensue. In other cases only part of the set of downstream events triggered by MPT would occur. This would prevent the development of apoptotic morphology in the dying cell and thus lead to necrosis. Prevention of caspase-3 activation by ATP depletion in CD95-treated Jurkat cells has been demonstrated to result in necrotic cell demise (Leist et al. 1997b).

5.2
Pharmacological Prevention of Apoptosis

Since the signal transduction of CD95 and TNF-R1 has been identified only over the last few years, earlier intervention strategies could not follow a rational approach at the post-receptor level. Partial prevention of TNF-induced apoptosis in hepatocyte cultures and a reduction of liver damage in vivo was obtained by cyclic adenosine monophosphate (cAMP)-raising substances (Jilg et al. 1996; Gantner et al. 1997; Fladmark et al. 1997). A selective and potent reduction of TNF-induced apoptosis, but not of that induced by CD95, was obtained with fructose treatment (unpublished data), possibly due to the ATP-depleting action (Zeid et al. 1997; Valeri et al.

1997) of this sugar. Liver damage due to CD95 activation was prevented by linomide, a substance possibly preventing the intracellular signaling of CD95 via the sphingomyelinase pathway (Redondo et al. 1996).

The most rational pharmacological approach in the past was based on the assumption that components of the death program may require de novo protein synthesis. ActD-sensitized murine hepatocyte cultures were indeed protected by various inhibitors of protein synthesis from TNF-induced apoptosis. Concentration-dependent protection was observed with cycloheximide, puromycin, ricin, and tunicamycin (Leist et al. 1994; Leist and Wendel 1995), which may suggest a requirement for de novo protein synthesis. However, cycloheximide may also induce apoptosis in whole livers (Ledda-Columbano et al. 1992; Furukawa et al. 1997) and alternative mechanisms of action have been suggested to explain cytoprotective effects of cycloheximide. These include upregulation of the anti-apoptotic protein Bcl-2 and an improvement of endogenous antioxidant defense (Ratan et al. 1994). Protein synthesis inhibitors alone had hardly any sensitizing effect towards TNF in murine hepatocytes. Notably, when human hepatoma cells were used, they could be sensitized towards TNF by cycloheximide or ActD. Protein synthesis inhibitors did not protect from apoptosis elicited by CD95 stimulation, but rather had a sensitizing effect (Ni et al. 1994).

In 1995, the intracellular pathway leading from TNF-R stimulation to apoptosis was shown in various cell types to involve activation and proteolytic action of caspases (Los et al. 1995; Tewari and Dixit 1995; Enari et al. 1995). This family of proteases is structurally related to the *ced-3* cell death gene products of *C. elegans* (Kumar and Lavin 1996; Zhivotovsky et al. 1997; Henkart 1996; Patel et al. 1996). Inhibition of these proteases was tested as a potentially useful pharmacological approach to stop disease processes involving hepatocyte apoptosis (Künstle et al. 1997; Rouquet et al. 1996b; Rodriguez et al. 1996b). The results showed unambiguously that both TNF- and CD95-mediated hepatic apoptosis in mice was completely prevented when caspase activities were blocked. In addition, liver damage could even be stopped after its initiation by curative application of caspase inhibitors. Measurement of caspase activities in hepatocytes suggests a caspase-3-related enzyme as key mediator (Leist et al. 1997c). In agreement with this, measurement of caspase activities in vivo showed that this enzyme was particularly activated in the liver by CD95 stimulation (Rodriguez et al. 1996b). Finally, caspase inhibitors were shown not only to delay hepatotoxicity or to shift the toxicity to another organ, but rather, a

single dose of inhibitor was sufficient to protect from an otherwise lethal challenge with TNF or αCD95 and to ensure long-term survival (Fig. 4). Although the inhibitors used are still at an experimental stage, they suggest a novel pharmacological approach to apoptosis-related liver disease.

5.3 Immunological and Genetic Modulation of Apoptosis

TNF-induced murine hepatic apoptosis can be inhibited in vivo by immune modulators. For example, it has been shown that injection of the NO donor sodium nitroprusside or interleukin (IL)-1 completely prevented liver damage (Bohlinger et al. 1995; Leist et al. 1995a). Conversely, inhibition of endogenous NO formation significantly enhanced TNF-dependent liver damage (Bohlinger et al. 1995, 1996), so that NO production seems to represent an endogenous protective mechanism in the liver. In fact, direct protective effects of NO pretreatment against TNF-induced apoptosis have been observed with a liver-specific NO donor (Saavedra et al. 1997). Under this situation inhibition of apoptosis seems to have been due to upregula-

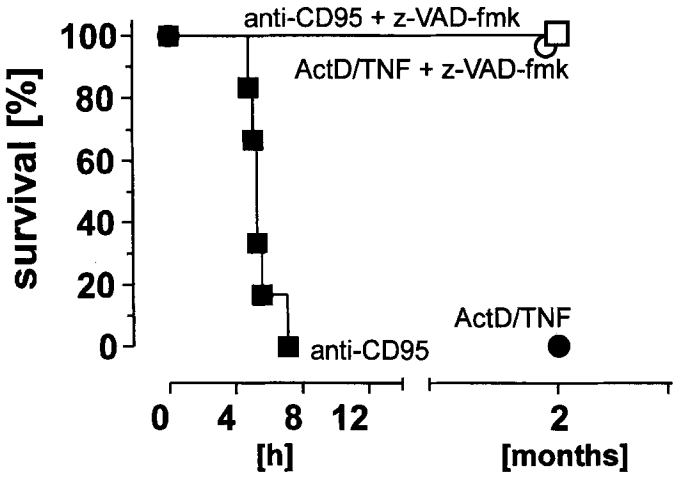

Fig. 4. Prevention by caspase inhibition of lethality due to apoptosis receptor stimulation. Mice were injected with actinomycin D/tumor necrosis factor (*ActD/TNF*) (*circle*) or anti-CD95 antibody (*squares*) with (*open symbols*) or without (*solid symbols*) pretreatment with the caspase inhibitor (10 mg/kg) z-VAD-fmk (intraperitoneally, 15 min before challenge). Survival was recorded over a period of 2 months

tion of heat shock protein hsp70 (Kim et al. 1997). The protective effect of IL-1 in vivo is specific for TNF-induced toxicity since liver damage due to CD95 stimulation was not reduced by this cytokine (Leist et al. 1996a). In addition to direct effects of NO on hepatotoxicity, NO or IL-1 may have indirect in vivo actions, e.g., the synthesis of protective acute phase proteins (Libert et al. 1991, 1994; Van Molle et al. 1997), or the prevention of ischemia-reperfusion (Bohlinger et al. 1996).

Molecules modifying the CD95 apoptosis signal inside the cell have been examined by using transgenic mice. In an elegant approach *bcl-2*, a gene putatively controlling apoptosis at the mitochondrial level and upstream of caspase-3 activation, was overexpressed selectively in murine livers (Lacronique et al. 1996; Rodriguez et al. 1996a). Such transgenic mice were resistant to CD95-induced hepatic apoptosis and, in part, lethality. This approach shows that lethality induced by systemic CD95 stimulation in mice is to a large extent due to stimulation of apoptosis in hepatocytes and the subsequent liver failure.

In another approach a non-transforming mutant of simian virus (SV)-40 T antigen was overexpressed in mice. This molecule does not transform cells, but it is able to inactivate the putatively proapoptotic protein p53 (Rouquet et al. 1996a). Hepatocytes from such mice were protected from CD95-mediated apoptosis, but not from TNF. These findings suggest a variance of the two signal transduction pathways of TNF-RI and CD95, although both have caspase activation in common. The possible involvement of p53 in CD95 killing but not in TNF-triggered apoptosis suggests that hepatic apoptosis may be modulated differentially.

6
Apoptosis in Hepatotoxicology

Hepatotoxins may induce apoptosis (Corcoran et al. 1994; Columbano 1995) in two fundamentally different ways (Fig. 5): (1) In vitro, substances such as valinomycin (Sun et al. 1994), colchicine (Tsukidate et al. 1993), bile salts (Zeid et al. 1997; Botla et al. 1995; Kwo et al. 1995; Patel et al. 1994; Jones et al. 1997), and okadaic acid (Böe et al. 1991) directly induce cellular alterations that finally lead to apoptosis, possibly via the activation of caspases. (2) In vivo, the same direct mechanisms may operate. Alternatively, toxins may lead to the stimulation of hepatocytes with proapoptotic cytokines and sensitize them in parallel to the action of such mediators,

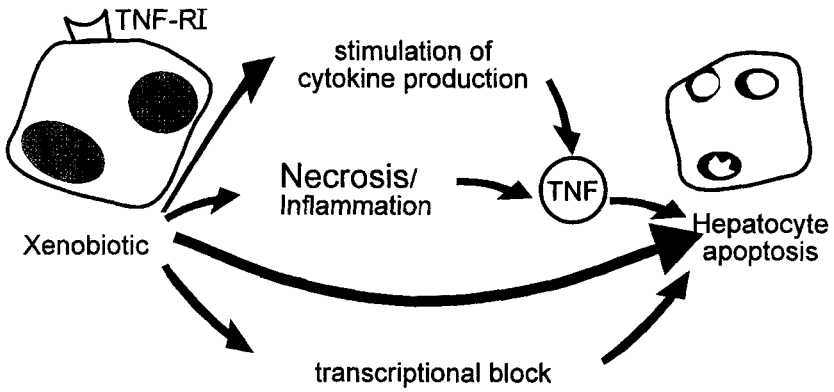

Fig. 5. Putative actions of toxins eventually causing apoptosis of hepatocytes. *TNF*, tumor necrosis factor; *TNF-R1*, tumor necrosis factor receptor-1

e.g., by weakening defense mechanisms or by inhibiting transcription. Particularly the second, indirect mode of action has found little attention and will be briefly reviewed below.

6.1 Mediators Derived From Non-parenchymal Cells and Cytokines in Hepatotoxicology

It seems that in vivo a large fraction of the most typical hepatotoxins alter the intercellular signaling (e.g., induce cytokine release or response) or act in synergy with intercellular signals (Table 2). This would imply that the explanation of their toxicity involves detailed intercellular molecular events in addition to their directly damaging effect on membranes or on vital structures within the ultimate target cell. The evidence for the involvement of immune mediators, non-parenchymal liver cells, and macrophage-derived products in toxicity has been compiled by Laskin and Pendino (1995). There are various studies showing that modulation of macrophage function or neutralization of immune mediators alters xenobiotic- induced toxicity (Table 2). One of the most prominent mediators is the proapoptotic cytokine TNF.

6.2
Toxin-Induced Apoptosis

Evidence is accumulating to show that many xenobiotics cause apoptosis (Corcoran et al. 1994; Columbano 1995) or symptoms of hepatocyte apoptosis in rodents (see Table 2). This suggests that apoptosis in the liver is not restricted to physiological situations alone. The frequent co-occurrence of apoptosis and necrosis in the liver may imply that the default mode of demise for hepatocytes is apoptosis, as for many other cell types. However, many intoxications would damage hepatocytes so severely that the apoptotic program would not be continued to the end and cell death would take the shape of necrosis (Leist and Nicotera 1997).

6.3
TNF as Mediator of Toxin-Induced Apoptosis

If a single toxin releases TNF and simultaneously sensitizes cells towards the apoptotic actions of this cytokine, then TNF-induced hepatocyte apoptosis should contribute significantly to overall toxicity (see Fig. 5). For some toxins such a scenario has been demonstrated. For example, the toxicity of CCl_4, the prototype of a directly acting hepatotoxin, is inhibited by scavenging of TNF with recombinant soluble TNF-receptor constructs (Czaja et al. 1995).

In another study, the role of TNF and hepatocyte apoptosis during the poisoning of mice with α-amanitin or with ActD, respectively, was examined (Leist et al. 1997a). Indeed, the two toxins displayed similar actions on the liver. At low doses they induced hepatocyte apoptosis in vivo and in vitro highly synergistic with TNF. At high doses they induced liver damage alone that was associated with the occurrence of apoptotic hepatocytes and oligonucleosomal DNA fragmentation. This toxicity was inhibited by passive immunization of mice against TNF. Toxicity was also prevented by IL-1 pretreatment, which has been shown to prevent TNF-induced hepatocyte apoptosis (Bohlinger et al. 1996). The necessity of TNF for hepatotoxicity was further confirmed by the resistance of tnf-r1° mice and the unaltered sensitivity of tnf-r2° mice to α-amanitin. Thus, different lines of evidence suggest that hepatotoxicity of ActD or α-amanitin, a prototype "direct-acting" hepatotoxin, involves the actions of TNF and the induction of apoptosis in hepatocytes.

Also, the "direct" hepatotoxic effect of GalN was reexamined. Selective liver failure caused by this substance in rodents was suggested 30 years ago to represent a model for human viral hepatitis (Keppler et al. 1968). In fact, hepatocyte apoptosis (Councilman bodies) was noted to be one of the most conspicuous phenomena of GalN-induced pathology (Reutter et al. 1968, 1970; Keppler et al. 1968; Medline et al. 1970). A series of studies in the 1970s and 1980s showed that the substance exerted a very pronounced toxicity in synergy with endogenous and exogenous immune modulators (Grün and Liehr 1976; Liehr et al. 1978; Mihas et al. 1990; Galanos et al. 1979; Czaja et al. 1994). Finally, it was shown that GalN specifically sensitized mice to the lethality of TNF (Lehmann et al. 1987), which is due to selective liver failure (Tiegs et al. 1989) associated with apoptotic hepatocyte death (Leist et al. 1995a). In analogy to the studies on ActD and α-amanitin toxicity, it was examined whether endogenous TNF would contribute to the putatively direct hepatotoxic effect of pure GalN. In fact, inhibition of liver failure and hepatocyte apoptosis by blunting the effects of endogenously formed TNF demonstrates the role of TNF in GalN hepatotoxicity (Fig. 6).

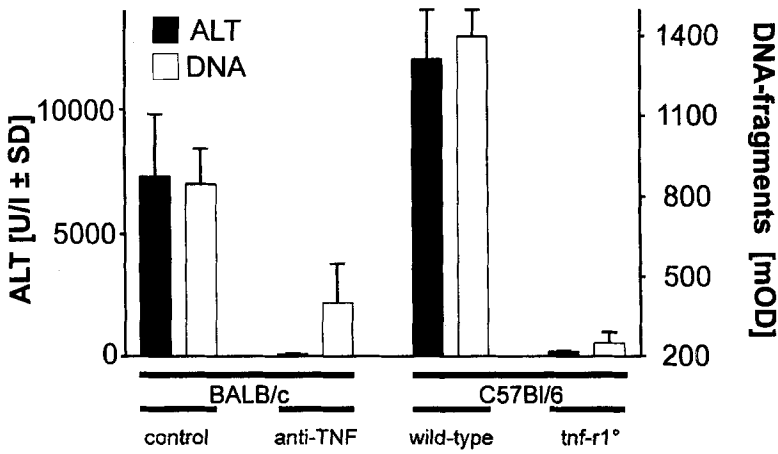

Fig. 6. The role of endogenous tumor necrosis factor (*TNF*) in D-galactosamine (GalN)-induced liver damage. All mice were injected with 2.1 g/kg GalN. Serum transaminases (*ALT*) and hepatic DNA fragmentation were determined after 24 h. Animals pretreated with neutralizing anti-TNF antibodies or mice lacking TNF receptor-1 (*tnf-r1°*) were protected

These findings appear to close a historic circle. Transcriptional inhibition by the xenobiotic GalN sensitizes hepatocytes to apoptosis triggered by endogenous TNF. As suggested initially, this may indeed resemble the situation during viral hepatitis. This may not only apply to the morphological appearance, but also to the mechanisms of hepatocyte death. The simple xenobiotic GalN may model some aspects of viral infection where transcription of the hepatocyte genome is partially blocked by viral protein synthesis and apoptosis is induced in virus-sensitized cells by endogenous TNF (Guilhot et al. 1996; Su and Schneider 1997).

Acknowledgements. We are grateful to Ms. C. Hoffmann for help in the preparation of the manuscript and to Prof. P. Nicotera for stimulating discussion. This work was supported by the Deutsche Forschungsgemeinschaft (grants We 686/17-1), as well as the Graduiertenkolleg "Biochemische Pharmakologie".

References

Adachi M, Suematsu S, Kondo T, Ogasawara J, Tanaka T, Yoshida N, Nagata S (1995) Targeted mutation in the Fas gene causes hyperplasia in peripheral lymphoid organs and liver. Nature Genet 11:294–300

Adachi Y, Bradford BU, Gao W, Bojes HK, Thurman RG (1994) Inactivation of Kupffer cells prevents early alcohol-induced liver injury. Hepatology 20:453–460

Adam-Klages S, Adam D, Wiegmann K, Struve S, Kolanus W, Schneider-Metgener J, Krönke M (1996) FAN, a novel WD-repeat protein, couples the p55 TNF-receptor to neutral sphingomyelinase. Cell 86:937–947

Adamson GM, Billings RE (1992) Tumor necrosis factor induced oxidative stress in isolated mouse hepatocytes. Arch Biochem Biophys 294:223–229

Adamson GM, Billings RE (1993) Cytokine toxicity and induction of NO synthase activity in cultured mouse hepatocytes. Toxicol Appl Pharmacol 119:100–107

Adjei PN, Kaufmann SH, Leung W-Y, Mao F, Gores GJ (1996) Selective induction of apoptosis in Hep 3B cells by toposiomerase I inhibitors: evidence for a protease-dependent pathway that does not activate cysteine protease P32. J Clin Invest 98:2588–2596

Aggarwal BB, Vilcek J (eds) (1992) Tumor necrosis factors. Structure, function and mechanisms of action. Dekker, New York

Aguilar HI, Botla R, Arora AS, Bronk SF, Gores GJ (1996) Induction of the mitochondrial permeability transition by protease activity in rats: a mechanism of hepatocyte necrosis. Gastroenterology 110:558–566

Ankarcrona M, Dypbukt JM, Bonfoco E, Zhivotovsky B, Orrenius S, Lipton SA, Nicotera P (1995) Glutamate-induced neuronal death: a succession of necrosis or apoptosis depending on mitochondrial function. Neuron 15:961–973

Arora AS, Jones BJ, Patel TC, Bronk SF, Gores GJ (1997) Ceramide induces hepatocyte cell death through disruption of mitochondrial function in the rat. Hepatology 25:958–963

Barriault C, Audet M, Yousef IM, Tuchweber B (1995) Effect of agents which modify reticuloendothelial function on acute phalloidin-induced lethality and hepatotoxicity in mice. Toxicol Appl Pharmacol 131:206–215

Bate CA, Taverne J, Playfair JH (1989) Soluble malarial antigens are toxic and induce the production of tumor necrosis factor in vivo. Immunol 66:600–605

Bathal PS, Powell LW, Mackay IR (1982) Apoptosis in autoimmune chronic active Hepatitis (CAH). Hepatol 2:154–155

Battersby C, Egerton WS, Balderson G, Kerr JF, Burnett W (1974) Another look at rejection in pig liver homografts. Surgery 76:617–623

Bedossa P, Peltier E, Terris B, Franco D, Poynard T (1995) Transforming growth factor-beta 1 (TGF-beta1) and TGF-beta1 receptors in normal, cirrhotic, and neoplastic human livers. Hepatology 21:760–766

Benedetti A, Jezequel AM, Orlandi F (1988) A quantitative evaluation of apoptotic bodies in rat liver. Liver 8:172–177

Beutler B (ed) (1992) Tumor necrosis factors. The molecules and their emerging role in medicine. Raven, New York

Biava C, Mukhlova-Montiel M (1965) Electron microscopic observation on councilman-like acidophilic bodies and other forms of acidophilic changes in human liver cells. Am J Pathol 46:775–802

Blazka ME, Wilmer JL, Holladay SD, Wilson RE, Luster MI (1995) Role of proinflammatory cytokines in acetaminophen hepatotoxicity. Toxicol Appl Pharmacol 133:43–52

Blazka ME, Elwell MR, Holladay SD, Wilson RE, Luster MI (1996) Histopathology of acetaminophen-induced liver changes: role of interleukin 1 alpha and tumor necrosis factor alpha. Toxicol Pathol 24:181–189

Böe R, T, Gjertsen, Vintermyr OK, Houge G, Lanotte M, Döskeland SO (1991) The protein phosphatase inhibitor okadaic acid induces morphological changes typical of apoptosis in mammalian cells. Exp Cell Res 195:237–246

Bohlinger I, Leist M, Barsig J, Uhlig S, Tiegs G, Wendel A (1995) Interleukin-1 and nitric oxide protect against tumor necrosis-factor alpha-induced liver injury through distinct pathways. Hepatology 22:1829–1837

Bohlinger I, Leist M, Gantner F, Angermüller S, Tiegs G, Wendel A (1996) DNA-fragmentation in mouse organs during endotoxic shock. Am J Pathol 149:1381–1393

Boldin MP, Goncharov TM, Goltsev YV, Wallach D (1996) Involvement of MACH, a novel MORT1/FADD-interacting protease, in Fas/APO-1- and TNF receptor-induced cell death. Cell 85:803–815

Bonfoco E, Krainc D, Ankarcrona M, Nicotera P, Lipton SA (1995) Apoptosis and necrosis: two distinct events induced respectively by mild and intense insults with NMDA or nitric oxide/superoxide in cortical cell cultures. Proc Natl Acad Sci USA 92:72162–72166

Botla R, Spivey JR, Aguilar H, Bronk SF, Gores GJ (1995) Ursodeoxycholate (UDCA) inhibits the mitochondrial membrane permeability transition induced by glychenodeoxycholate: a mechansism of UDCA cytoprotection. J Pharmacol Exp Ther 272:930–938

Bour ES, Ward LK, Cornman GA, Isom HC (1996) Tumor necrosis factor-alpha-induced apoptosis in hepatocytes in long-term culture. Am J Pathol 148:485–495

Bronk SF, Gores GJ (1993) pH-dependent nonlysosomal proteolysis contributes to lethal anoxic injury of rat hepatocytes. Am J Physiol 264:G744–G751

Browning JL, Ngam-ek A, Lawton P, DeMarinis J, Tizard R, Chow EP (1993) Lymphotoxin beta, a novel member of the TNF family that forms a heteromeric complex with lymphotoxin on the cell surface. Cell 72:847–856

Bursch W, Oberhammer F, Schulte-Hermann R (1992) Cell death by apoptosis and its protective role against disease. Trends Pharmacol Sci 13:245–251

Cascales M, Alvarez A, Gasco P, Fernandez Simon L, Sanz N, Bosca L (1994) Cocaine-induced liver injury in mice elicits specific changes in DNA ploidy and induces programmed death of hepatocytes. Hepatology 20:992–1001

Child P, Ruiz LA (1968) Acidophilic bodies. Their chemical and physical nature in patients with bolivian hemorrhagic fever. Arch Pathol 85:45–50

Chinnaiyan AM, Chaudhary D, O'Rourke K, Koonin EV, Dixit VM (1997a) Role of CED-4 in the activation of CED-3. Nature 388:728–729

Chinnaiyan AM, O'Rourke KO, Lane BR, Dixit VM (1997b) Interaction of ced-4 with ced-3 and ced-9: a molecular framework for cell death. Nature 275:1122–1126

Columbano A (1995) Cell death: current difficulties in discriminating apoptosis from necrosis in the context of pathological processes in vivo. J Cell Biochem 58:181–190

Columbano A, Ledda-Columbano GM, Coni PP, Faa G, Liguori C, Santa Cruz G, Pani P (1985) Occurrence of cell death (apoptosis) during the involution of liver hyperplasia. Lab Invest 52:670–675

Corcoran GB, Ray SD (1992) Contemporary issues in toxicology. The role of the nucleus and other compartments in toxic cell death produced by alkylating hepatotoxicants. Toxicol Appl Pharmacol 113:167–183

Corcoran GB, Fix L, Jones DP, Moslen MT, Nicotera P, Oberhammer FA, Buttyan R (1994) Contemporary issues in toxicology. Apoptosis: molecular control point in toxicity. Toxicol Appl Pharmacol 128:169–181

Councilman WT (1890) Report on the etiology and prevention of yellow fever. In: Sternberg GM (ed) United states marine hospital service, Treasury Department, document no 1328. Government Printing Office, Washington DC, pp 151–159 (Public health bulletin 2)

Crowe PD, VanArsdale TL, Walters BN, Ware CF, Hession C, Ehrenfels B, Browning JL, Din WS, Goodwin RG, Smith CA (1994) A lymphotoxin-beta-specific receptor. Science 264:707–710

Czaja MJ, Xu J, Ju Y, Alt E, Schmiedeberg P (1994) Lipopolysaccharide-neutralizing antibody reduces hepatocyte injury from acute hepatotoxin administration. Hepatology 19:1282–1289

Czaja MJ, Xu J, Alt E (1995) Prevention of carbon tetrachloride-induced rat liver injury by soluble tumor necrosis factor receptor. Gastroenterology 108:1849–1854

Darnay BG, Aggarwal BB (1997) Early events in TNF signaling: a story of associations and dissociations. J Leukoc Biol 61:559–566

Decker K, Keppler D (1974) Galactosamine hepatitis: key role of the nucleotide deficiency period in the pathogenesis of cell injury and cell death. Rev Physiol Biochem Pharmacol 71:77–100

Ding-feng Z, Hong R, Xiao-ping J, Ya-su Z (1993) Serum tumor necrosis factor (TNF) in the pathogenesis of clinical hepatic failure of HCV and/or HBV infection. Chin Med J 106:335–338

Dypbukt JM, Ankarcrona M, Burkitt M, Sjöholm A, Ström K, Orrenius S, Nicotera P (1994) Different prooxidant levels stimulate growth, trigger apoptosis, or produce necrosis of insulin-secreting RINm5F cells. J Biol Chem 269:30533–30560

Enari M, Hug H, Nagata S (1995) Involvement of an ICE-like protease in fas-mediated apoptosis. Nature 375:78–81

Fabregat I, Sanchez A, Alvarez AM, Nakamura T, Benito M (1996) Epidermal growth factor, but not hepatocyte growth factor, suppresses the apoptosis induced by transforming growth factor-beta in fetal hepatocytes in primary culture. FEBS Lett 384:14–18

Fladmark KE, Gjertsen BT, Doskeland SO, Vintermyr OK (1997) Fas/Apo-1-induced apoptosis of primary hepatocytes is inhibited by cAMP. Biochem Biophys Res Commun 232:20–25

Flemming W (1885) Über die Bildung von Richtungsfiguren in Säugethiereiern beim Untergang Graaf'scher Follikel. Arch Anat Physiol (Anat Abt) 221–244 + Taf X/XI

French LE, Hahne M, Viard I, Radlgruber G, Zanone R, Becker K, Müller C, Tschopp J (1996) Fas and Fas ligand in embryos and adult mice: ligand expression in several immune-privileged tissues and coexpression in adult tissues characterized by apoptotic cell turnover. J Cell Biol 133:335–343

Fukuda K, Kojiro M, Chiu J-F (1993) Demonstration of extensive chromatin cleavage in transplanted morris hepatoma 7777 tissue: apotosis or necrosis? Am J Pathol 142:935–946

Furukawa K, Estus S, Fu W, Mark RJ, Mattson MP (1997) Neuroprotective action of cycloheximide involves induction of bcl-2 and antioxidant pathways. J Cell Biol 136:1137–1149

Galanos C, Freudenberg MA, Reutter W (1979) Galactosamine-induced sensitization to the lethal effects of endotoxin. Proc Natl Acad Sci USA 76:5939–5943

Galle PR, Hofmann WJ, Walczak H, Schaller H, Otto G, Stremmel W, Krammer PH, Runkel L (1995) Involvement of the CD95 (APO-1/Fas) receptor and ligand in liver damage. J Exp Med 182:1223–1230

Gantner F, Leist M, Jilg S, German PG, Freudenberg MA, Tiegs G (1995a) Tumor necrosis factor-induced hepatic DNA fragmentation as an early marker of T cell-dependent liver injury in mice. Gastroenterology 109:166–176

Gantner F, Leist M, Lohse AW, Germann PG, Tiegs G (1995b) Concanavalin A-induced T Cell-mediated hepatic injury in mice: the role of tumor necrosis factor. Hepatology 21:190–198

Gantner F, Leist M, Küsters S, Vogt K, Volk D, Tiegs G (1996) T cell stimulus-induced crosstalk between lymphocytes and liver macrophages results in augmented cytokine release. Exp Cell Res 229:137–146

Gantner F, Küsters S, Wendel A, Hatzelmann A, Schudt C, Tiegs G (1997) Protection from T cell-mediated murine liver failure by phosphodiesterase inhibitors. J Pharmacol Exp Ther 280:53–60

Gilles PN, Guerrette DL, Ulevitch RJ, Schreiber RD, Chisari FV (1992) HBsAg retention sensitizes the hepatocyte to injury by physiological concentrations of interferon-gamma. Hepatology 16:655–663

Glücksmann A (1951) Cell death in normal vertebrate ontogeny. Biol Rev Camb Philos Soc 26:59–86

Goldin RD, Hunt NC, Clark J, Wickramasinghe SN (1993) Apoptotic bodies in a murine model of alcoholic liver disease: reversibility of ethanol-induced changes. J Pathol 171:73–76

Golstein P (1997) Controlling cell death. Science 275:1081–1082

González-Amaro R, Garcia-Monzón C, Garcia-Buey L, Moreno-Otero R, Alonso JL, Yagüe E, Pivel JP, López-Cabrera M, Fernandez-Ruiz E, Sánchez-Madrid F (1994) Induction of tumor necrosis factor alpha by human hepatocytes in chronic viral hepatitis. J Exp Med 179:841–848

Gräper L (1914) Eine neue Anschauung über physiologische Zellausschaltung. Arch Zellforsch 12:373–394

Grasl Kraupp B, Bursch W, Ruttkay Nedecky B, Wagner A, Lauer B, Schulte Hermann R (1994) Food restriction eliminates preneoplastic cells through apoptosis and antagonizes carcinogenesis in rat liver. Proc Natl Acad Sci USA 91:9995–9999

Grell M, Douni E, Wajant H, Löhden M, Clauss M, Maxeiner B, Georgopoulos S, Lesslauer W, Kollias G, Pfizenmaier K, Scheurich P (1995) The transmembrane form of tumor necrosis factor is the prime activating ligand of the 80 kDa tumor necrosis factor receptor. Cell 83:793–802

Grün M, Liehr H (1976) Significance of endotoxemia in experimental "galactosamine-hepatitis" in rat. Acta Hepato Gastroenterol 23:64–81

Guilhot S, Miller T, Cornman G, Isom HC (1996) Apoptosis induced by tumor necrosis factor-alpha in rat hepatocyte cell lines expressing Hepatitis B virus. Am J Pathol 148:801–814

Gut J, Schmitt S, Bingen A, Anton M, Kirn A (1984) Probable role of endogenous endotoxins in hepatocytolysis during murine hepatitis caused by frog virus 3. J Infect Dis 149:621–629

Gutierrez-Ramos JC, Bluethmann H (1997) Molecules and mechanisms operating in septic shock: lessons from knockout mice. Immunol Today 18:323–333

Hansen J, Cherwitz DL, Allen JI (1994) The role of tumor necrosis factor alpha in acute endotoxin-induced hepatotoxicity in ethanol-fed rats. Hepatology 20:461–474

Hartley A, Stone JM, Heron C, Cooper JM, Schapira AHV (1994) Complex I Inhibitors induce dose-dependent apoptosis in PC12 cells: relevance to Parkinson's disease. J Neurochem 63:1987–1990

Hengartner MO (1997) Apoptosis. CED-4 is a stranger no more. Nature 388:714–715

Henkart PA (1996) ICE family proteases: mediators of all apoptotic cell death? Immunity 4:195–201

Hewett JA, Jean PA, Kunkel SL, Roth RA (1993) Relationship between tumor necrosis factor-alpha and neutrophils in endotoxin-induced liver injury. Am J Physiol 256:G1011–G1015

Higuchi H, Kurose I, Kato S, Miura S, Ishii H (1996) Ethanol-induced apoptosis and oxidative stress in hepatocytes. Alcohol Clin Exp Res 20:340A-346A

Higuchi M, Aggarwal BB, Yeh ETH (1997) Activation of CPP32-like protease in tumor necrosis factor-induced apoptosis is dependent on mitochondrial function. J Clin Invest 99:1751–1758

Hiramatsu N, Hayashi N, Katayama K, Mochizuki K, Kawanishi Y, Kasahara A, Fusamoto H, Kamada T (1994) Immunohistochemical detection of fas antigen in liver tissue of patients with chronic hepatitis C. Hepatology 19:1354–1359

Honchel R, Marsano L, Cohen D, Shedlofsky S, McClain CJ (1991) Lead enhances lipopolysaccharide and tumor necrosis factor liver injury. J Lab Clin Med 117:202–208

Huang AS, Wagner RR (1965) Inhibition of cellular RNA synthesis by non-replicating vesicular stomatitis virus. Proc Natl Acad Sci USA 54:1579

Hully JR, Chang L, Schwall RH, Widmer HR, Terrell TG, Gillett NA (1994) Induction of apoptosis in the murine liver with recombinant human activin A. Hepatology 20:854–861

Inayat-Hussain SH, Couet C, Cohen GM, Cain K (1997) Processing/activation of CPP32-like proteases is involved in transforming growth factor beta1-induced apoptosis in rat hepatocytes. Hepatology 25:1516–1526

Irmler M, Thome M, Hahne M, Schneider P, Hofmann K, Steiner V, Bodmer J-L, Schröter M, Burns K, Mattmann C, Rimoldi D, French LE, Tschopp J (1997) Inhibition of death receptor signals by cellular FLIP. Nature 388:190–195

Ishiyama H, Ogino K, Hobara T (1995) Role of Kupffer cells in rat liver injury induced by diethyldithiocarbamate. Eur J Pharmacol 292:135–141

Itoh N, Nagata S (1993) A novel protein domain required for apoptosis. Mutational analysis of human fas antigen. J Biol Chem 268:10932–10937

Jakobsen PH, Bate CA, Taverne J, Playfair JH (1997) Malaria: toxins, cytokines and disease. Parasite Immunol 17:223–231

Jensen JC, Pogrebniak HW, Pass HI, Buresh C, Merino MJ, Kauffmann D, Venzon D, Langstein HN, Norton JA (1992) Role of tumor necrosis factor in oxygen toxicity. J Appl Physiol 5:1902–1907

Jilg S, Barsig J, Leist M, Küsters S, Volk H-D, Wendel A (1996) Enhanced release of interleukin-10 and soluble tumor necrosis factor receptors as novel principles of methylxanthine action in murine models of endotoxic shock. J Pharmacol Exp Ther 278:421–431

Jones AL, Selby P (1989) Tumor necrosis factor: clinical relevance. Cancer Surv 8:817–836

Jones BA, Rao YP, Stravitz RT, Gores GJ (1997) Bile salt-induced apoptosis of hepatocytes involves activation of protein kinase C. Am J Physiol 272:G1109–G1115

Karvountzis GG, Redeker AG, Peters RL (1974) Long-term follow-up studies of patients surviving fulminant viral hepatitis. Gastroenterology 67:870–877

Katschinski T, Galanos C, Coumbos A, Freudenberg M (1992) Gamma interferon mediates proponibacterium acnes-induced hypersensitivity to lipopolysaccharide in mice. Infect Immun 60:1994–2001

Kehrer JP, Jones DP, Lemasters JJ, Farber JL, Jaeschke H (1990) Contemporary issues in toxicology. Mechanisms of hypoxic cell injury. Toxicol Appl Pharmacol 106:165–178

Keppler D, Lesch R, Reutter W, Decker K (1968) Experimental hepatitis induced by D-galactosamine. Exp Mol Pathol 9:279–290

Kerr JFR (1969) An electron-microscopic study of liver cell necrosis due to heliotrine. J Pathol 97:557–562

Kerr JFR (1971) Shrinkage necrosis: a distinct mode of cellular death. J Pathol 105:13–22

Kerr JF, Wyllie AH, Currie AR (1972) Apoptosis: a basic biological phenomenon with wide ranging implications in tissue kinetics. Br J Cancer 26:239–247

Kerr JFR, Searle J, Halliday WJ, Roberts I, Cooksley WGE, Halliday JW, Holder L, Burnett W, Powell LW (1979) The nature of piecemeal necrosis in chronic active hepatitis. Lancet 2:827–828

Kim Y-M, de Vera ME, Watkins SC, Billiar TR (1997) Nitric oxide protects cultured rat hepatocytes from tumor necrosis factor-alpha-induced apoptosis by inducing heat shock protein 70 expression. J Biol Chem 272:1402–1411

Klion FM, Schaffner F (1966) The ultrastructure of acidophilic bodies. Am J Pathol 48:755–765

Kluck RM, Bossy-Wetzel E, Green DR, Newmeyer DD (1997) The release of cytochrome c from mitochondria: a primary site for bcl-2 regulation of apoptosis. Science 275:1132–1136

Kondo T, Suda T, Fukuyama H, Adachi M, Nagata S (1997) Essential roles of the fas ligand in the development of hepatitis. Nat Med 3:409–413

Koop DR, Klopfenstein B, Iimuro Y, Thurman RG (1997) Gadolinium chloride blocks alcohol-dependent liver toxicity in rats treated chronically with intragastric alcohol despite the induction of CYP2E1. Mol Pharmacol 51:944–950

Krams SM, Egawa H, Quinn MB, Villanueva JC, Garcia-Kennedy R, Martinez OM (1995) Apoptosis as a mechanism of cell death in liver allograft rejection. Transplantation 59:621–625

Krippner A, Matsuno-Yagi A, Gottlieb RA, Babior BM (1996) Loss of function of cytochrome c in Jurkat cells undergoing Fas-mediated apoptosis. J Biol Chem 271:21629–21636

Kroemer G (1997a) Mitochondrial implication in apoptosis. Towards an endosymbiont hypothesis of apoptosis evolution. Cell Death Differ 4:443–456

Kroemer G (1997b) The proto-oncogene bcl-2 and its role in regulating apoptosis. Nat Med 3:614–620

Kroemer G, Zamzami N, Susin SA (1997) Mitochondrial control of apoptosis. Immunol Today 18:44–51

Kumar S, Lavin MF (1996) The ICE family of cysteine proteases as effectors of cell death. Cell Death Differ 3:255–267

Künstle G, Leist M, Uhlig S, Revesz L, Feifel R, MacKenzie A, Wendel A (1997) ICE-protease inhibitors block murine liver injury and apoptosis caused by CD95 or TNF-alpha. Immunol Lett 55:5–10

Küsters S, Gantner F, Kunstle G,Tiegs G (1996) Interferon gamma plays a critical role in T cell-dependent liver injury in mice initiated by concanavalin A. Gastroenterology 111:462–471

Küsters S, Tiegs G, Alexopoulou L, Pasparakis M, Douni E, Kuenstle G, Bluethmann H, Wendel A, Pfizenmaier K, Kollias G, Grell M (1997) In vivo evidence for a functional role of both tumor necrosis factor (TNF) receptors and transmembrane TNF in experimental hepatitis.. Eur J Immunol 27: (2870–2875)

Kwo P, Patel T, Bronk SF, Gores GJ (1995) Nuclear serine protease activity contributes to bile acid-induced apoptosis in hepatocytes. Am J Physiol 268:G613–G621

Lacronique V, Mignin A, Fabre M, Viollet B, Rouquet N, Molina T, Porteu A, Henrion A, Bouscary D, Varlet P, Joulin V, Kahn A (1996) Bcl-2 protects from lethal hepatic apoptosis induced by an anti-Fas antibody in mice. Nature Med 2:80–86

Lancaster JR, Laster SM, Gooding LR (1989) Inhibition of target cell mitochondrial electron transfer by tumor necrosis factor. FEBS Lett 248:169–174

Laskin DL, Pendino KJ (1995) Macrophages and inflammatory mediators in tissue injury. Annu Rev Pharmacol Toxicol 35:655–677

Laskin DL, Gardner CR, Price VF, Jollow DJ (1995) Modulation of macrophage functioning abrogates the acute hepatotoxicity of acetaminophen. Hepatology 21:1045–1050

Leach BE, Forbes JC (1941) Sulfonamide drugs as protective agents against carbon tetrachloride poisoning. Proc Soc Exp Biol Med 48:361–363

Ledda-Columbano GM, Coni P, Curto M, Giacomini L, Faa G, Olivero S, Piacentini M, Columbano A (1991) Induction of two different modes of cell death, apoptosis and necrosis, in rat liver after a single dose of thioacetamide. Am J Pathol 139:1099–1109

Ledda-Columbano GM, Coni P, Faa G, Manenti G, Columbano A (1992) Rapid induction of apoptosis in rat liver by cycloheximide. Am J Pathol 140:545–549

Ledda-Columbano GM, Shinozuka H, Katyal SL, Columbano A, (1996) Cell proliferation, cell death and hepatocarcinogenesis. Cell Death Differ 3:17–22

Lehmann V, Freudenberg MA, Galanos C (1987) Lethal toxicity of lipopolysaccharide and tumor necrosis factor in normal and D-galactosamine-treated mice. J Exp Med 165:657–663

Leist M, Nicotera P (1997) The shape of cell death. Biochem Biophys Res Commun 236:1–9

Leist M, Wendel A (1995) Tunicamycin potently inhibits tumor necrosis factor-induced hepatocyte apoptosis. Eur J Pharmacol 292:201–204

Leist M, Wendel A (1996) A novel mechanism of murine hepatocyte death inducible by concanavalin A. J Hepatol 24:948–959

Leist M, Gantner F, Bohlinger I, German PG, Tiegs G, Wendel A (1994) Murine hepatocyte apoptosis induced in vitro and in vivo by TNF-alpha requires transcriptional arrest. J Immunol 153:1778–1787

Leist M, Gantner F, Bohlinger I, Tiegs G, Germann PG, Wendel A (1995a) Tumor necrosis factor-induced hepatocyte apoptosis precedes liver failure in experimental murine shock models. Am J Pathol 146:1220–1234

Leist M, Gantner F, Jilg S, Wendel A (1995b) Activation of the 55 kDa TNF-receptor is necessary and sufficient for TNF-induced liver failure, hepatocyte apoptosis and nitrite release. J Immunol 154:1307–1316

Leist M, Gantner F, Künstle G, Bohlinger I, Tiegs G, Bluethmann H, Wendel A (1996a) The 55 kD tumor necrosis factor receptor and CD95 independently signal murine hepatocyte apoptosis and subsequent liver failure. Mol Med 2:109–124

Leist M, Auer-Barth S, Wendel A (1996b) Tumor necrosis factor production in the perfused mouse liver and its pharmacological modulation by methylxanthines. J Pharmacol Exp Ther 276:968–976

Leist M, Gantner F, Naumann H, Bluethmann H, Vogt K, Brigelius-Flohe R, Nicotera P, Volk H, Wendel A (1997a) Tumor necrosis factor-induced apoptosis during poisoning of mice with hepatotoxins. Gastroenterology 112:924–935

Leist M, Single B, Castoldi AF, Kühnle S, Nicotera P (1997b) Intracellular ATP concentration: a switch deciding between apoptosis and necrosis. J Exp Med 185:1481–1486

Leist M, Single B, Künstle G, Volbracht C, Hentze H, Nicotera P (1997c) Apoptosis in the absence of poly-(ADP-ribose) polymerase. Biochem Biophys Res Commun 233:518–522

Lennon SV, Martin SJ, Cotter TG (1991) Dose-dependent induction of apoptosis in human tumor cell lines by widely diverging stimuli. Cell Prolif 24:203–214

Levy E, Slusser RJ, Ruebner BH (1968) Hepatic changes produced by a single dose of endotoxin in the mouse. Am J Pathol 52:477–502

Lewis M, Tartaglia LA, Lee A, Bennett GL, Rice GC, Wong GH, Chen E, Goeddel DV (1991) Cloning and expression of cDNAs for two distinct murine tumor necrosis factor receptors demonstrate one receptor is species specific. Proc Natl Acad Sci USA 88:2830–2834

Libert C, Van Bladel S, Brouckaert P, Shaw A, Fiers W (1991) Involvement of the liver, but not of IL-6, in IL-1-induced desensitization to the lethal effects of tumor necrosis factor. J Immunol 146:2625–2632

Libert C, Brouckaert P, Fiers W (1994) Protection by alpha-1 acid-glycoprotein against tumor necrosis factor-induced lethality. J Exp Med 180:1571–1575

Liehr H, Grün M, Seelig H, R, Seelig, Reutter W, Heine W (1978) On the pathogenesis of galactosamine hepatitis. Virchows Arch [B] 26:331–344

Lin J-K, Chou C-K (1992) In vitro apoptosis in the human hepatoma cell line induced by transforming growth factor beta-1. Cancer Res 52:385–388

Liu X, Kim CN, Yang J, Jemmerson R, Wang X (1996) Induction of apoptotic program in cell-free extracts: requirement for dATP and cytochrome c. Cell 86:147–157

Liu X, Zou H, Slaughter C, Wang X (1997) DFF, a heterodimeric protein that functions downstream of caspase-3 to trigger DNA fragmentation during apoptosis. Cell 89:175–184

Liu ZG, Hsu H, Goeddel DV, Karin M (1996) Dissection of TNF receptor 1 effector functions: JNK activation is not linked to apoptosis while NF-kB activation prevents cell death. Cell 87:565–576

Lockshin RA, Beaulaton J (1974) Programmed cell death. Life Sci 15:1549–1565

Lockshin RA, Williams CM (1965) Programmed cell death I. Cytology of degeneration in the intersegmental muscles of the pernyi silkmoth. J Insect Physiol 11:123–133

Los M, van de Craen M, Penning LC, Schenk H, Westendorp M, Baeuerle PA, Dröge W, Krammer PH, Flers W, Schulze-Osthoff K (1995) Requirement of an ICE/CED-3 protease for Fas/APO-1-mediated apoptosis. Nature 375:81–83

Majno G, Joris I (1995) Apoptosis, oncosis, and necrosis. An overview of cell death. Am J Pathol 146:3–15

Martin-Sanz P, Diaz-Guerra MJ, Casado M, Bosca L (1996) Bacterial lipopolysaccharide antagonizes transforming growth factor beta 1-induced apoptosis in primary cultures of hepatocytes. Hepatology 23:1200–1207

Medline A, Schaffner F, Popper H (1970) Ultrastructural features in galactosamine-induced hepatitis. Exp Mol Pathol 12:201–212

Merrill JE, Zimmerman RP (1991) Natural and induced cytotoxicity of oligodendrocytes by microglia is inhibitable by TGFbeta. GLIA 4:327–331

Miethke T, Wahl C, Heeg K, Echtenacher B, Krammer PH, Wagner H (1992) T cell-mediated lethal shock triggered in mice by the superantigen staphylococcal enterotoxin B: critical role of tumor necrosis factor. J Exp Med 175:91–98

Miethke T, Duschek K, Heeg K, Wagner H (1993) Pathogenesis of the toxic shock syndrome: T cell mediated lethal shock caused by the superantigen TSST-1. Eur J Immunol 23:1494–1500

Mihas AA, Ceballos R, Mihas TA, Hirshowitz BI (1990) Modification of the hepatotoxicity of D-galactosamine in the rat by an anti-endotoxin. J Med 21:301–311

Miyai K, Slusser RJ, Ruebner BH (1962) Viral hepatitis in mice: an electron microscopic study. Exp Mol Pathol 2:464–480

Mohler KM, Sleath PR, Fitzner JN, Cerretti DP, Alderson M, Kerwar SS, Torrance DS, Otten-Evans C, Weerawarna T, Greenstreet K, Kronheim SR, Petersen M, Gerhart M, Kozlosky CJ, March CJ, Black RA (1994) Protection against a lethal dose of endotoxin by an inhibitor of tumor necrosis factor processing. Nature 370:218–220

Moldawer LL, Gelin J, Schersten T, Lundholm KG (1987) Circulating interleukin 1 and tumor necrosis factor during inflammation. Am J Physiol 253:R922–R928

Moppert J, Ekesparre D, Bianchi L (1967) Zur Morphogenese der eosinophilen Einzelzellnekrose im Leberparenchym des Menschen. Eine licht- und elektronenoptisch korrelierte Untersuchung. Virchows Arch Pathol Anat 342:210–220

Mori W, Aoki N, Shiga J (1981) Acute hepatic cell necrosis experimentally produced by viral agents in rabbits. Am J Pathol 103:31–38

Morita M, Watanabe Y, Akaike T (1995) Protective effect of hepatocyte growth factor on interferon-gamma-induced cytotoxicity in mouse hepatocytes. Hepatology 21:1585–1593

Muzio M, Chinnaiyan AM, Kischkel FC, O'Rourke K, Shevchenko A, Ni J, Scaffidi C, Bretz JD, Zhang M, Gentz R, Mann M, Krammer PH, Peter ME, Dixit VM (1996) FLICE, a novel FADD-homologous ICE/CED-3-like protease, is recruited to the CD95 (Fas/APO-1) death-inducing signaling complex. Cell 85:817–827

Nagata S (1997) Apoptosis by death factor. Cell 99:355–365

Nagata S, Golstein P (1995) The Fas death factor. Science 267:1449–1455

Nakano Y, Shirai M, Mori N, Nakano M (1991) Neutralization of microcystin shock in mice by tumor necrosis factor alpha antiserum. Appl Environ Microbiol 57:327–330

Ni R, Tomita Y, Matsuda K, Ichihara A, Ishimura K, Ogasawara J, Nagata S (1994) Fas-mediated apoptosis in primary cultured mouse hepatocytes. Exp Cell Res 215:332–337

Nicotera P, Leist M (1997) Energy supply and the shape of death in neurons and lymphoid cells. Cell Death Differ 4:435–442

Nicotera P, Hartzell P, Baldi C, Svensson S-A, Bellomo G, Orrenius S (1986a) Cystamine induces toxicity in hepatocytes through the elevation of cytosolic Ca^{2+} and the stimulation of a nonlysosomal proteolytic system. J Biol Chem 261:14628–14635

Nicotera P, Hartzell P, Davis G, Orrenius S (1986b) The formation of plasma membrane blebs in hepatocytes exposed to agents that increase cytosolic Ca^{2+} is mediated by the activation of a non-lysosomal proteolytic system. FEBS Lett 209:139–144

Nieminen A-L, Saylor AK, Tesfai SA, Herman B, Lemasters JJ (1995) Contribution of the mitochondrial permeability transition to lethal injury after exposure of hepatocytes to t-butylhydroperoxide. Biochem J 307:99–106

Nissen F (1886) Über das Verhalten der Kerne in den Milchdrüsenzellen bei der Absonderung. Arch Mikroskop Anat 26:337–342

Nolan JP (1989) Intestinal endotoxins as mediators of hepatic injury-an idea whose time has come again. Hepatology 10:887–891

Oberhammer F, Bursch W, Parzefall W, Breit P, Erber E, Stadler M, Schulte-Hermann R (1991) Effects of transforming growth factor beta on cell death of cultured rat hepatocytes. Cancer Res 51:2478–2485

Oberhammer FA, Pavelka M, Sharma S, Tiefenbacher R, Purchio AF, Bursch W, Schulte-Hermann R (1992) Induction of apoptosis in cultured hepatocytes and in regressing liver by transforming growth factor ß1. Proc Natl Acad Sci USA 89:5408–5412

Oberhammer F, Bursch W, Tiefenbacher R, Fröschl G, Pavelka M, Purchio T, Schulte-Hermann R (1993a) Apoptosis is induced by transforming growth factor-beta1 within 5 hours in regressing liver without significant fragmentation of the DNA. Hepatology 18:1238–1246

Oberhammer F, Wilson JW, Dive C, Morris ID, Hickman JA, Wakeling AE, Walker PR, Sikorska M (1993b) Apoptotic death in epithelial cells: cleavage of DNA to 300 and/or 50 kb fragments prior to or in the absence of internucleosomal fragmentation. EMBO J 12:3679–3684

Oberhammer F, Nagy P, Tiefenbacher R, Fröschl G, Bouzanza B, Thorgeirsson SS, Carr B (1996) The antiandrogen cyproterone acetate induces synthesis of transforming factor beta-1 in the parenchymal cells of the liver accompanied by an enhanced sensitivity to undergo apoptosis and necrosis without inflammation. Hepatology 23:329–337

Oberhammer FA, Qin H (1995) Effect of three tumor promoters on the stability of hepatocyte cultures and apoptosis after transforming growth factor-beta1. Carcinogenesis 16:1363–1371

Oehm A, Behrmann I, Kalk W, Pawlita M, Maier G, Klas C, Li-Weber M, Richards S, Dhein J, Trauth BC, Ponsting H, Krammer PH (1992) Purification and molecular cloning of the APO-1 cell surface antigen, a member of the tumour necrosis factor/nerve growth factor receptor family. J Biol Chem 267:10709–10715

Ogasawara J, Watanabe-Fukunaga R, Adachi M, Matsuzawa A, Kasugai T, Kitamura Y, Itoh N, Suda T, Nagata S (1993) Lethal effect of the anti-fas antibody in mice. Nature 364:806–809

Ohno K, Maier P (1995) Tumor necrosis factor alpha differentially modulates the cellular response of rat hepatocytes in periportal- and pericentral-equivalent cultures. Eur J Pharmacol 292:205–214

Ohno K, Nakano T, Matsumoto Y, Watari T, Goitsuka R, Nakayama H, Tsujimoto H, Hasegawa A (1993) Apoptosis induced by tumor necrosis factor in cells chronically infected with feline immunodeficiency virus. J Virol 67:2429–2433

Orrenius S, McConkey DJ, Bellomo G, Nicotera P (1989) Role of Ca^{2+} in toxic cell killing. Trends Pharmacol Sci 10:281–285

Otto F, Schmid P, Mackensen A, Wehr U, Seiz A, Braun M, Galanos C, Mertelsmann R, Engelhard R (1996) Phase II trial of intravenous endotoxin in patients with colorectal and non-small cell lung cancer. Eur J Cancer 32 A:1712–1718

Pastorino JG, Snyder JW, Serroni A, Hoek JB, Farber JL (1993) Cyclosporin and carnitine prevent the anoxic death of cultured hepatocytes by inhibiting the mitochondrial permeability transition. J Biol Chem 268:13791–13798

Pastorino JG, Simbula G, Yamamoto K, Glascott Jr PA, Rothman RJ, Farber JL (1996) The cytotoxicity of tumor necrosis factor depends on induction of the mitochondrial permeability transition. J Biol Chem 271:29792–29798

Patel T, Bronk SF, Gores GJ (1994) Increases of intracellular magnesium promote glycodeoxycholate-induced apoptosis in rat hepatocytes. J Clin Invest 94:2183–2192

Patel T, Gores GJ, Kaufmann SH (1996) The role of proteases during apoptosis. FASEB J 10:587–597

Pensati L, Costanzo A, Ianni A, Accapezzato D, Iorio R, Natoli G, Nisini R, Almerighi C, Balsano C, Vajro P, Vegnente A, Levrero M (1997) Fas/Apo1 mutations and autoimmune lymphoproliferative syndrome in a patient with type 2 autoimmune hepatitis. Gastroenterology 113:1384–1389

Peter ME, Kischkel FC, Hellbardt S, Chinnaiyan AM, Krammer PH, Dixit VM (1996) CD95(APO-1/Fas)-associating signalling proteins. Cell Death Differ 3:161–170

Pfitzner W (1886) Zur pathologischen Anatomie des Zellkerns. Virchows Arch Pathol Anat 103:275–300

Prehn JHM, Bindokas VP, Marcuccilli CJ, Krajewski S, Reed JC, Miller RJ (1994) Regulation of neuronal Bcl-2 protein expression and calcium homeostasis by transforming growth factor type beta confers wide-ranging protection on rat hippocampal neurons. Proc Natl Acad Sci USA 91:12599–12603

Pritchard DJ, Butler WH (1989) Apoptosis – the mechanism of cell death in dimethylnitrosamine-induced hepatotoxicity. J Pathol 158:253–260

Que FG, Gores GJ (1996) Cell death by apoptosis: basic concepts and disease relevance for the gastroenterologist. Gastroenterology 110:1238–1243

Randow F, Syrbe U, Meisel C, Krausch D, Zuckermann H, Platzer C, Volk H-D (1995) Mechanism of endotoxin desensitization: involvement of interleukin 10 and transforming growth factor beta. J Exp Med 181:1887–1892

Ratan RR, Murphy TH, Baraban JM (1994) Macromolecular synthesis inhibitors prevent oxidative stress-induced apoptosis in embryonic cortical neurons by shunting cysteine from protein synthesis to glutathione. J Neurosci 14:4385–4392

Ray SD, Sorge CL, Kamendulis LM, Corcoran GB (1992) Ca^{++}-activated DNA fragmentation and dimethylnitrosamine-induced hepatic necrosis: effects of Ca^{++}-endonuclease and poly(ADP-ribose) polymerase inhibitors in mice. J Pharmacol Exp Ther 263:387–394

Ray SD, Kamendulis LM, Gurule MW, Yorkin RD, Corcoran GB (1993) Ca^{2+} antagonists inhibit DNA fragmentation and toxic cell death induced by acetaminophen. FASEB J 7:453–463

Ray SD, Mumaw VR, Raje RR, Fariss MW (1996) Protection of acetaminophen-induced hepatocellular apoptosis and necrosis by cholesteryl hemisuccinate pretreatment. J Pharmacol Exp Ther 279:1470–1483

Redondo C, Flores I, Gonzalez A, Nagata S, Carrera AC, Merida I, Martinez AC (1996) Linomide prevents the lethal effect of anti-Fas antibody and reduces Fas-mediated ceramide production in mouse hepatocytes. J Clin Invest 98:1245–1252

Rensing-Ehl A, Frei K, Flury R, Matiba B, Mariani SM, Weller M, Aebischer P, Krammer PH, Fontana A (1995) Local Fas/APO-1 (CD95) ligand-mediated tumor cell killing in vivo. Eur J Immunol 25:2253–2258

Reutter W, Lesch R, Keppler D, Decker K (1968) Galactosamine-hepatitis. Naturwissenschaften 55:497

Reutter W, Bauer CH, Lesch R (1970) On the mechanism of action of galactosamine: different response to D-galactosamine of rat liver during development. Naturwissenschaften 57:674–675

Rodriguez I, Matsuura K, Khatib K, Reed JC, Nagata S, Vassalli P (1996a) A bcl-2 transgene expressed in hepatocytes protects mice from fulminant liver destruction but not from rapid death induced by anti-Fas antibody injection. J Exp Med 183:1031–1036

Rodriguez I, Matsuura K, Ody C, Nagata S, Vassalli P (1996b) Systemic injection of a tripeptide inhibits the intracellular activation of CPP32-like proteases in vivo and fully protects mice against fas-mediated fulminant liver destruction and death. J Exp Med 184:2067–2072

Rosser BG, Gores GJ (1995) Liver cell necrosis: cellular mechanisms and clinical implications. Gastroenterology 108:252–275

Rouquet N, Allemand I, Grimber G, Molina T, Briand P, Joulin V (1996a) Protection of hepatocytes from Fas-mediated apoptosis by a non-transforming SV40 T-antigen mutant. Cell Death Differ 3:91–96

Rouquet N, Pagès J-C, Molina T, Briand P, Joulin V (1996b) ICE inhibitor YVADcmk is a potent therapeutic agent against in vivo liver apoptosis. Curr Biol 6:1192–1195

Rubin BY (1992) TNF and viruses: multiple interrelationships. In: Aggarwal BB, Vilcek J (eds) Tumor necrosis factors. Structure, function and mechanisms of action. Dekker, New York, pp 331–340

Saavedra JE, Billiar TR, Williams DL, Kim YM, Watkins SC, Keefer LK (1997) Targeting nitric oxide (NO) delivery in vivo. Design of a liver-selective NO donor prodrug that blocks tumor necrosis factor-alpha-induced apoptosis and toxicity in the liver. J Med Chem 40:1947–1954

Sanderson M, Factor V, Nagy P, Kopp J, Kondaiah P, Wakefield L, Roberts AB, Sporn MB, Thorgeirsson SS (1995) Hepatic expression of mature transforming growth factor beta1 in transgenic mice results in multiple tissue lesions. Proc Natl Acad Sci USA 92:2572–2576

Sasaki H, Matsuno T, Tanaka N, Orita K (1996) Activation of apoptosis during the reperfusion phase after rat liver ischemia. Transplant Proc 28:1908–1909

Sauer A, Hartung T, Aigner J, Wendel A (1996) Endotoxin-inducible granulocyte-mediated hepatotoxicity requires adhesion and serine protease release. J Leukoc Biol 60:633–643

Saunders JW (1966) Death in embryonic systems. Science 154:604–612

Savill J, Fadok V, Henson P, Haslett C (1993) Phagocyte recognition of cells undergoing apoptosis. Immunol Today 14:131–136

Schulte-Hermann R, Bursch W, Grasl-Kraupp B (1995) Active cell death (apoptosis) in liver biology and disease. Prog Liver Dis 15:1–35

Schwartz LM, Osborne BA (1993) Programmed cell death, apoptosis and killer genes. Immunol Today 14:582–590

Schwartz LM, Smith SW, Jones MEE, Osborne BA (1993) Do all programmed cell deaths occur via apoptosis? Proc Natl Acad Sci USA 90:980–984

Searle J, Kerr JFR, Bishop CJ (1982) Necrosis and apoptosis: distinct modes of cell death with fundamentally different significance. Pathol Ann 17:229–259

Searle J, Harmon BV, Bishop CJ, Kerr JFR (1987) The significance of cell death by apoptosis in hepatobiliary disease. J Gastroenterol Hepatol 2:77–96

Searle JW, Balderson G (1996) Apoptosis as a mechanism of cell death in liver allograft rejection. Transplantation 61:168–169

Selye H, Tuchweber B, Bertok L (1966) Effect of lead acetate on the susceptibility of rats to bacterial endotoxins. J Bacteriol 91:884–890

Seyberth HW, Schmidt-Gayk H, Hackental E (1972) Toxicity, clearance and distribution of endotoxin in mice as influenced by actinomycin D, cycloheximide, a-amanitin and lead acetate. Toxicon 10:491–500

Shi J, Fujeda H, Kokubo Y, Wake K (1997) Evidence of hepatocyte apoptosis in the rat liver after the administration of carbon tetrachloride (in press)

Shikata N, Oyaizu T, Senzaki H, Uemura Y, Tsubura A (1996) Liver apoptosis after dimethylnitrosamine administration in shrews. Exp Toxicol Pathol 48:307–311

Shimizu S, Eguchi Y, Kamiike W, Akao Y, Kosaka H, Hasegawa J, Matsuda H, Tsujimoto Y (1996) Involvement of ICE family proteases in apoptosis induced by reoxygenation of hypoxic hepatocytes. Am J Physiol 271:G949–G958

Shimizu S, Eguchi Y, Kamiike W, Itoh Y, Hasegawa J-I, Yamabe K, Otsuki Y, Matsuda H, Tsujimoto Y (1996) Induction of apoptosis as well as necrosis by hypoxia and predominant prevention of apoptosis by Bcl-2 and Bcl-xL. Cancer Res 56:2161–2166

Shinagawa T, Yoshioka K, Kakumu S, Wakita T, Ishikawa T, Itoh Y, Takayanaki M (1991) Apoptosis in cultured rat hepatocytes: the effect of tumour necrosis factor alpha and interferon gamma. J Pathol 165:247–253

Solorzano CC, Ksontini R, Pruitt JH, Hess PJ, Edwards PD, Kaibara A, Abouhamze A, Auffenberg T, Galardy RE, Vauthey JN, Copeland EM III, Edwards CK III, Lauwers GY, CLare-Salzler M, MacKay SL, Moldawer LL, Lazarus DD (1997) Involvement of 26-kDa cell-associated TNF-alpha in experimental hepatitis and exacerbation of liver injury with a matrix metalloproteinase inhibitor. J Immunol 158:414–419

Sparwasser T, Miethke T, Lipford G, Erdmann A, Hacker H, Heeg K, Wagner H (1997) Macrophages sense pathogens via DNA motifs: induction of tumor necrosis factor-alpha-mediated shock. Eur J Immunol 27:1671–1679

Stadler J, Bentz BG, Harbrecht BG, Di Silvio M, Curran RD, Billiar T, Hoffman RA, Simmons RL (1992) Tumor necrosis factor alpha inhibits hepatocyte mitochondrial respiration. Ann Surg 216:539–546

Stanger BZ (1996) Looking beneath the surface: the cell death pathway of Fas/APO-1 (CD95). Mol Med 2:7–20

Stauber GB, Aggarwal BB (1989) Characterization and affinity cross-linking of receptors for human recombinant lymphotoxin (tumor necrosis factor-beta) on a human histiocytic lymphoma cell line, U-937. J Biol Chem 264:3573–3576

Strand S, Hofmann WJ, Hug H, Müller. M., Otto G, Strand D, Mariani SM, Stremmel W, Krammer PH, Galle PR (1996) Lymphocyte apoptosis induced by CD95 (APO-1/Fas) ligand expressing tumor cells – a mechanism of immune evasion? Nature Med 2:1361–1366

Su F, Schneider RJ (1997) Hepatitis B virus HBx protein sensitizes cells to apoptotic killing by tumor necrosis factor alpha. Proc Natl Acad Sci USA 94:8744–8749

Sun DY, Jiang S, Zheng L, Ojcius DM, Young JD (1994) Separate metabolic pathways leading to DNA fragmentation and apoptotic chromatin condensation. J Exp Med 179:559–568

Susin SA, Zamzami N, Castedo M, Hirsch T, Marchetti P, Macho A, Daugas E, Geuskens M, Kroemer G (1996) Bcl-2 inhibits the mitochondrial release of an apoptogenic protease. J Exp Med 184:1331–1341

Susin SA, Zamzami N, Castedo M, Daugas E, Wang H-G, Geley S, Fassy F, Reed JC, Kroemer G (1997) The central executioner of apoptosis: multiple connections between protease activation and mitochondria in Fas/APO-1/CD95- and ceramide-induced apoptosis. J Exp Med 186:25–37

Svoboda D, Nielson A, Werder A, Higginson J (1962) An electron microscopic study of viral hepatitis in mice. Am J Pathol 41:205–224

Tagawa Y, Sekikawa K, Iwakura Y (1997) Suppression of concanavalin A-induced hepatitis in IFN-gamma (-/-) mice, but not in TNF-alpha (-/-) mice: role for IFN-gamma in activating apoptosis of hepatocytes. J Immunol 159:1418–1428

Talmadge JE, Bowersox O, Tribble H, Lee SH, Shepard M, Liggitt D (1987) Toxicity of tumor necrosis factor is synergistic with gamma-interferon and can be reduced with cyclooxygenase inhibitors. Am J Pathol 128:410–425

Tanaka M, Suda T, Yatomi T, Nakamura N, Nagata S (1997) Lethal effect of recombinant human fas ligand in mice pretreated with Propionibacterium acnes. J Immunol 158:2303–2309

Tartaglia LA, Ayres M, Wong GHW, Goeddel DV (1993) A novel domain within the 55 kd TNF receptor signals cell death. Cell 74:845–853

Tartaglia LA, Goeddel DV (1992) Two TNF receptors. Immunol Today 13:151–153

Taverne J, Bate CA, Sarkar DA, Meager A, Rook GA, Playfair JH (1990) Human and murine macrophages produce TNF in response to soluble antigens of plasmodium falciparum. Parasite Immunol 12:33–43

Tewari M, Dixit VM (1995) Fas- and tumor necrosis factor-induced apoptosis is inhibited by the poxvirus crmA gene product. J Biol Chem 270:3255–3260

Thome M, Schneider P, Hofmann K, Fickenscher H, Meinl E, Neipel F, Mattmann C, Burns K, Bodmer J-L, Schröter M, Scaffidi C, Krammer PH, Peter ME, Tschopp J

(1997) Viral FLICE-inhibitory proteins (FLIPs) prevent apoptosis induced by death receptors. Nature 386:517–520

Tiegs G, Wolter M, Wendel A (1989) Tumor necrosis factor is a terminal mediator in galactosamine/endotoxin-induced hepatitis in mice. Biochem Pharmacol 38:627–631

Tiegs G, Niehörster M, Wendel A (1990) Leukocyte alterations do not account for hepatitis induced by endotoxin or TNF-alpha in galactosamine-sensitized mice. Biochem Pharmacol 40:1317–1322

Torre D, Zeroli C, Giola M, Ferrario G, Fiori GP, Bonetta G, Tambini R (1994) Serum levels of interleukin-1 alpha, interleukin-1 beta, interleukin-6, and tumor necrosis factor in patients with acute viral hepatitis. Clin Infect Dis 18:194

Tsuji H, Harada A, Mukaida N, Nakanuma Y, Bluethmann H, Kaneko S, Yamakawa K, Nakamura S-I, Kobayashi K-I, Matsushima K (1997) Tumor necrosis factor receptor p55 is essential for intrahepatic granuloma formation and hepatocellular apoptosis in a murine model of bacterium-induced fulminant hepatitis. Infect Immun 65:1892–1898

Tsukidate K, Yamamoto K, Snyder JW, Farber JL (1993) Microtubule antagonists activate programmed cell death (apoptosis) in cultured rat hepatocytes. Am J Pathol 143:918–925

Valeri F, Boess F, Wolf A, Göldlin C, Boelsteri UA (1997) Fructose and tagatose protect against oxidative cell injury by iron chelation. Free Radic Biol Med 22:257–268

Van Molle W, Libert C, Fiers W, Brouckaert P (1997) Alpha 1-acid glycoprotein and alpha 1-antitrypsin inhibit TNF-induced but not anti-Fas-induced apoptosis of hepatocytes in mice. J Immunol 159:3555–3564

Virchow R (1858) Cellular pathology as based upon physiological and pathological histology. In: Birmingham AL (ed) Classics of medicine library, 2nd edn, p 361

Wallach D (1997) Placing death under control. Nature 388:123–126

Wallach D, Boldin M, Goncharov T, Goltsev Y, Mett I, Malinin N, Adar R, Kovalenko A, Varfolomeev E (1996) Exploring cell death mechanisms by analyzing signaling cascades of the TNF/NGF receptor family. Behring Inst Mitt 97:144–155

Ware CF, Crowe PD, Grayson MH, Androlewicz MJ, Browning JL (1992) Expression of surface lymphotoxin and tumor necrosis factor on activated T, B, and natural killer cells. J Immunol 149:3881–3888

Watanabe Y, Morita M, Akaike T (1996) Concanavalin A induces perforin-mediated but not fas-mediated hepatic injury. Hepatology 24:702–710

Weil M, Jacobson MD, Coles HSR, Davies TJ, Gardner RL, Raff KD, Raff MC (1996) Constitutive expression of the machinery for programmed cell death. J Cell Biol 133:1053–1059

Weiner FR, Giambrone M, Czaja MJ, Shah A, Annoni G, Takahashi S, Eghbali M, Zern MA (1990) Ito-cell gene expression and collagen regulation. Hepatology 11:111–120

Wendel A (1990) Biochemical pharmacology of inflammatory liver injury in mice. Methods Enzymol 186:675–680

Williamson R (1970) Properties of rapidly labelled deoxyribonucleic acid fragments isolated from the cytoplasm of primary cultures of embryonic mouse liver cells. J Mol Biol 51:157–168

Wong GHW, Kamb A, Goeddel DV (1992) Antiviral properties of TNF. In: Beutler B (ed) Tumor necrosis factors. The molecules and their emerging role in medicine. Raven, New York, pp 371–382

Wyllie AH, Kerr JF, Currie AR (1980) Cell death: the significance of apoptosis. Int Rev Cytol 68:251–306

Yang J, Liu X, Bhalla K, Kim CN, Ibrado AM, Cai J, Peng T, Jones DP, Wang X (1997) Prevention of apoptosis by Bcl-2: release of cytochrome c from mitochondria blocked. Science 275:1129–1132

Yonehara S, Ishii A, Yonehara M (1989) A cell-killing monoclonal antibody (anti-Fas) to a cell surface antigen co-downregulated with the receptor of tumor necrosis factor. J Exp Med 169:1747–1756

Zabel P, Wolter DT, Schönharting MM, Schade UF (1989) Oxpentifylline in endotoxemia. Lancet II:1474–1477

Zamzami N, Susin SA, Marchetti P, Hirsch T, Gómez-Monterrey I, Castedo M, Kroemer G (1996) Mitochondrial control of nuclear apoptosis. J Exp Med 183:1533–1544

Zeid IM, Bronk SF, Fesmier PJ, Gores GJ (1997) Cycloprotection by fructose and other ketohexoses during bile salt-induced apoptosis of hepatocytes. Hepatol 25:81–86

Zhivotovsky B, Burgess DH, Vanags DM, Orrenius S (1997) Involvement of cellular proteolytic machinery in apoptosis. Biochem Biophys Res Commun 230:481–488

Zou H, Henzel WJ, Liu X, Lutschg A, Wang X (1997) Apaf-1, a human protein homologous to C. elegans CED-4, participates in cytochrome c-dependent activation of caspase-3. Cell 90:405–413

Editor-in-charge: Professor D. Pette